Green's function approach for quantum graphs: an overview

Fabiano M. Andrade[a,b], Alexandre G. M. Schmidt[c], Eduardo Vicentini[d], Bin K. Cheng[e], Marcos G. E. da Luz[e]

[a] *Department of Computer Science and Department of Physics and Astronomy, University College London, WC1E 6BT London, United Kingdom*
[b] *Departamento de Matemática e Estatística, Universidade Estadual de Ponta Grossa, 84030-900 Ponta Grossa-PR, Brazil*
[c] *Departamento de Física, Universidade Federal Fluminense, 27215-350 Volta Redonda-RJ, Brazil*
[d] *Departamento de Física, Universidade Estadual do Centro Oeste, 85010-990 Guarapuava-PR, Brazil*
[e] *Departamento de Física, Universidade Federal do Paraná, 81531-980 Curitiba-PR, Brazil*

Abstract

Here we review the many interesting aspects and distinct phenomena associated to quantum dynamics on general graph structures. For so, we discuss such class of systems under the energy domain Green's function (G) framework. Such approach is particularly interesting because G can be written as a sum over classical-like paths, where local quantum effects are taking into account through the scattering matrix amplitudes (basically, transmission and reflection coefficients) defined on each one of the graph vertices. So, the *exact* G has the functional form of a generalized semiclassical formula, which through different calculation techniques (addressed in details here) always can be cast into a closed analytic expression. This allows to solve exactly arbitrary large (although finite) graphs in a recursive and fast way. Using the Green's function method, we survey many properties for open and closed quantum graphs, like scattering solutions for the former and eigenspectrum and eigenstates for the latter, also addressing quasi-bound states. Concrete examples, like cube, binary trees and Sierpiński-like, topologies are considered. Along the work, possible distinct applications using the Green's function methods for quantum graphs are outlined.

Keywords: quantum graphs, Green's function, scattering, bound states, quasi-bound state

Contents

Email addresses: f.andrade@ucl.ac.uk,fmandrade@uepg.br (Fabiano M. Andrade), luz@fisica.ufpr.br (Marcos G. E. da Luz)

1. Introduction

A graph can be understood intuitively as a set of elements (the vertices), attached ones to the others through connections (the edges). The topological arrangement of a graph is thus completely determined by the way the vertices are joined by the edges. The more general concept of a network – essentially a graph – has found applications in many branches of science and engineering. Some representative examples include: the analysis of electrical circuits, verification (in different contexts) of the shortest paths in grid structures, traffic planning, charge transport in complex chemical compounds, ecological webs, cybernetics architectures, linguistic families, and social connection relations, to cite just a few. In fact, given that as diverse as the street system of a city, the web of neurons in the human brain, and the organization of digital database in distinct storage devices, can all be described as 'graphs', we might be lead to conclude that such idea is one of the most useful and broadly used abstract mathematical notion in our everyday lives.

Less familiar is which we call quantum graphs[1], or more precisely quantum metric graphs (by associating lengths to the edges), basically comprising the study of the Helmholtz operator $\nabla^2 + k^2$ – when the external potentials for the underlying Hamiltonian along the edges are null, see later – on these topological structures. Nevertheless, they still attract a lot of attention in the physics and mathematics specialized literature because their rich behavior and potential applications [1, 2], for instance, regarding wave propagation and diffusive properties (actually, this latter aspect allowing a possible formal association between the Schrödinger and the diffusion equations [3]).

Historically, Linus Pauling seems to be the first to foresee the usefulness of considering quantum dynamics on graph structures, e.g., to model free electrons in organic molecules [4–10]. Indeed, in a first approximation the

[1] Depending on the particular aspect to be studied, quantum graphs are also named quantum networks or quantum wires.

molecules can be viewed as a set of fixed atoms (vertices) connected by chemical bonds (edges), along which the electrons obey a 1D Schrödinger equation with an effective potential. Moreover, quantum transport in multiply connected systems [11], like electron transport in organic molecules [12] as proteins and polymers, may be described by one-dimensional pathways (trajectories through the edges), changing from one path to another due to scattering at the vertices centers. More recently, quantum graphs have also been used to characterize molecular connectivity [13, 14].

In the realm of condensed matter physics, under certain conditions [15, 16] charge transport in solids is likewise well described by one-dimensional dynamics in branched (so network-like) structures, as in polymer films [17, 18]. Quantum graphs have also been applied in the analysis of disordered superconductors [19], Anderson transition in disordered wires [20, 21], quantum Hall systems [22], superlattices [23], quantum wires [24], mesoscopic quantum systems [25–28], and in connection with laser tomography technologies [29].

To understand fundamental aspects of quantum mechanics, graphs are idealized exactly soluble models to address, e.g., band spectrum properties of lattices [30, 31], the relation between periodic-orbit theory and Anderson localization [32], general scattering [33], chaotic and diffusive scattering [34–36], and quantum chaos [37]. In particular, quantum graphs relevance in grasping distinct features of quantum chaotic dynamics have been demonstrated in two pioneer papers [38, 39]. Through elucidating examples, such works show that the corresponding spectral statistics follow very closely the predictions of the random-matrix theory [40]. They also present an alternative derivation of the trace formula[2], highlighting the similarities with the famous Gutzwiller's expression for chaotic Hamiltonian systems [41, 42]. Actually, a very welcome fact in the area is the possibility to obtain exact analytic results for quantum graphs even when they present chaotic behavior [43–46]. Important advances and distinct approaches to spectrum statistics analysis in quantum graphs, as well as the relation with quantum chaos, can be found in a nice review in [47].

As a final illustration of the vast applicability of graphs we mention the important fields of quantum information and quantum computing [48]. For the metric case (the focus in this review), it has been proposed that the logic gates necessary to process and operate qubits could be implemented by tailoring the scattering properties of the vertices along a quantum graph [49, 50]. However, much more common in quantum information is to consider only the topological features of the graphs [51], hence not ascribing lengths to the edges. Such structures are usually referred as discrete or combinatorial graphs (for a parallel between metric and combinatorial see, e.g., [52]). They are the basis to construct the so called graph-states [53–57], in which the vertices are the states themselves (e.g., spins 1/2 constituting the qubits) and the edges represent the pairwise interactions (for instance, an Ising-like coupling [58]) between two vertices states [59]. Graph-states are very powerful tools to unveil different aspects of quantum computation. For instance, to establish relations between different computational methods schemes [57, 60] and to demonstrate that entanglement can help to outperform the Shannon limit capacity (of the classical case) in transmitting a message with zero probability of error throughout a channel presenting noise [61, 62].

Extremely relevant in quantum information processing is the concept of quantum walks, loosely speaking, the quantum version of classical random walks [63–65]. Quantum walks are quite useful either theoretically, as primitives of universal quantum computers [66–68], or operationally, as building blocks to quantum algorithms [65, 69–71]. Thus, since there is a close connection between quantum walks and quantum graphs [72–75], this might open the possibility of extending different techniques to treat quantum graphs to the study of quantum walks [76–79], therefore helping in the development of quantum algorithms.

The physical construction of quantum graphs is obviously an essential issue. In such regard, an important result is that in Ref. [80]. It shows that quantum graphs can be implemented through microwave networks due to the formal equivalence between the Schrödinger equation (describing the former) and the telegraph equation (describing the latter) [80]. Currently, these kind of systems are among the most preeminent experimental realizations of quantum graphs – as demonstrated by the vast literature on the topic [81–101]. Nonetheless, microwave networks are not the only possibility. In particular, optical lattices [102–104] and quasi-1D structures of large donor-acceptor molecules (with quasi-linear optical responses) [105] might also constitute very appropriate setups for building quantum graphs.

The implementation of quantum graphs – of course, besides the concrete applications – can be quite helpful in settling relevant theoretical questions. As an illustrative example, consider the famous query posed by Mark Kac in 1966: 'can one hear the shape of a drum?' [106]. Its modified version in the present context is [107]: 'can one

[2] For $G(\mathbf{r}'', \mathbf{r}'; E)$ the energy dependent Green's function of a quantum system (Sec. 3), the trace of G, or $g(E) = \int d\mathbf{r}\, G(\mathbf{r}, \mathbf{r}; E)$, is important because it leads to the problem density of states $\rho(E) = -(1/\pi)\lim_{\epsilon\to 0}\mathrm{Im}[g(E + i\epsilon)]$. The Gutzwiller trace formula [41] is an elegant semiclassical approximation for $\rho(E)$, in which $g(E)$ is given in terms of sums over classical periodic orbits.

hear the shape of a graph?'. It has been proved that for simple graphs (see next Sec.) whose all edges lengths are incommensurable, the spectrum is uniquely determined [107]. In other words, in this case one should be able to reconstruct the graph just from its eigenmodes. But if these assumptions are not verified, then distinct graphs can be isospectral [108, 109]. An interesting perspective to the problem arises by adding infinity leads to originally closed graphs [110, 111]. So, we have scattering system which can be analyzed in terms of their scattering matrices $\mathcal{S}$. Two metric graphs, Γ_A and Γ_B, are said isoscattering either if $\mathcal{S}_A$ and $\mathcal{S}_B$ share the same set of poles or the phases of $\det[\mathcal{S}_A]$ and $\det[\mathcal{S}_B]$ are equal [112]. Hence, the question is now: can the poles of $\mathcal{S}$ and phases of $\det[\mathcal{S}]$ *alone* to define the graph's shape? The answer is again negative [88, 110], as nicely confirmed through microwave networks experiments [88] (see also [82]). However, by analyzing in more details actual scattering data (e.g., in the time instead of frequency domain [84]) it does become possible to distinguish isoscattering graphs which are topologically different.

Quantum graphs as a well posed general mathematical problem requires the establishment of the underlying self-adjoint operator, i.e., the proper definition of the wave equation with its correct boundary conditions. Probably, the first important step along this direction was taken in 1953 in Ref. [7]. There, graphs were thought of as idealized web of wires or wave guides, but for the widths being much smaller than any other spatial scale. Assuming the lateral size of the wire small enough, any propagating wave remains in a single transverse mode. Therefore, instead of the corresponding partial differential Schrödinger equation, one can deal with ordinary differential operators. Also, if no external field is applied or no potential V for the wires is assumed, the one dimensional motion along the edges is free and everywhere in the graph the wave number is $k = \sqrt{2\mu E/\hbar^2}$, with the energy E a constant. Concerning the nodes, they either can be faced as scattering centers (thus, conceivably described by local $\mathcal{S}$ matrices) or the *loci* where consistent matching conditions for the partial wave functions (i.e., the ψ's in the distinct edges) must be imposed (Sec. 2).

In contrast, graphs with non-vanishing potentials – sometimes referred to as 'dressed' [44, 113] – lead to solutions with spatially dependent k's along the edges. An important subset of dressed are scaling quantum graphs[3] [43, 44, 114–117], whose mathematical foundations are discussed in [118]. They are particularly interesting because although their classical limit is chaotic, the quantum spectrum is exactly obtained through analytic periodic orbit expansions [43]. Another very relevant class of dressed quantum graphs is that described by magnetic Schrödinger operators [119]. In this case one assumes arbitrary inhomogeneous magnetic fields in the network [120], such that for each edge e there is a corresponding vector potential A_e. So, formally we have to make the traditional momentum operator substitution in the Schrödinger equation: $d/dx_e \to d/dx_e - iA_e$. Recently, quantum graphs with magnetic flux have attracted a lot of attention due to the many distinct phenomena emerging in these systems [121–128].

Given the discussion so far, it is already clear that a quantum graph is, after all, just an usual quantum problem. As such, its solution basically means to determine properties like wave packets propagation [129, 130], eigenstates (either bound and scattering states) [131, 132], eigenenergies [133], etc. This can be accomplished from, say, a suitable Schrödinger equation and appropriate boundary conditions for each specific graph topology, Sec. 2. But operationally there are many ways to deal with these systems, so different techniques can be employed. For instance, we can cite self-adjoint extension approaches [134], and the previously mentioned scattering $\mathcal{S}$ matrix methods [38] and the trace formula based on classical periodic orbits expansions [39].

It is well known that the energy Green's function G is a very powerful tool in quantum mechanics [135, 136]. Its knowledge allows to determine essentially any relevant quantity for the problem (e.g., the time evolution can be calculated from the time-dependent propagator, which is the Fourier transform of G). So, it should be quite natural to consider Green's function approaches in the study of graph structures. In fact, one of the first works in this direction [35] has employed G to describe transport in open graphs. Later, the many possibilities in utilizing Green's functions techniques for arbitrary quantum graphs have been discussed and exemplified in [137], with general and rigorous results further obtained from such a method in [138, 139]. Recently, Green's functions have been used to investigate (always in the context of quantum graphs): searching algorithms for shortest paths [140], Casimir effects [141], vacuum energy in quantum field theories [142], and resonances on unbounded star-shaped networks [143]. Finally, but not the least important, the special topological features of networks make it possible (at least in the undressed case[4]) to obtain the exact G in a closed analytic form for any finite (i.e., a large although limited number of nodes and

[3] Briefly, to each edge e of a scaling quantum graph one can associate a numerical constant γ_e. Then, along e the wave number is $k_e = \gamma_e k_0$, with $k_0 = \sqrt{2\mu E/\hbar^2}$ a constant.

[4] The Green's function for scaling quantum graphs can also be calculated exactly. This will be briefly discussed in Sec. 3.

edges) arbitrary graph. Certainly, this contrasts with most problems in quantum mechanics, for which exact analytic solutions are very hard to find [144, 145].

Therefore, the purpose in this review is twofold. As for the first, we start observing there is a huge literature discussing general features and applications of classical graphs. To cite just one, more physics-oriented, we mention communicability (so, signal transport) in classical networks [146]. In the quantum case comprehensive overviews are not so abundant, notwithstanding particular relevant aspects can be found addressed in details in some very interesting works [1, 39, 47, 52, 147, 148]. Also, for a formal and rigorous treatment, a good source is [149]. In this way, our first goal is to survey graphs as ordinary quantum mechanics problems. However, highlighting that their special characteristics can give rise to rich quantum phenomena.

The second is to do so by specifically considering one of the most powerful methods to treat quantum graphs, namely, the Green's function approach. For arbitrary graphs, we discuss in an unified manner how to obtain the exact energy domain G as a general sum over paths '*a la Feynman*' [150–152]. These paths must be weighted by the proper quantum amplitudes, given by energy-dependent scattering matrices elements associated to the vertices. We examine a schematic way to regroup the multi-scattering contributions (essentially a factorization method [134, 153–155]), leading to a final closed analytic expression for G. This particular procedure to construct the exact G is very useful to interpret many results concerning quantum graphs, like interference in transport processes [35, 156, 157]. With the help of illustrative examples, we elaborate on how to extract from G the graphs quantum properties.

The work is organized as the following. In Section 2 we define and discuss general quantum graphs. In Section 3 we consider in great detail the Green's function approach for such systems. In Section 4 we present (with examples) the factorization protocols which allow to cast G as a closed analytic formula. Distinct applications are addressed in the next three Sections. More specifically, the general determination of bound and scattering states, analysis of representative graphs (cube, binary trees, and Sierpiński-like graphs), and quasi-bound states in open structures, are considered, respectively, in Secs. 5, 6, and 7. Finally, we drawn our final remarks and conclusion in Section 8.

2. Quantum mechanics on graphs: general aspects

2.1. Graphs

A finite *graph* $X(V,E)$ is a pair consisting of two sets, of vertices (or nodes) $V(X) = \{1, 2, \ldots, n\}$ and of edges (or bonds) $E(X) = \{e_1, e_2, \ldots, e_m\}$ [158, 159]. Thus, the total number of vertices and edges is given, respectively, by $n = |V(X)|$ and $m = |E(X)|$. If the vertices i and j are linked by the edge e_s, then $e_s \equiv \{i, j\}$ (hereafter $i, j = 1, \ldots, n$ and $r, s = 1, \ldots, m$). For an undirected graph, any edge $\{i, j\}$ has the same properties [160] in both $i \to j$ and $j \to i$ 'directions': $\{i, j\} \equiv \{j, i\}$. For simple graphs $e_s \neq \{j, j\}$ and $e_r = e_s$ only if $r = s$. Hence, in this case there are no loops or pair of edges multiple-connected. Finally, for connected graphs the vertices cannot be divided into two non-empty subsets such that there is no edge joining the two subsets.

The graph topology, i.e., the way the vertices and edges are associated, can be described in terms of the adjacency matrix $A_{ij}(X)$ of dimension $n \times n$. For simple undirected graphs, $A_{ij}(X)$ reads

$$A_{ij}(X) = \begin{cases} 1, & \text{if } \{i, j\} \in E(X), \\ 0, & \text{otherwise.} \end{cases} \tag{1}$$

Two vertices are said neighbors whenever they are connected by an edge. Thus, the set

$$E_i(X) = \{j : \{i, j\} \in E(X)\} \tag{2}$$

is the neighborhood of the vertex $i \in V(X)$ and the degree (or valence) of i is

$$v_i = |E_i(X)| = \sum_{j=1}^{n} A_{ij}(X). \tag{3}$$

Note that

$$|E(X)| = \frac{1}{2} \sum_{i=1}^{n} |E_i(X)|. \tag{4}$$

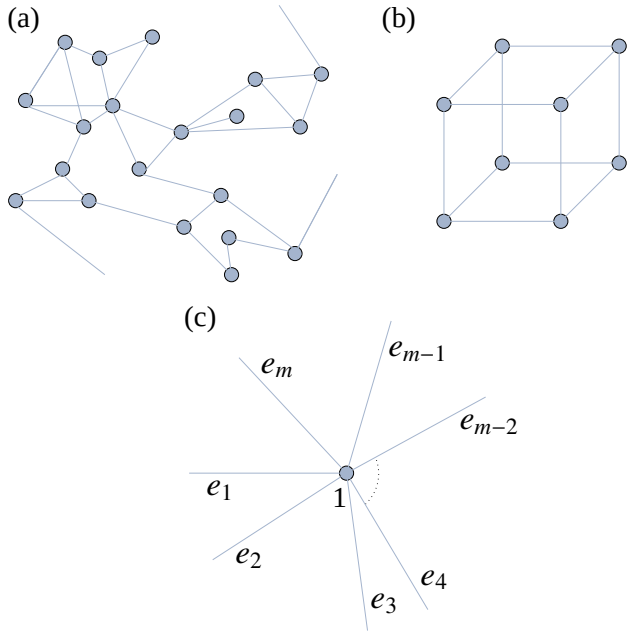

Figure 1: (Color online). Examples of (a) open and (b) closed quantum graphs. (c) A open star graph with a single vertex $V(\Gamma) = \{1\}$ connected to $E(\Gamma) = \{e_1, \ldots, e_m\}$ leads.

So far, the above definitions refer to *discrete* or *combinatorial* graphs. To discuss quantum graphs it is necessary to equip the graphs with a metric. Therefore, a *metric graph* $\Gamma(V, E)$ is a graph $X(V, E)$ for which it is also assigned a positive length $\ell_{e_s} \in (0, +\infty)$ to each edge. If all edges have finite length the metric graph is called *compact*, otherwise it is *non-compact*. In this latter case Γ has one ore more 'leads'. A lead is a single ended edge e_r, which leaves from a vertex and extends to the semi-infinite ($\ell_{e_s} = +\infty$).

In the quantum description, for each edge e_s (with e_s either joining two vertices i and j or leaving from vertex j to the infinite) we assume a coordinate x_{e_s}, indicating the position along the edge. For $e_s = \{i, j\}$, to choose at which vertex (i or j) $x_{e_s} = 0$ is just a matter of convention, and can be set according to the convenience in each specific system. Of course, for e_s a lead attached to j, a natural choice is $x_{e_s} = 0$ at j.

In the remaining of this review we will focus on simple connected graphs, the most studied situation in quantum mechanics [73]. But we stress that the Green's function discussed here is also valid for non-simple graphs, i.e., for many edges joining the same two vertices and for the existence of loops: one just need to consider the proper reflections and transmissions quantum amplitudes (Sec. 3) for the propagation along these extra edges.

2.2. The time-independent Schrödinger equation on graphs

A *quantum graph* is a metric graph structure $\Gamma(V, E)$, on which we can define a differential operator H (usually the Schrödinger Hamiltonian) together with proper vertices boundary conditions [39, 47]. In others words, a quantum graph problem is a triple

$$\{\Gamma(V, E), \text{Hamiltonian operator } H \text{ on } E(\Gamma), \text{boundary conditions for } V(\Gamma)\}.$$

A quantum graph is called *closed* if the respective metric graph is compact, otherwise it is called *open*. A schematic representation of quantum graphs [160] is depicted in Figure 1.

The total wave function Ψ is a vector with m components, written as

$$\Psi = \begin{pmatrix} \psi_{e_1}(x_{e_1}) \\ \psi_{e_2}(x_{e_2}) \\ \vdots \\ \psi_{e_m}(x_{e_m}) \end{pmatrix}. \tag{5}$$

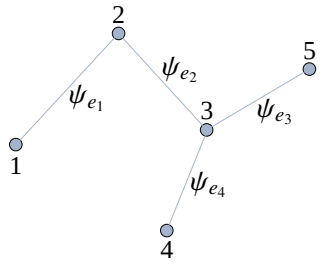

Figure 2: (Color online). A quantum graph $\Gamma(V,E)$, $V(\Gamma)=\{1,2,3,4,5\}$, $E(\Gamma)=\{\{1,2\},\{2,3\},\{3,4\},\{3,5\}\}$ and the Ψ components in each one of its edges. The wave functions must be matched through the boundary condition at each vertex $i\in V(\Gamma)$. Specifically: at $i=1$: ψ_{e_1}; at $i=2$: ψ_{e_1},ψ_{e_2}; at $i=3$: $\psi_{e_2},\psi_{e_3},\psi_{e_4}$; at $i=4$: ψ_{e_4}; at $i=5$: ψ_{e_3}.

The Hamiltonian operator on $E(\Gamma)$ consists of the following unidimensional differential operators defined on each edge e_s [19, 161] (the dressed case)

$$H_{e_s}(x_{e_s})=-\frac{\hbar^2}{2\mu}\frac{d^2}{dx_{e_s}^2}+V_{e_s}(x_{e_s}). \tag{6}$$

Here, $V_{e_s}(x_{e_s})$ is the potential assumed to be non-negative and smooth in the interval $0<x_{e_s}<\ell_{e_s}$. Different works have addressed the above Hamiltonian for non-vanishing potentials (for instance, see [43, 44, 116, 137, 162–165]). However, in the literature, even in papers discussing quantum chaos [37–39, 47, 166], it is usual to have for any e_s that $V_{e_s}=0$ (the case we assume in this review). Then, the component $\psi_{e_s}(x_{e_s})$ of the total wave function Ψ is the solution of ($k=\sqrt{2\mu E}/\hbar$)

$$-\frac{d^2\psi_{e_s}}{dx_{e_s}^2}=k^2\psi_{e_s}(x_{e_s})\;\Rightarrow\;\psi_{e_s}(x_{e_s})=c_{+,e_s}\,\exp[+i\,k\,x_{e_s}]+c_{-,e_s}\,\exp[-i\,k\,x_{e_s}], \tag{7}$$

with the c's constants. All these wave functions must satisfy appropriate boundary conditions at the vertices, ensuring continuity, global probability current conservation, divergence free ψ's and uniqueness. Technically, the match of the boundary conditions in each vertex is the most cumbersome step in obtaining the final full Ψ (in Figure 2 we illustrate which components must be matched in which vertices for a particular example of a graph with $V(\Gamma)=\{1,2,3,4,5\}$ and $E(\Gamma)=\{\{1,2\},\{2,3\},\{3,4\},\{3,5\}\}$).

Furthermore, the imposition of these boundary conditions [39, 47, 167] renders the Hamiltonian operator to be self-adjoint [5]. In fact, the most general boundary conditions at a vertex of a quantum graph (consistent with flux conservation [30]) can be determined through self-adjoint extension techniques [168, 169]. Let us denote by [134, 153] $\Psi_j=(\psi_{e_{j_1}},\psi_{e_{j_2}},\ldots,\psi_{e_{jv_j}})^T$ and $\Psi'_j=(\psi'_{e_{j_1}},\psi'_{e_{j_2}},\ldots,\psi'_{e_{jv_j}})^T$, respectively, the wave functions and their derivatives associated to the v_j edges attached to the vertex j. Then, the boundary conditions can be specified through $v_j\times v_j$ matrices $\mathcal{A}_j$ and $\mathcal{B}_j$, with $\mathcal{A}_j\Psi_j=\mathcal{B}_j\Psi'_j$ at j. One ensures self-adjointeness of the Hamiltonian operator by imposing current conservation $\Psi_j^\dagger\Psi'_j=\Psi'^\dagger_j\Psi_j$. As shown in [134, 153], the general solution for this problem implies that $\mathcal{A}_j\mathcal{B}_j^\dagger=\mathcal{B}_j\mathcal{A}_j^\dagger$, resulting in a set of v_j^2 independent real parameters to characterize the boundary conditions at j. More on this is discussed in the Appendix A, but here we comment that in physical terms, the self-adjointness of the Hamiltonian implies that the dynamics does not allow the vertices to behave as sinks or sources.

2.3. The vertices as zero-range potentials

From the previous discussion, in an undressed quantum graph the edges e_s can be viewed as free unidimensional spatial directions of length ℓ_{e_s} and the vertices as point structures (0D), whose action is to impose the proper boundary conditions on the ψ's. In the usual 1D quantum mechanics, arbitrary zero-range potentials, also known as point

[5] Consider a continuous linear (so bounded) operator O of domain $\mathcal{D}(O)$ in a Hilbert space $\mathcal{H}$. The adjoint $O^\dagger$ (also bounded) of the operator O is such that $\langle O\psi|\phi\rangle=\langle\psi|O^\dagger\phi\rangle$ for $\psi\in\mathcal{D}(O)$ and $\varphi\in\mathcal{H}$. O is self-adjoint if and only if $O=O^\dagger$ and $\mathcal{D}(O)=\mathcal{D}(O^\dagger)$ [167].

interactions, have exactly such effect [170, 171] (see Appendix A.1). A textbook example is the Dirac delta-function potential that simply determines, at its location, a specific boundary conditions to the wave function [172].

Hence, to describe the quantum dynamics along a graph we can take the j's as arbitrary zero-range interactions, an approach fully consistent with the general boundary conditions treatment described in Sec. 2.2, Appendix A. Moreover, to assume the vertices as potentials brings up an important advantage: the j's become point scatterers. As such, they are completely characterized by their scattering features, given in terms of the reflections and transmission amplitudes. For example, this is exactly the case for a delta-function, for which ψ can be obtained without considering any boundary conditions. Instead, a purely scattering treatment solves the problem (see, e.g., the pedagogical discussion in [173]). General point interactions are very diverse in their scattering properties. For instance, the intriguing aspects of transmission and reflection from point interactions have been discussed in distinct contexts, such as, time-dependent potentials [174], nonlinear Schrödinger equation [175] and shredding by sparse barriers [176].

Actually, for a point interaction on the line (say, at $x_0 = 0$), as demonstrated in the Appendix A.1, to determine which boundary conditions its impose to the wave function, at $x = 0$, is entirely equivalent to specify its scattering $\mathcal{S}$ matrix elements. This holds true when the vertex, a zero-range potential, instead of being attached to two edges (the 'left' ($-\infty < x < 0$) and 'right' ($0 < x < +\infty$) semi-infinite leads for the 1D line case), has v_j 1D directions or edges (see Figure 1 (c)). From the Appendix A.2, we then can define for each vertex j a matrix $\mathcal{S}_j$, of elements $\mathcal{S}_j^{(s,s)}(k) = r_j^{(s)}(k)$ and $\mathcal{S}_j^{(s,r)}(k) = r_j^{(s,r)}(k)$ (from now on, we will label edges e_{j_s} and e_{j_r} simply as s and r). Here

- $t_j^{(s,r)}(k)$ is the quantum amplitude for a plane wave, of wave number k, incoming from the edge s towards the vertex j to be transmitted to the edge r outgoing from j.
- $r_j^{(s)}(k)$ is the quantum amplitude for a plane wave, of wave number k, incoming from the edge s towards the vertex j to be reflected to the edge s outgoing from j.

The required conditions for self-adjointeness (i.e., probability flux conservation) along the whole graph (Appendix A.3), demands that $\mathcal{S}(k)\mathcal{S}^{\dagger}(k) = \mathcal{S}^{\dagger}(k)\mathcal{S}(k) = \mathbf{1}$ and $\mathcal{S}(k) = \mathcal{S}^{\dagger}(-k)$, so yielding

$$\sum_{l=1}^{v_j} \mathcal{S}_j^{(s,l)}(k)\,\mathcal{S}_j^{(r,l)^*}(k) = \sum_{l=1}^{v_j} \mathcal{S}_j^{(l,s)}(k)\,\mathcal{S}_j^{(l,r)^*}(k) = \delta_{sr}, \quad \mathcal{S}_j^{(s,r)}(k) = \mathcal{S}_j^{(r,s)^*}(-k). \tag{8}$$

Summarizing, for quantum graphs it is complete equivalent to set either the boundary conditions for the ψ's at each vertex, as mentioned in Sec. 2.2, or to specify the scattering properties of the different j's through the $\mathcal{S}_j^{(r,s)}$ matrices obeying to Eq. (8). We also observe that eventually one could have bound states for a given point interaction potential j depending on the particular BC imposed to ψ at the vertex location. In the scattering description, the quantum coefficients R and T have poles at the upper-half of the complex plane k, corresponding to the possible eigenenergies. The eigenfunctions can then be obtained from an appropriate extension of the scattering states to those k's values [177]. This will be exemplified in Section 6.

3. Energy domain Green's functions for quantum graphs

3.1. Basic results in the usual 1D case

The Green's function $G(E)$ is an important tool in quantum mechanics [135]. In the usual 1D case, it is defined by the inhomogeneous differential equation ($H(x) = -(\hbar^2/(2\mu))\, d^2/dx^2 + V(x)$)

$$[E - H(x_f)]G(x_f, x_i; E) = \delta(x_f - x_i), \tag{9}$$

where also $G(x_f, x_i; E)$ is subjected to proper boundary conditions.

Suppose we have a complete set of normalized eigenstates $\psi_s(x)$ ($s = 0, 1, ...$, discrete spectrum) and $\psi_\sigma(x)$ ($\sigma > 0$, continuum spectrum), with

$$H\psi_s = E_s\psi_s, \qquad H\psi_\sigma = \frac{\hbar^2\sigma^2}{2\mu}\psi_\sigma. \tag{10}$$

Then, the solution of Eq. (9) is formally

$$G(x_f, x_i; E) = \sum_s \frac{\psi_s(x_f)\,\psi_s{}^*(x_i)}{(E - E_s)} + \int_0^\infty d\sigma\, \frac{\psi_\sigma(x_f)\,\psi_\sigma{}^*(x_i)}{(E - \hbar^2\sigma^2/(2\mu))}. \tag{11}$$

Thus, from Eq. (11) we can identify the poles of the Green's function with the bound states eigenenergies E_s and the residues at each pole with a tensorial product of the corresponding bound state eigenfunction. The continuous part of the spectrum corresponds to a branch cut of $G(x_f, x_i; E)$ [178, 179]. Given Eq. (11), the limit

$$\lim_{E\to E_s} (E - E_s)\, G(x_f, x_i; E) = \psi_s(x_f)\,\psi_s{}^*(x_i) \tag{12}$$

can be used to extract the discrete bound states from G.

3.2. The exact Green's function written as a generalized semiclassical expression

There are basically three methods for calculating the Green's function [135]: solving the differential equation in (9); summing up the spectral representation in (11); or performing the Feynman path integral expansion for the propagator in the energy representation [180, 181]. In particular, for contexts similar to the present work (see next), the latter approach has been used to study scattering by multiple potentials in 1D [150, 151], to calculate the eigenvalues of multiple well potentials [152], to study scattering quantum walks [77, 78], and to construct exact Green's function for rectangular potentials [182, 183].

The exact Green's function for an arbitrary finite array of potentials of compact support[6] has been obtained in [150], with an extension for more general cases presented in [151]. For the derivations in [150], it is necessary for the r's and t's of each localized potential to satisfy to certain conditions, which indeed are the ones in the Appendix A, Eq. (A.14) (note that point interactions constitute a particular class of potentials of compact support [184]). Thus, based on [150] we can calculate the Green's function for general point interactions by using the corresponding reflection and transmission coefficients, which are quantities with a very clear physical interpretation and conceivably, even amenable to be determined through experiments [185, 186].

So, for these general array of potentials, according to Refs. [150–152] the *exact* (hence in contrast with usual semiclassical approximations, see footnote 2) Green's function for a particle of fixed energy E and end points x_i and x_f is given by

$$G(x_f, x_i; E) = \frac{\mu}{i\hbar^2 k} \sum_{\text{sp}} W_{\text{sp}} \exp\left[\frac{i}{\hbar} S_{\text{sp}}(x_f, x_i; k)\right]. \tag{13}$$

The above sum is performed over all scattering paths (sp) starting in x_i and ending in x_f. A 'scattering path' represents a trajectory in which the particle leaves from x_i, suffers multiple scattering, and finally arrives at x_f. For each sp, S_{sp} is the classical-like action, i.e., $S_{\text{sp}} = k\, L_{\text{sp}}$, with L_{sp} the trajectory length. The term W_{sp} is the sp quantum amplitude (or weight), constructed as it follows: each time the particle hits a localized potential V_n, quantically it can be reflected or transmitted by the potential. In the first case, W_{sp} gets a factor r_n and in the second, W_{sp} gets a factor t_n. The total W_{sp} is then the product of all quantum coefficients r_n's and t_n's acquired along the sp.

The direct extension of Eq. (13) – often called generalized semiclassical Green's function formula because its functional form – to quantum graphs is natural. In fact, the two main ingredients necessary in the rigorous derivation [150, 151] of Eq. (13), namely, unidimensionality and localized potentials, are by construction present in quantum graphs. First, since the quantum evolution takes place along the graph edges, regardless the Γ topology, the dynamics is essentially 1D. Second, the potentials (scatters) are the vertices, which as we have seen, can be treated as point interactions, so a particular class of compact support potentials [184, 187].

In the Appendix B we outline the main steps necessary to prove that the exact Green's function for arbitrary quantum graphs has the very same form of Eq. (13). Moreover, as we are going to discuss in length in Sec. 4, different techniques can be used to identify and sum up all the scattering paths. So, for general finite (i.e., $|V(\Gamma)|$ and $|E(\Gamma)|$ both finites) connected undirected simple metric quantum graphs Γ, in principle one always can obtain a

[6] If $V_n(x)$ is said to have compact support in the interval $\mathcal{I}_n \equiv \{x \,|\, a_n < x < b_n\}$, then $V_n(x)$ identically vanishes for $x \notin \mathcal{I}_n$. An arbitrary array of N potentials of compact support is given by $V(x) = \sum_{n=1}^{N} V_n(x)$, for all $\mathcal{I}_n$'s disjoint.

closed analytical expression for G. Therefore, given that any information about a quantum system can be extracted directly from the corresponding Green's function, the results here constitute a very powerful tool in the analysis of many distinct aspects of quantum graphs.

As a final observation, we recall that for scaling quantum graphs [118], for each edge e_s we have $k_{e_s} = \gamma_{e_s} k_0$ (see footnote 3). This behavior for the wave number can result from constant potentials V_{e_s} along the distinct e_s's. But as discussed in [183], the correct G for these kind of piecewise constant potential systems can also be cast as above. Therefore, the exact Green's function for scaling quantum graphs are likewise given by Eq. (13).

4. Obtaining the Green's function for quantum graphs: general procedures

The formula in Eq. (13) gives the correct Green's function for arbitrary connected undirected simple quantum graphs. However, it has no universal practical utility unless we are able to identify all the possible scattering paths and to sum up the resulting infinite series – regardless the specific system. So, here we shall describe different protocols to handle Eq. (13), allowing to write the exact G as a closed analytic expression. To keep the discussion as accessible as possible, we start with few straightforward illustrative examples. In the sequence we extend the analysis to more general situations.

We adopt the following notation:

- $r_j^{(s)}$ and $t_j^{(s,r)}$ are the reflection and transmission amplitudes for the vertex j, as described in the end of Sec. 2.
- P_l represents the contribution from an entire infinite family l of sp to Eq. (13), so that $G = \mu/(i\hbar^2 k)\sum_l P_l$.
- $G_{sr}(x_f, x_i; k)$ is the Green's function for a particle with energy $E = \hbar^2k^2/2\mu$, whose initial point x_i lies in the edge e_s and the final point x_f in the edge e_r.

Also, whenever there is no room for doubt, for simplicity we represent edges by s (instead of e_s) and vertices by capital letters, A, B, etc.

4.1. Constructing the Green's function: a simple example

Consider the open graph shown in Figure 3(a). It has two vertices, A and B, one finite edge (of length ℓ_1), labeled 1, and two semi-infinite edges (leads), labeled i and f. By assuming $-\infty < x_i < 0$ in i and $0 < x_f < +\infty$ in f, the Green's function $G_{if}(x_f, x_i; k)$ essentially describes the transmission across the full graph structure, i.e., from the left to the right leads. To obtain G we need to sum up all the possible sp for a quantum particle starting at x_i, in i, going through multiple reflections between the vertices A and B, and finally ending up at x_f, in f. As we are going to show, Eq. (13) yields a convergent geometric series, which therefore can be calculated exactly [150–152, 188–193].

In Fig. 3 (b)–(d) it is depicted three examples of sp. Consider the scattering path in 3 (b), representing the 'direct' propagation from x_i to x_f. The particle starts by leaving x_i towards A. From this first stretch of the trajectory, one gets a factor $\exp[-ikx_i]$ to G. Upon hitting the vertex, the particle is then transmitted through A. This process yields a factor $t_A^{(i,1)}$ to G. Next, the particle goes to the vertex B location, leading to a factor $\exp[ik\ell_1]$. Once in B, the particle is then transmitted through B, thus resulting in $t_B^{(1,f)}$. Finally, from the final trajectory stretch (B to x_f), one gets $\exp[ikx_f]$. Putting all this together, the sp of Fig. 3 (b) contributes to Eq. (13) with $W_{sp} = t_A^{(i,1)}\, t_B^{(1,f)}$ and $L_{sp} = (x_f - x_i) + \ell_1 = |x_f| + |x_i| + \ell_1$ (hence the length of this sp).

Following the same type of analysis, for the other two examples in Fig. 3 we have:

(c) $\exp[-ikx_i]\, t_A^{(i,1)}\, \exp[ik\ell_1]\, r_B^{(1)}\, \exp[ik\ell_1]\, r_A^{(1)}\, \exp[ik\ell_1]\, t_B^{(1,f)}\, \exp[ikx_f]$:

$W_{sp} = r_A^{(1)}\, r_B^{(1)}\, t_A^{(i,1)}\, t_B^{(1,f)}, \qquad L_{sp} = (x_f - x_i) + 3\ell_1;$

(d) $\exp[-ikx_i]\, t_A^{(i,1)}\, \exp[ik\ell_1]\, r_B^{(1)}\, \exp[ik\ell_1]\, r_A^{(1)}\, \exp[ik\ell_1]\, r_B^{(1)}\, \exp[ik\ell_1] r_A^{(1)}\, \exp[ik\ell_1]\, t_B^{(1,f)}\, \exp[ikx_f]$:

$W_{sp} = (r_A^{(1)})^2\, (r_B^{(1)})^2\, t_A^{(i,1)}\, t_B^{(1,f)}, \qquad L_{sp} = (x_f - x_i) + 5\ell_1.$

Thus, the full Green's function is written as a sum over all the existing terms of the above form, or

$$G_{if}(x_f, x_i; k) = \frac{\mu}{i\hbar^2 k}\, \exp[-ikx_i]\, t_A^{(i,1)} \Big(\sum_{n=0}^{\infty} [r_A^{(1)}]^n\, [r_B^{(1)}]^n\, \exp[ik(2n+1)\ell_1] \Big)\, t_B^{(1,f)}\, \exp[ikx_f]. \tag{14}$$

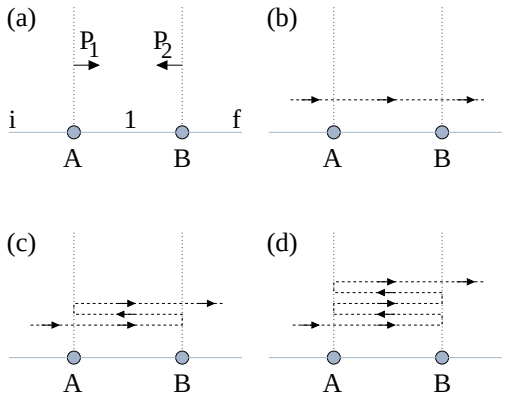

Figure 3: (Color online). A simple graph with two vertices, A and B, a finite edge labeled 1 (of length ℓ_1), and left, i, and right, f, leads. (a) The starting positions of two families, P_1 and P_2, of sp. (b)-(d) Schematic examples of individual sp.

Equation (14) is in fact a geometric series and since for the quantum amplitudes we have that $|r_j^{(s)}|^2 \leq 1$ and $|t_j^{(s,r)}|^2 \leq 1$, the sum in Eq. (14) always converges. So, the Green's function reads

$$G_{if}(x_f, x_i; k) = \frac{\mu}{i\hbar^2 k}\, T_{if}\, \exp[ik(x_f - x_i + \ell_1)], \tag{15}$$

with

$$T_{if} = \frac{t_A^{(i,1)}\, t_B^{(1,f)}}{1 - r_A^{(1)} r_B^{(1)} \exp\left[2ik\ell_1\right]}. \tag{16}$$

Note that Eq. (16) can be recognized as the transmission amplitude for the whole system [150]. This illustrates the fact that by properly regrouping several vertices, they can be treated as a 'single' vertex, effectively contributing with overall reflection and transmission amplitudes to G. As we discuss in details in Sec. 4.2, such an approach strongly simplifies the calculation of the Green's function for more complicated systems.

For the present example, to identify all the infinite possible sp is relatively direct. But when the number of vertices and edges increases, this can become a very tedious and cumbersome enterprise. Fortunately, the task can be accomplished by means of a simple diagrammatic classification scheme, separating the sp into families.

To exemplify it, consider again G_{if} for the graph of Fig. 3. For any sp, necessarily at the beginning the particle leaves x_i, goes to A, and then is transmitted through A. Once tunneling to $x_1 = 0^+$ (always with positive velocity), there are infinite possibilities to follow (some displayed in Fig. 3 (b)–(d)). So, schematically we represent all the trajectories headed to the right, departing from $x_1 = 0^+$, as the family P_1, Fig. 3 (a). Now, a sp in P_1 initiates traveling from A to B. Then, in B it may either cross the vertex B, finally arriving at the final point x_f, or be reflected from B, reversing its movement direction (at $x_1 = \ell_1^-$). For this latter situation, all the subsequent trajectories from $x_1 = \ell_1^-$ can be represented as the family P_2, Fig. 3 (a). But exactly the same reasoning shows that for any sp in P_2, the particle leaves B towards A, it is reflected from A[7], and then becomes one of the paths in P_1.

Hence, the above prescription yields for the Green's function

$$G_{if}(x_f, x_i; k) = \frac{\mu}{ik\hbar^2}\, \exp[-ikx_i]\, t_A^{(i,1)}\, P_1, \tag{17}$$

where

$$P_1 = \exp[ik\ell_1] \left\{ \begin{array}{l} r_B^{(1)}\, P_2 \\ t_B^{(1,f)}\, \exp[ikx_f], \end{array} \right. \tag{18}$$

and

$$P_2 = \exp[ik\ell_1]\, r_A^{(1)}\, P_1. \tag{19}$$

[7]To be transmitted through A would lead the particle to travel towards $x_i \to -\infty$, with no returning (there are no vertices for $x_i < 0$). So, obviously this sp cannot contribute to G_{if}.

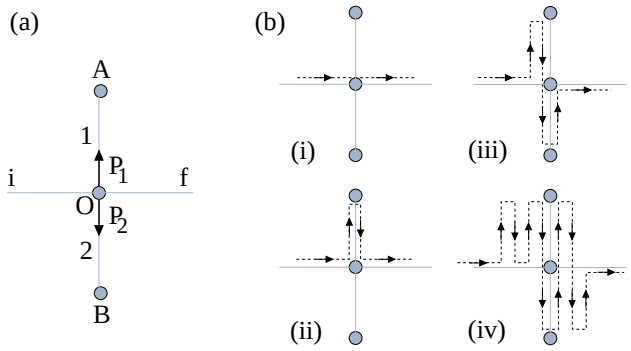

Figure 4: (Color online). The cross shaped graph, with two leads, i and f (left and right), two finite edges, 1 and 2 (up and down), and three vertices, A, O, B. (a) The P_s's represent all the trajectories starting at vertex O along an edge s and finally tunneling O, to get to the lead f. (b) Four schematic examples of possible sp.

In Eq. (18), '{' represents the possible splitting for the sp in the family P_1. The algebraic equation equivalent to Eq. (18) is

$$P_1 = \exp[ik\ell_1]\Big(r_B^{(1)}\, P_2 + t_B^{(1,f)}\, \exp[ikx_f]\Big). \tag{20}$$

Thus, solving Eqs. (19) and (20) for P_1, one obtains

$$P_1 = \frac{t_B^{(1,f)}\, \exp[ik\ell_1]\, \exp[ikx_f]}{1 - r_A^{(1)}\, r_B^{(1)}\, \exp[2ik\ell_1]}, \tag{21}$$

which by direct substitution into Eq. (17), leads to the exact G in Eq. (15).

In this way, the identification and summation of an infinite number of sp is reduced to the solution of a simple system of linear algebraic equations. Such strong recursive nature of the scattering paths in quantum graphs constitutes a key procedure to solve more complicated problems.

4.2. Simplification procedures: further details

From the previous example, it is clear that two protocols which drastically simplify the calculations for G are: (a) to regroup infinite many scattering paths into finite number of families of trajectories; and (b) to divide a large graph into smaller blocks, to solve the individual blocks, and then to connect the pieces altogether.

Thus, given their importance, here we further elaborate on (a) and (b), unveiling certain technical aspects which do not arise from a so simple graph as that in Sec. 4.1. Hence, we explicit address two different systems below: a cross shaped structure, useful to illustrate details about (a), and a tree-like quantum graph, a system whose solution is considerably facilitated by the block separation technique (b).

4.2.1. Regrouping the sp into families: a cross shaped graph case study

The cross-shaped graph is shown in Fig. 4. It is composed by three vertices, two edges and two leads. Observe that the vertex O is the origin (end) of the lead f (i). Let us first discuss the Green's function for the particle leaving $-\infty < x_i < 0$, along the lead i, and getting to $0 < x_f < +\infty$, along the lead f. In the sum Eq. (13), the sp are all the trajectories starting from i, suffering multiple transmissions and reflections between the edges 1 and 2 (of lengths ℓ_1 and ℓ_2), and arriving at f. In Fig. 4 (b) we show schematic examples of possible sp: (i) direct transmission from i to f through the central vertex O, so that $W_{sp} = t_O^{(i,f)}$ and $L_{sp} = x_f - x_i$; (ii) transmission from i to the edge 1, a reflection at vertex A, and a final transmission from the central vertex to the lead f, then $W_{sp} = t_O^{(i,1)}\, r_A^{(1)}\, t_O^{(1,f)}$ and $L_{sp} = x_f - x_i + 2\ell_1$; (iii) transmission to edge 1, a reflection from A, then a transmission to edge 2, a new reflection, this time from vertex B, and finally at O a transmission to lead f, in this way $W_{sp} = t_O^{(i,1)}\, r_A^{(1)}\, t_O^{(1,2)}\, r_B^{(2)}\, t_O^{(2,f)}$ and $L_{sp} = x_f - x_i + 2(\ell_1 + \ell_2)$; (iv) transmission to edge 1, a double bouncing within edge 1, then transmission to edge 2, a reflection from vertex B, a transmission to edge 1, a reflection from vertex A, another transmission to edge 2, a reflection from vertex B, and finally a transmission to lead f from edge 2 (through vertex O), thus $W_{sp} = t_O^{(i,1)}\, [r_A^{(1)}]^3\, r_O^{(1)}\, [t_O^{(1,2)}]^2\, [r_B^{(2)}]^2\, t_O^{(2,1)}\, t_O^{(2,f)}$ and $L_{sp} = x_f - x_i + 6\ell_1 + 4\ell_2$.

Such infinite large proliferation of paths can be factorized in a simple way. Indeed, since for any sp we have initially a propagation from x_i to O along i and finally a propagation from O to x_f along f, we can write

$$G_{if}(x_f, x_i; k) = \frac{\mu}{i\hbar^2 k}\, T_{if}\, \exp[ik(x_f - x_i)]. \tag{22}$$

Here T_{if} comprises all the contributions resulting from sp in the region A—O—B of the graph, or

$$T_{if} = \begin{cases} t_O^{(i,f)} \\ t_O^{(i,1)}\, P_1 \\ t_O^{(i,2)}\, P_2 \end{cases} . \tag{23}$$

As before, the symbol '{' represents the trajectories splitting, which reads

$$T_{if} = t_O^{(i,f)} + t_O^{(i,1)}\, P_1 + t_O^{(i,2)}\, P_2. \tag{24}$$

The first term is just the amplitude for the direct path, i.e., a simple tunneling from i to f through O. The second (third) term represents the tunneling from lead i to edge 1 (2) and all the subsequent possible trajectories that the particle can follow until reaching lead f, represented by P_1 and P_2, Fig. 4 (a).

The reasoning to obtain the two families of infinite trajectories, P_1 and P_2, is quite simple. Take, for instance, P_1: all such paths start at $x_1 = 0^+$, travel along edge 1 towards vertex A, suffer a reflection at A, and then return to vertex O. This part of the trajectories results in the term $r_A^{(1)} \exp[2ik\ell_1]$. Once reaching back vertex O they can either, be reflected from it, then going into the set of paths P_1 again, or to tunnel to edge 2, so going into the family of paths P_2, or yet to tunnel to lead f, thus terminating the A—O—B part of the sp. The same type of analysis follows for P_2, so

$$\begin{cases} P_1 = r_A^{(1)} \exp[2ik\ell_1] \begin{cases} r_O^{(1)} P_1 \\ t_O^{(1,2)} P_2 \\ t_O^{(1,f)} \end{cases} \\ \\ P_2 = r_B^{(2)} \exp[2ik\ell_2] \begin{cases} r_O^{(2)} P_2 \\ t_O^{(2,1)} P_1 \\ t_O^{(2,f)} \end{cases} \end{cases} , \tag{25}$$

leading to the algebraic equations

$$\begin{cases} P_1 = r_A^{(1)} \exp[2ik\ell_1]\Big(r_O^{(1)} P_1 + t_O^{(1,2)} P_2 + t_O^{(1,f)}\Big) \\ P_2 = r_B^{(2)} \exp[2ik\ell_2]\Big(r_O^{(2)} P_2 + t_O^{(2,1)} P_1 + t_O^{(2,f)}\Big), \end{cases} \tag{26}$$

whose solution reads

$$\begin{aligned} P_1 &= \frac{1}{g}\left\{r_A^{(1)} t_O^{(1,f)} \exp[2ik\ell_1] + r_A^{(1)} r_B^{(2)}\Big(t_O^{(1,2)} t_O^{(2,f)} - r_O^{(2)} t_O^{(1,f)}\Big) \exp[2ik(\ell_1 + \ell_2)]\right\} \\ P_2 &= \frac{1}{g}\left\{r_B^{(2)} t_O^{(2,f)} \exp[2ik\ell_2] + r_A^{(1)} r_B^{(2)}\Big(t_O^{(2,1)} t_O^{(1,f)} - r_O^{(1)} t_O^{(2,f)}\Big) \exp[2ik(\ell_1 + \ell_2)]\right\}, \end{aligned} \tag{27}$$

for

$$g = \Big(1 - r_A^{(1)} r_O^{(1)} \exp[2ik\ell_1]\Big)\Big(1 - r_B^{(2)} r_O^{(2)} \exp[2ik\ell_2]\Big) - r_A^{(1)} r_B^{(2)} t_O^{(1,2)} t_O^{(2,1)} \exp[2ik(\ell_1 + \ell_2)]. \tag{28}$$

Similarly, we can consider both the initial and end points at the edge i ($-\infty < x_i, x_f < 0 \in i$), for which G_{ii} is given by

$$G_{ii}(x_f, x_i; k) = \frac{\mu}{i\hbar^2 k}\Big\{\exp[ik|x_f - x_i|] + R_{ii}\, \exp[-ik(x_f + x_i)]\Big\}. \tag{29}$$

In this case, it is not difficult to see that

$$R_{ii} = r_O^{(i)} + t_O^{(i,1)} P_1 + t_O^{(i,2)} P_2. \tag{30}$$

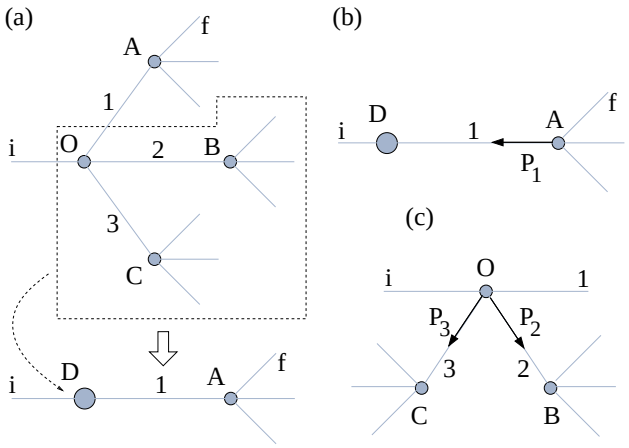

Figure 5: (Color online). A tree-like quantum graph. (a) By regarding the whole region C—O—B (including the leads) as an 'unique' effective vertex D, the original graph is reduced as illustrated. (b) In the reduced graph, P_1 represents the family of trajectories which suffer multiple reflections between D and A, and finally tunnel the vertex A to the lead f. (c) The auxiliary graph (and the corresponding sp families) necessary to calculate $r_D^{(1)}$ and $t_D^{(i,1)}$.

The expressions leading to the correct P's are those in (27) where, however, we must make the obvious substitution of $t_O^{(s,f)}$ by $t_O^{(s,i)}$ ($s = 1, 2$).

Finally, we consider the end point x_f in one of the edges, say edge 1. We assume that the origin of the this edge is at vertex O, so $0 < x_f < \ell_1$. Then, we have that

$$G_{i1}(x_f, x_i; k) = \frac{\mu}{i\hbar^2 k}\, \exp[-ikx_i]\left(t_O^{(i,1)} P_1 + t_O^{(i,2)} P_2\right). \tag{31}$$

Of course here we should not take into account any sp for which the particle tunnels to the edge f (for a reason similar to that explained in footnote 7). Thus, we have for the P's:

$$\begin{cases} P_1 = \exp[ikx_f] + r_A^{(1)}\, \exp[2ik\ell_1]\left(\exp[-ikx_f] + r_O^{(1)}\, P_1 + t_O^{(1,2)}\, P_2\right) \\ P_2 = r_B^{(2)}\, \exp[2ik\ell_2]\left(r_O^{(2)}\, P_2 + t_O^{(2,1)}\, P_1\right). \end{cases} \tag{32}$$

By solving the above system and substituting into the expression (31), we get

$$\begin{aligned} G_{1i}(x_f, x_i; k) = \frac{\mu}{i\hbar^2 k g} &\left\{t_O^{(i,1)} + r_B^{(2)}\left(t_O^{(i,2)} t_O^{(2,1)} - r_O^{(2)} t_O^{(i,1)}\right)\exp[2ik\ell_2]\right\} \\ &\times \left\{\exp[ik(x_f - x_i)] + r_A^{(1)}\exp[ik(2\ell_1 - x_f - x_i)]\right\}, \end{aligned} \tag{33}$$

with g given by Eq. (28).

4.2.2. Treating a graph in terms of blocks: a tree-like case study

Next we discuss how to shorten the calculations for a large quantum graph by decomposing it in blocks. For so, we consider the example shown in Fig. 5 (a), a relatively simple tree-like graph: a lead i is attached to a vertex O, from which emerges three edges 1, 2 and 3, ending, respectively, at vertices A, B, and C. Each of these vertices, by their turn, are connected to three leads.

Here we just analyze the Green's function for the initial position $-\infty < x_i < 0$ in lead i and the end position $0 < x_f < +\infty$ in lead f, which is connected to vertex A, see Fig. 5 (a). Observe that in this particular situation we do not need to consider any sp that goes into another lead before to f. In such case the particle would leave the graph, being impossible to come back to f.

The first step to simplify the problem is to face the whole block indicated in Fig. 5 (a) as a single vertex D. Any information about the inner structure of such region will be contained in the vertex quantum amplitudes $t_D^{(i,1)}$ and $r_D^{(1)}$.

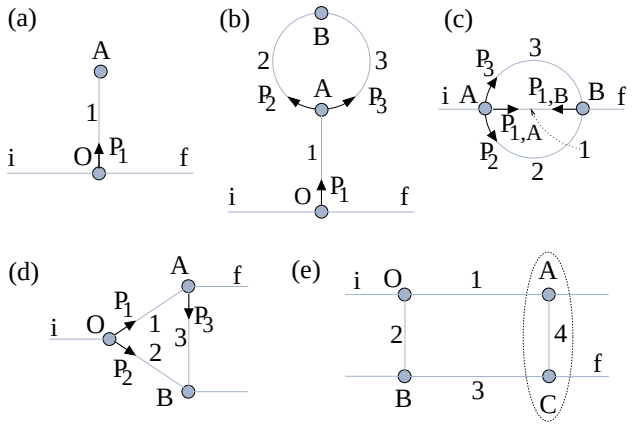

Figure 6: (Color online). Several graphs whose G's can be obtained from the solutions of other topologies by eliminating, redefining or regrouping the vertices reflections and transmissions quantum amplitudes. (a) The cross shaped graph, Fig. 4, but with both the bottom edge and vertex removed. (b) The same as in (a), but with the simple vertex A substituted by a circle-like structure. (c) A circle-like graph attached to two leads. (d) Triangle (e) and rectangle graphs attached to semi-infinite leads.

Thus, we reduce the original graph to the simpler one depicted in Fig. 5 (b). From Fig. 5 (b), we have that the Green's function can be written as $G_{if}(x_f, x_i; k) = \mu/(i\hbar^2 k)\, T_{if}\, \exp[ik(x_f - x_i)]$, with $T_{if} = t_D^{(i,1)} \exp[ik\ell_1]\left(r_A^{(1)} P_1 + t_A^{(1,f)}\right)$. Then, based on our previous discussions, one quickly realizes that the infinite family of trajectories P_1 is given by $P_1 = r_D^{(1)} \exp[2ik\ell_1]\left(r_A^{(1)} P_1 + t_A^{(1,f)}\right)$, or

$$P_1 = \frac{r_D^{(1)} t_A^{(1,f)} \exp[2ik\ell_1]}{1 - r_D^{(1)} r_A^{(1)} \exp[2ik\ell_1]}. \tag{34}$$

It remains to determine the coefficients $t_D^{(i,1)}$ and $r_D^{(1)}$. We can do so with the help of the auxiliary quantum graph of Fig. 5 (c). We first recall that $t_D^{(i,1)}$ ($r_D^{(1)}$) represents the sp contribution for the particle to go from lead i (edge 1) to edge 1 through the region B—O—C. Inspecting Fig. 5 (c), we see that $t_D^{(i,1)} = t_O^{(i,1)} + t_O^{(i,3)} P_3 + t_O^{(i,2)} P_2$ and $r_D^{(1)} = r_O^{(1)} + t_O^{(1,3)} P_3 + t_O^{(1,2)} P_2$, where for the P's

$$\begin{cases} P_3 = r_C^{(3)} \exp[2ik\ell_3]\left(r_O^{(3)} P_3 + t_O^{(3,2)} P_2 + t_O^{(3,1)}\right) \\ P_2 = r_B^{(2)} \exp[2ik\ell_2]\left(r_O^{(2)} P_2 + t_O^{(2,3)} P_3 + t_O^{(2,1)}\right). \end{cases} \tag{35}$$

The solution of Eq. (35) is given by Eq. (27) with the appropriate labels substitutions in (27): $A \to C$, $1 \to 3$ and $f \to 1$.

4.3. The Green's function solutions by eliminating, redefining or regrouping scattering amplitudes

A great advantage in writing the Green's function in terms of the general scattering amplitudes of each vertex is that by setting appropriate values for or regrouping these quantities, we can obtain G for some graphs based on the solutions for other topologies.

Indeed, for a vertex j attached to two edges (e_{j_1} and e_{j_2}), to set $r_j^{(s)} = 0$ and $t_j^{(s,r)} = 1$ $(s, r = 1, 2)$ is equivalent to remove the vertex j from the graph. On the other hand, if for all e_{j_s} we set $t_j^{(s,r)} = 0$ for the two (one) vertices j attached to the finite (semi-infinite) edge e_{j_r}, then we eliminate e_{j_r} from the structure. For instance, consider the graph in Fig. 6 (a). We obtain its exact G_{if}, G_{ii} and G_{i1} just by assuming $t_O^{(i,2)} = t_O^{(1,2)} = 0$ for the solutions of the cross shaped graph of Fig. 4.

As for regrouping, the G's for the graph in Fig. 6 (b) – if x_i and x_f are not in the edges 2 and 3 – follow from the exact Green's functions for the graph of Fig. 6 (a) by just supposing the whole region A—B—A as a single vertex, say C, and making the substitution $r_A^{(1)} \to r_C^{(1)}$. From the Fig. 6 (b) we see that $r_C^{(1)}$ is given by $r_C^{(1)} = r_A^{(1)} + t_A^{(1,2)} P_2 + t_A^{(1,3)} P_3$,

with the P's obtained from

$$\begin{cases} P_2 = r_B^{(2)} \exp[2ik\ell_2]\Big(r_A^{(2)} P_2 + t_A^{(2,3)} P_3 + t_A^{(2,1)}\Big) \\ \quad\quad + t_B^{(2,3)} \exp[ik(\ell_2+\ell_3)]\Big(r_A^{(3)} P_3 + t_A^{(3,2)} P_2 + t_A^{(3,1)}\Big) \\ P_3 = r_B^{(3)} \exp[2ik\ell_3]\Big(r_A^{(3)} P_3 + t_A^{(3,2)} P_2 + t_A^{(3,1)}\Big) \\ \quad\quad + t_B^{(3,2)} \exp[ik(\ell_2+\ell_3)]\Big(r_A^{(2)} P_2 + t_A^{(2,3)} P_3 + t_A^{(2,1)}\Big). \end{cases} \tag{36}$$

Consider now the more involving example in Fig. 6 (c) and G_{11} for which both end points are in edge 1, i.e., $0 < x_i, x_f < \ell_1$. We define $r_C^{(1)}$ ($t_C^{(1,1)}$) as the resulting quantum amplitude for the particle to hit the vertex A from edge 1, to suffer all the multiple scattering in edges 2 and 3 and finally to come back to edge 1 from the vertex A (B). We likewise define $r_D^{(1)}$ and $t_D^{(1,1)}$ for the particle initially hitting the vertex B. So, we have that (dropping the superscripts (1) and (1, 1) for simplicity)

$$G_{11}(x_f, x_i; k) = \frac{\mu}{i\hbar^2 k}\Big\{ \exp[ik|x_f - x_i|] + \exp[ik(\ell_1 - x_i)]\Big(r_D P_{1,B} + t_D P_{1,A}\Big) + \exp[ikx_i]\Big(r_C P_{1,A} + t_C P_{1,B}\Big)\Big\}, \tag{37}$$

where

$$\begin{cases} P_{1,A} = \exp[ikx_f] + \exp[ik\ell_1]\Big(r_D P_{1,B} + t_D P_{1,A}\Big) \\ P_{1,B} = \exp[ik(\ell_1 - x_f)] + \exp[ik\ell_1]\Big(r_C P_{1,A} + t_C P_{1,B}\Big). \end{cases} \tag{38}$$

Solving the above system, the Green's function (37) reads

$$\begin{aligned} G_{11}(x_f, x_i; k) = \frac{\mu}{i\hbar^2 k g}\Big\{ & g \exp[ik|x_f - x_i|] + r_C \exp[ik(x_f + x_i)] + r_D \exp[ik(2\ell_1 - x_f + x_i)] \\ & + r_C\, r_D \exp[ik(2\ell_1 + x_f - x_i)] + r_C\, r_D \exp[ik(2\ell_1 - x_f + x_i)] \\ & + \Big(1 - t_C \exp[ik\ell_1]\Big) \exp[ik(\ell_1 + x_f - x_i)] \\ & + \Big(1 - t_D \exp[ik\ell_1]\Big) \exp[-ik(\ell_1 - x_f + x_i)]\Big\}, \end{aligned} \tag{39}$$

with $g = \Big(1 - t_C \exp[ik\ell_1]\Big)\Big(1 - t_D \exp[ik\ell_1]\Big) - r_C\, r_D \exp[2ik\ell_1]$.

Lastly (see Fig. 6 (c)), the coefficients are given by $r_C = r_A^{(1)} + t_A^{(1,2)} P_2 + t_A^{(1,3)} P_3$, with P_2 and P_3 obeying to

$$\begin{cases} P_2 = r_B^{(2)} \exp[2ik\ell_2]\Big(r_A^{(2)}\, P_2 + t_A^{(2,3)}\, P_3 + t_A^{(2,1)}\Big) \\ \quad\quad + t_B^{(2,3)} \exp[ik(\ell_2+\ell_3)]\Big(r_A^{(3)}\, P_3 + t_A^{(3,2)}\, P_2 + t_A^{(3,1)}\Big) \\ P_3 = r_B^{(3)} \exp[2ik\ell_3]\Big(r_A^{(3)}\, P_3 + t_A^{(3,2)}\, P_2 + t_A^{(3,1)}\Big) \\ \quad\quad + t_B^{(3,2)} \exp[ik(\ell_2+\ell_3)]\Big(r_A^{(2)}\, P_2 + t_A^{(2,3)}\, P_3 + t_A^{(2,1)}\Big) \end{cases}. \tag{40}$$

By its turn, $t_C = t_A^{(1,2)} P_2 + t_A^{(1,3)} P_3$, where this time P_2 and P_3 satisfy to

$$\begin{cases} P_2 = r_B^{(2)} \exp[2ik\ell_2]\Big(r_A^{(2)}\, P_2 + t_A^{(2,3)}\, P_3\Big) \\ \quad\quad + t_B^{(2,3)} \exp[ik(\ell_2+\ell_3)]\Big(r_A^{(3)}\, P_3 + t_A^{(3,2)}\, P_2\Big) + \exp[ik\ell_2] t_B^{(2,1)} \\ P_3 = r_B^{(3)} \exp[2ik\ell_3]\Big(r_A^{(3)}\, P_3 + t_A^{(3,2)}\, P_2\Big) \\ \quad\quad + t_B^{(3,2)} \exp[ik(\ell_2+\ell_3)]\Big(r_A^{(2)}\, P_2 + t_A^{(2,3)}\, P_3\Big) + \exp[ik\ell_3] t_B^{(3,1)} \end{cases}. \tag{41}$$

The amplitudes r_D and t_D are obtained from the expression for r_C and t_C by just exchanging the indices $A \leftrightarrow B$.

Finally, if for both graphs of Fig. 6 (d) and (e), the G initial and final points are, respectively, in the edges i and f (so that $-\infty < x_i < 0$ and $0 < x_f < +\infty$), the Green's function is simply

$$G_{fi}(x_f, x_i; k) = \frac{\mu}{i\hbar^2 k} T_{if} \exp[ik(x_f - x_i)]. \tag{42}$$

The coefficient T_{if} is then given by $T_{if} = t_O^{(i,1)}\, P_1 + t_O^{(i,2)}\, P_2$.

For the case of Fig. 6 (d), P_1 and P_2 are obtained from the following

$$\left\{\begin{array}{l} P_1 = r_A^{(1)}\exp[2ik\ell_1]\Big(r_O^{(1)}P_1 + t_O^{(1,2)}P_2\Big) + \exp[ik\ell_1]\Big(t_A^{(1,3)}P_3 + t_A^{(1,f)}\Big) \\ P_2 = r_B^{(2)}\exp[2ik\ell_2]\Big(r_O^{(2)}P_2 + t_O^{(2,1)}P_1\Big) \\ \quad + t_B^{(2,3)}\exp[ik(\ell_2+\ell_3)]\Big(r_A^{(3)}P_3 + t_A^{(3,f)}\Big) \\ \quad + t_B^{(2,3)}t_A^{(3,1)}\exp[ik(\ell_1+\ell_2+\ell_3)]\Big(r_O^{(1)}P_1 + t_O^{(1,2)}P_2\Big) \\ P_3 = r_B^{(3)}\exp[2ik\ell_3]\Big(r_A^{(3)}P_3 + t_A^{(3,f)}\Big) \\ \quad + t_B^{(3,2)}\exp[ik(\ell_2+\ell_3)]\Big(r_O^{(2)}P_2 + t_O^{(2,1)}P_1\Big) \\ \quad + r_B^{(3)}t_A^{(3,1)}\exp[ik(\ell_1+2\ell_3)]\Big(r_O^{(1)}P_1 + t_O^{(1,2)}P_2\Big), \end{array}\right. \tag{43}$$

with P_3 an auxiliary family of infinite trajectories, introduced just to help in the recursive definitions of P_1 and P_2 (see Fig. 6 (d)). The solution of the above system put into the expression for T_{if} yields the final exact Green's function.

For G_{if} for the graph of Fig. 6 (e) we can use the above same set of equations if we treat the region comprising vertices A and C of Fig. 6 (e) as a single effective vertex, corresponding to A in Fig. 6 (d). Therefore, by using the previous analysis, we find that we need only to make the following substitutions in the Green's function expression for the graph of Fig. 6 (d):

$$\begin{aligned} r_A^{(1)} &\to r_A^{(1)} + t_A^{(1,4)}\,r_C^{(4)}\,t_A^{(4,1)}\exp[2ik\ell_4]/g, \\ t_A^{(1,f)} &\to t_A^{(1,4)}\,t_C^{(4,f)}\exp[ik\ell_4]/g, \\ t_A^{(1,3)} &\to t_A^{(1,4)}\,t_C^{(4,3)}\exp[ik\ell_4]/g, \\ r_A^{(3)} &\to r_C^{(3)} + t_C^{(3,4)}\,r_A^{(4)}\,t_C^{(4,3)}\exp[2ik\ell_4]/g, \\ t_A^{(3,f)} &\to t_C^{(3,f)} + t_C^{(3,4)}\,r_A^{(4)}t_C^{(4,f)}\exp[2ik\ell_4]/g, \\ t_A^{(3,1)} &\to t_C^{(3,4)}\,t_A^{(4,1)}\exp[ik\ell_4]/g, \end{aligned}$$

where $g = 1 - r_A^{(4)}\,r_C^{(4)}\exp[2ik\ell_4]$.

5. Eigenstates and scattering states in quantum graphs

From the previous Sec. we have seen that different techniques enable one to obtain G in a relatively straightforward manner. On the other hand, we also have mentioned that the calculation of the wave function in certain contexts may be lengthy. Hence, the natural question is how easily one can extract from G the system eigenvalues, eigenstates and scattering states, allowing to bypass the more traditional approach of directly solving the Schrödinger equation. In the following we give some examples along this line. For definiteness, we concentrate on the graph of Fig. 6(a).

5.1. Eigenstates

The explicit expression for the Green's function with $-\infty < x_i < 0$ in lead i and $0 < x_f < +\infty$ in lead f is (Fig. 6(a))

$$\begin{aligned} G_{if}(x_f, x_i; k) &= \frac{\mu}{i\hbar^2 k}\,T_{if}\,\exp[ik(x_f - x_i)], \\ T_{if} &= t_O^{(i,f)} + \frac{t_O^{(i,1)}\,r_A^{(1)}\,t_O^{(1,f)}\exp[2ik\ell_1]}{1 - r_O^{(1)}\,r_A^{(1)}\exp[2ik\ell_1]}. \end{aligned} \tag{44}$$

For both x_i and x_f ($0 < x_i, x_f < \ell_1$, $x_f > x_i$) in the edge 1, we get

$$\begin{aligned} G_{11}(x_f, x_i; k) = \frac{\mu}{i\hbar^2 k}&\frac{1}{\Big(1 - r_O^{(1)}\,r_A^{(1)}\exp[2ik\ell_1]\Big)} \\ &\times\Big(\exp[-ikx_i] + r_O^{(1)}\exp[ikx_i]\Big) \\ &\times\Big(\exp[ikx_f] + r_A^{(1)}\exp[2ik\ell_1]\exp[-ikx_f]\Big), \end{aligned} \tag{45}$$

For open graphs, like that in Fig. 6 (a), depending on the characteristics of the vertices, the system may support bound states[8]. In these cases, the eigenstates are calculated from the residues of $G(x_f, x_i; k)$ at the poles $k = k_n$ [135]. Furthermore, the problem eigenenergies are given by $E_n = \hbar^2 k_n^2/(2\mu)$.

By inspecting the above Green's functions, we see that they can diverge (consequently presenting poles [30]) only if $g(k = k_n) = 0$, with

$$g(k) = 1 - r_O^{(1)}(k)\, r_A^{(1)}(k) \exp[2ik\ell_1]. \tag{46}$$

As a concrete example, consider the vertex O being a generalized δ interaction (here attached to $N = 3$ edges, Fig. 6 (a)) of strength γ [30]. Then, the reflection coefficients for the vertex O are given by ($\hbar = \mu = 1$)

$$r_O^{(1)} = r_O^{(i)} = r_O^{(f)} = r_O = \frac{2\gamma - (N-2)ik}{Nik - 2\gamma} = \frac{2\gamma - ik}{3ik - 2\gamma}, \tag{47}$$

and the transmission coefficients by

$$t_O^{(i,1)} = t_O^{(1,i)} = t_O^{(i,f)} = t_O^{(f,i)} = t_O = \frac{2ik}{Nik - 2\gamma} = \frac{2ik}{3ik - 2\gamma}. \tag{48}$$

For the vertex A, we take the boundary condition $\psi'(A) = \lambda\psi(A)$, which is equivalent to the following reflection coefficient

$$r_A^{(1)} = \frac{ik - \lambda}{ik + \lambda}. \tag{49}$$

It is a well-known fact that any pole of the scattering amplitudes in the upper half of complex k plane along the imaginary axis represents a bounded energy [194]. For example, for the usual (1D) Dirac δ-function with intensity $\gamma < 0$ (attractive δ), the transmission coefficient is $t_\delta = ik/(ik - \gamma)$. In this case, the unique negative energy of the system reads $E_1 = k_1^2/2 = -\gamma^2/2$, where $k_1 = i|\gamma|$ is the only pole of $t_\delta(k)$ [195, 196].

So, for our graph the eigenvalues are obtained from the following transcendental equation (with $\mathrm{Re}[k_n] = 0$ and $\mathrm{Im}[k_n] > 0$)

$$g(k_n) = 1 - \left(\frac{2\gamma - ik_n}{2\gamma - 3ik_n}\right)\left(\frac{\lambda - ik_n}{\lambda + ik_n}\right)\exp[i2k_n\ell_1] = 0. \tag{50}$$

Moreover, using the formula ($g'(k_n) = dg(k)/dk|_{k=k_n}$)

$$\lim_{E\to E_n} \frac{(E - E_n)}{g(k)} = \frac{1}{2}\lim_{k\to k_n} \frac{(k^2 - k_n^2)}{g(k)} = \frac{k_n}{g'(k_n)}, \tag{51}$$

the residues of Eq. (44) are obtained from

$$\begin{aligned}
\psi_n^{(f)}(x_f)\,\psi_n^{(i)^*}(x_i) &= \frac{1}{2}\lim_{k\to k_n}(k^2 - k_n^2)\, G_{if}(x_f, x_i; k) \\
&= \Big\{\mathcal{N}_l(k_n)\exp[ik_n x_f]\Big\}\Big\{\mathcal{N}_l(k_n)\exp[-ik_n x_i]\Big\}, \\
\mathcal{N}_l(k_n) &= \frac{t_O^{(1)}(k_n)}{\sqrt{ig'(k_n)\, r_O^{(1)}(k_n)}},
\end{aligned} \tag{52}$$

and of Eq. (45) from

$$\begin{aligned}
\psi_n^{(1)}(x_f)\,\psi_n^{(1)^*}(x_i) &= \frac{1}{2}\lim_{k\to k_n}(k^2 - k_n^2)\, G_{11}(x_f, x_i; k) \\
&= \Big\{\mathcal{N}_e(k_n)\Big(\exp[-ik_n x_f] + r_O^{(1)}(k_n)\exp[ik_n x_f]\Big)\Big\} \\
&\quad\times\Big\{\mathcal{N}_e(k_n)\Big(\exp[-ik_n x_i] + r_O^{(1)}(k_n)\exp[ik_n x_i]\Big)\Big\}, \\
\mathcal{N}_e(k_n) &= \frac{1}{\sqrt{ig'(k_n)\, r_O^{(1)}(k_n)}}.
\end{aligned} \tag{53}$$

[8] A trivial textbook example is the usual δ-function potential in 1D. If its strength γ is negative, it may allow bound states.

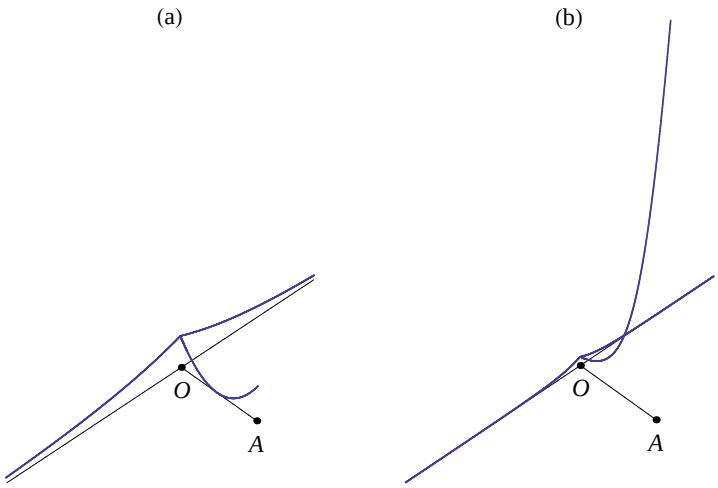

Figure 7: (Color online). The bound eigenstates probability distribution along the quantum graph of Fig. 6 (a), here $\ell_1 = 1.0$. The vertex O is a δ interaction of strength $\gamma = -3.0$. The boundary condition at the vertex A is given by $\psi'(A) = \lambda\psi(A)$, with $\lambda = 2.0$. (a) $|\psi_1(x)|^2$ for which $\kappa_1 = 0.463618$ and (b) $|\psi_2(x)|^2$ for which $\kappa_2 = 2.022448$.

Note that since for the poles $k_n = i\kappa_n$, with $\kappa_n > 0$, the wave functions in both leads have the general form $\psi_n(x) = \mathcal{N}_l \exp[-\kappa_n|x|]$, thus exponentially decaying away from the origin (at the vertex O), as it should be. The $\mathcal{N}$'s also lead to the correct normalization for the eigenstates. Exactly the same results follow from the Schrödinger equation solution.

As a numerical example, consider $\gamma = -3.0$, $\ell_1 = 1.0$ and $\lambda = 2.0$. Then, the system has two bound eigenstates, $n = 1, 2$. In Fig. 7 we show the resulting $|\psi_n(x)|^2$. The first eigenstate, with $\kappa_1 = 0.463618$, is mainly 'created' by the attractive δ potential. The second, with $\kappa_2 = 2.022448$, by the boundary condition at the vertex A. This can verified in Fig. 7: $|\psi_1|^2$ ($|\psi_2|^2$) is more concentrated around the vertex O (A).

5.2. Scattering

Consider again the Green function G_{if}, Eq. (44), for the open graph of Fig. 6 (a). As already discussed, the quantity $|T_{if}|^2$ in the expression for G_{if} can be interpreted as the total probability for a particle of wave number k incident from the lead i to be transmitted to the lead f. Similarly, supposing x_i and x_f in lead i, we have

$$G_{ii}(x_f, x_i; k) = \frac{\mu}{i\hbar^2 k}\Big\{\exp[ik|x_f - x_i|] + R_i \exp[-ik(x_f + x_i)]\Big\},$$
$$R_i = r_O^{(i)} + \frac{t_O^{(i,1)}\, r_A^{(1)}\, t_O^{(1,i)} \exp[2ik\ell_1]}{1 - r_O^{(1)}\, r_A^{(1)} \exp[2ik\ell_1]}. \tag{54}$$

Then, $|R_i|^2$ represents the total probability for a particle of wave number k incident from the lead i to be reflected to the lead i. By choosing different quantum amplitudes for the vertices, we naturally get different scattering patterns from R_i and T_{if}.

Two very common boundary conditions are those resulting from the (already mentioned) generalized δ interaction and the Neumann-Kirchhoff [2, 197]. Regarding the former, it has a very interesting property, however barely explored in the literature. Assume a vertex j linked to N edges as a generalized δ potential. Now, let us set its intensity γ to zero. From Eqs. (47) and (48) we have that $r_j = 2/N - 1$ and $t_j = 2/N$. Although trivial when $N = 2$ (yielding $r_j = 0$ and $t_j = 1$, i.e., the two edges become simply merged without a vertex in the middle), these expressions are exactly the matrix elements of a $N \geq 2$ dimensional Grover gate [67, 198, 199], an essential operator in quantum computation. So, quantum graphs with generalized δ functions of vanishing strengths at the vertices bear a close relation with quantum walks driving by Grover 'coins' [67]. As for the latter boundary condition, suppose that at a vertex j (being the origin of all edges e_{j_s} attached to it) we have $\sum_s \psi'_{e_{j_s}}(0) = \lambda \sum_s \psi_{e_{j_s}}(0)$ (actually, this is the case

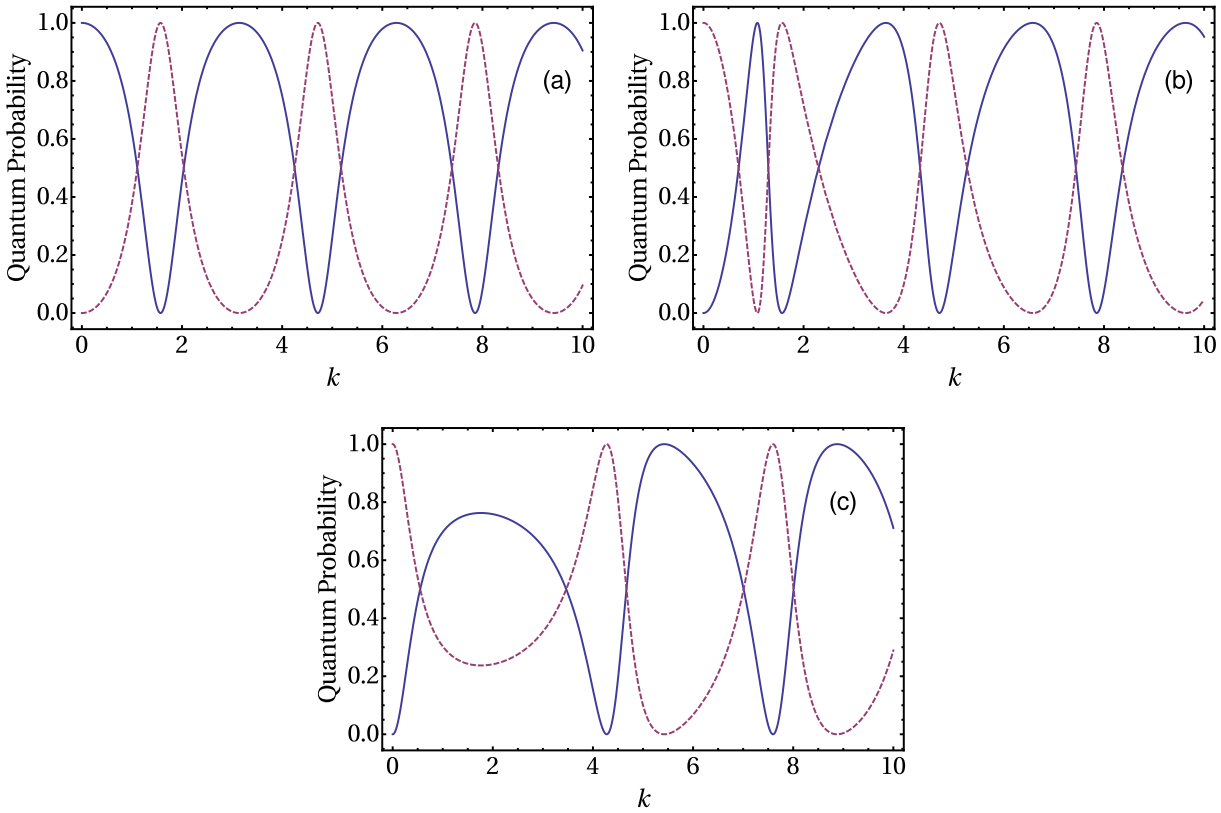

Figure 8: (Color online). The transmission $|T_{if}|^2$ (solid line) and reflection $|R_i|^2$ (dashed) probabilities as function of k for the quantum graph of Fig. 6 (a). In all cases $\ell_1 = 1.0$ and $\lambda = 0.0$ (Neumann-Kirchhoff boundary condition at A). The values of γ at O are: (a) 0.0, (b) 1.0, and (c) -1.5.

assumed for vertex A in the example of Fig. 7). The Neumann-Kirchhoff takes places for $\lambda = 0.0$. One of its curious consequences is that the corresponding reflection and transmission coefficients are k-independent.

To illustrate the graph distinct scattering behavior by assuming vertices with different properties, we consider for our graph (characterized by the parameters $\lambda = 0.0$, so Neumann-Kirchhoff, for A and γ for O) three situations: (a) $\gamma = 0.0$; and generalized δ of strengths (b) $\gamma = 1.0$ and (c) $\gamma = -1.5$. The resulting $|R_i|^2$ and $|T_{if}|^2$ as function of k are shown in Fig. 8, where distinctions in the scattering probabilities are clearly observed. In all cases $\ell_1 = 1.0$.

6. Representative quantum graphs

So far we have discussed the general ideas of how to use the energy domain Green's function method for quantum graphs through the explicit calculation of arbitrary examples. But in the pertinent literature one can find specific topologies which are of particular interest to study different quantum phenomena. For instance, the cases already discussed in Sec. 4, Fig. 6, are indeed proper structures to construct logic gates for quantum information processing [66, 68]. The graph in Fig. 6(b) can act as a phase shifter, whereas that in Fig. 6(e) could functioning as a basis-changing gate.

Other very important examples include:

- The widely analyzed (with the most distinct purposes [71, 200–203], like to investigate scattering features of 3D graphs [204]) hypercube;

- The binary tree [205–207], e.g., useful to highlight differences between classical and quantum walks [208] as well as to test the speed up gain – which is actually exponential – in searching algorithms based on quantum

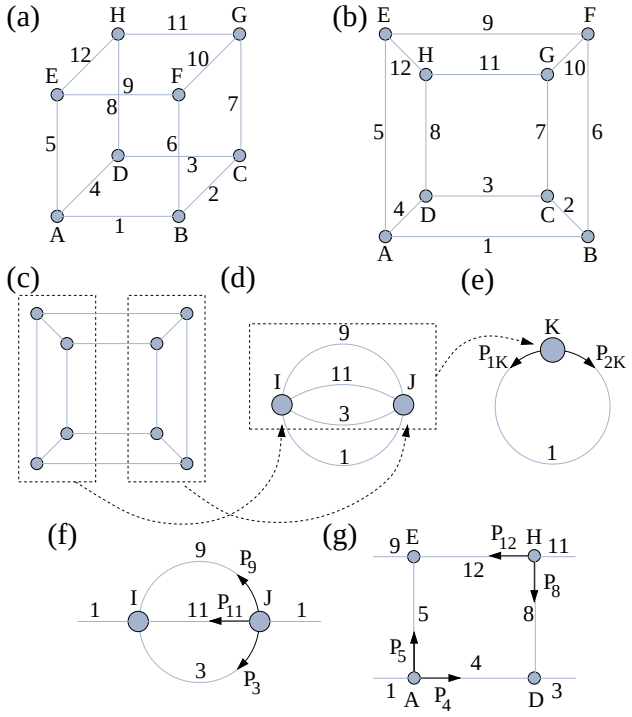

Figure 9: (Color online). A cube quantum graph. (a) The letters represent the vertices indices and the integers the edges indices. (b) A cube graph planar representation. (c)-(e) Regrouping procedures (see the main text). (f) Auxiliary graphs to determine the total R and T. (g) The inner structure of vertex I. The P_l's indicate the sp families.

dynamics [209] (here we should observe that the graph of Fig. 5(a) is in fact an extension of a binary tree, being a fragment of a large-scale ternary tree network [210]);

- Triangular Sierpiński-like structures [211], a nice illustration of graphs which in the limit of infinite vertices would be fractal. It has been considered in connection with molecular assembling [212] and with the mathematics of logical games like the Hanoi tower [213, 214].

Given the relevance of the above mentioned three graph systems, in the present section we shall address in details how to calculate the exact Green's function for each one of these problems.

6.1. Cube

The Green's function for closed quantum graphs can be obtained by a regrouping procedure discussed in the previous sections. We will exemplify applying this procedure to get the Green's function to the cube quantum graph in Fig. 9(a), with edges of length ℓ. In the Fig. 9(b) we show a planar representation of cube graph. Consider the case where the initial and final position are in the edge 1. Our first step to simplify the problem´s solution is to face the two regions marked by dashed line in Fig. 9(c) as two vertices I and J, see Fig. 9(d). The following step is to represent these two vertices as a single vertex K, with one R and T coefficients. All the information of internal structure of graph will be contained in these coefficients. Thus, we reduce the original graph in a simple circular graph. Considering Fig. 9(e), with x_i and $x_f (> x_i)$, the Green's function can be written as,

$$G_{11}(x_f, x_i; k) = \frac{\mu}{i\hbar^2 k}\frac{1}{g}\Big\{\exp[ik(x_f - x_i)] + \exp[ikx_i](RP_{1K} + TP_{2K}) + \exp[ik(\ell - x_i)](RP_{2K} + TP_{1K})\Big\}, \tag{55}$$

with P_{1K} and P_{2K} given by

$$\begin{cases} P_{1K} = \exp[ikx_f] + \exp[ik\ell](R\,P_{2K} + T\,P_{1K}) \\ P_{2K} = \exp[ik(\ell - x_f)] + \exp[ik\ell](R\,P_{1K} + T\,P_{2K}). \end{cases} \tag{56}$$

Solving the above system, the Green's function (55) reads

$$\begin{aligned} G_{11}(x_f, x_i; k) = \frac{\mu}{i\hbar^2 k}\frac{1}{g}\Big\{&\Big(1 - T\exp[ik\ell]\Big)\exp[ik(x_f - x_i)] \\ &+ R\Big(\exp[ik(x_f - x_i)] + \exp[ik(2\ell - x_f - x_i)]\Big) \\ &+ \Big(T + (R^2 - T^2)\exp[ik\ell]\Big)\exp[ik(\ell - x_f + x_i)]\Big\}, \end{aligned} \tag{57}$$

with $g = (1 - T\exp[ik\ell])^2 - R^2\exp[2ik\ell]$.

We need to determine the coefficients R and T. We do so with help of auxiliary quantum graph in Fig. 9(f). We first recall that the $T(R)$ represents the paths contribution for the particle to go from edge 1 to edge 1 by transmission (reflection). Inspecting figure 9(f), we see that:

$$\begin{aligned} T = &\, t_I^{(1,3)}\exp[ik\ell](r_J^{(3)}P_3 + t_J^{(3,9)}P_9 + t_J^{(3,11)}P_{11} + t_J^{(3,1)}) \\ &+ t_I^{(1,9)}\exp[ik\ell](r_J^{(9)}P_9 + t_J^{(9,3)}P_3 + t_J^{(9,11)}P_{11} + t_J^{(9,1)}) \\ &+ t_I^{(1,11)}\exp[ik\ell](r_J^{(11)}P_{11} + t_J^{(11,3)}P_3 + t_J^{(11,3)}P_{11} + t_J^{(11,1)}), \end{aligned} \tag{58}$$

where the P's are

$$\begin{cases} P_3 = r_I^{(3)}\exp[2ik\ell]\Big(r_J^{(3)}P_3 + t_J^{(3,9)}P_9 + t_J^{(3,11)}P_{11} + t_J^{(3,1)}\Big) \\ \quad + t_I^{(3,9)}\exp[2ik\ell]\Big(r_J^{(9)}P_9 + t_J^{(9,3)}P_3 + t_J^{(9,11)}P_{11} + t_J^{(9,1)}\Big) \\ \quad + t_I^{(3,11)}\exp[2ik\ell]\Big(r_J^{(11)}P_{11} + t_J^{(11,3)}P_3 + t_J^{(11,9)}P_9 + t_J^{(11,1)}\Big) \\ P_9 = r_I^{(9)}\exp[2ik\ell]\Big(r_J^{(9)}P_9 + t_J^{(9,3)}P_3 + t_J^{(9,11)}P_{11} + t_J^{(9,1)}\Big) \\ \quad + t_I^{(9,3)}\exp[2ik\ell]\Big(r_J^{(3)}P_3 + t_J^{(3,9)}P_9 + t_J^{(3,11)}P_{11} + t_J^{(3,1)}\Big) \\ \quad + t_I^{(9,11)}\exp[2ik\ell]\Big(r_J^{(11)}P_{11} + t_J^{(11,3)}P_3 + t_J^{(11,9)}P_9 + t_J^{(11,1)}\Big) \\ P_{11} = r_I^{(11)}\exp[2ik\ell]\Big(r_J^{(11)}P_{11} + t_J^{(11,3)}P_3 + t_J^{(11,9)}P_9 + t_J^{(11,1)}\Big) \\ \quad + t_I^{(11,3)}\exp[2ik\ell]\Big(r_J^{(3)}P_3 + t_J^{(3,9)}P_9 + t_J^{(3,11)}P_{11} + t_J^{(3,1)}\Big) \\ \quad + t_I^{(11,9)}\exp[2ik\ell]\Big(r_J^{(9)}P_9 + t_J^{(9,3)}P_3 + t_J^{(9,11)}P_{11} + t_J^{(9,1)}\Big). \end{cases} \tag{59}$$

And for R,

$$R = r_I^{(1)} + t_I^{(1,3)}P_3 + t_I^{(1,9)}P_9 + t_I^{(1,11)}P_{11}, \tag{60}$$

where the P's are the same that to T with the exchanges of indices $I \leftrightarrow J$.

The final step is to determine the coefficients $r_{I(J)}$ and $t_{I(J)}$ in terms of fundamental vertex coefficients. Because the symmetry of cube the I and J vertex coefficients have the same solution, so we just discuss the I vertex solution. Looking at equations in (59) we can think there are many quantum coefficients to calculated, but in the fact it is not true. Because of the symmetry of inner structure of I vertex only three coefficients need to be calculated, $r_I^{(1)}$, $t_I^{(1,3)}$ and $t_I^{(1,11)}$, see Fig. 9(g). From Fig. 9(g), we can write $r_I^{(1)} = r_A^{(1)} + t_A^{(1,4)}P_4 + t_A^{(1,5)}P_5$, where

$$\begin{cases} P_4 = r_D^{(4)}\exp[2ik\ell]\Big(r_A^{(4)}P_4 + t_A^{(4,5)}P_5 + t_A^{(4,1)}\Big) \\ \quad + t_D^{(4,8)}\exp[2ik\ell]\Big(r_H^{(8)}P_8 + t_H^{(8,12)}P_{12}\Big) \\ P_5 = r_E^{(5)}\exp[2ik\ell]\Big(r_A^{(5)}P_5 + t_A^{(5,4)}P_4 + t_A^{(5,1)}\Big) \\ \quad + t_E^{(5,12)}\exp[2ik\ell]\Big(r_H^{(12)}P_{12} + t_H^{(12,8)}P_8\Big) \\ P_8 = t_D^{(8,4)}\exp[2ik\ell]\Big(r_A^{(4)}P_4 + t_A^{(4,5)}P_5 + t_A^{(4,1)}\Big) \\ \quad + r_D^{(8)}\exp[2ik\ell]\Big(r_H^{(8)}P_8 + t_H^{(8,12)}P_{12}\Big) \\ P_{12} = t_E^{(12,5)}\exp[2ik\ell]\Big(r_A^{(5)}P_5 + t_A^{(5,4)}P_4 + t_A^{(5,1)}\Big) \\ \quad + r_E^{(12)}\exp[2ik\ell]\Big(r_H^{(12)}P_{12} + t_H^{(12,8)}P_8\Big). \end{cases} \tag{61}$$

And $t_I^{(1,3)} = \exp[ik\ell]\{t_A^{(1,4)}(r_D^{(4)}P_4 + t_D^{(4,8)}P_8 + t_D^{(4,3)}) + t_A^{(1,5)}(r_e^{(5)}P_5 + t_E^{(5,12)}P_{12})\}$, with the same P's give by the equations (61), with exchanges of indices $A \leftrightarrow B$,$1 \leftrightarrow 3$ and $5 \leftrightarrow 8$. Finally, $t_I^{(1,11)} = t_A^{(1,4)}P_4 + t_A^{(1,5)}P_5$, with again the same P's give by equations (61), with exchange of indices $A \leftrightarrow H$, $1 \leftrightarrow 11$, $4 \leftrightarrow 8$ and $5 \leftrightarrow 12$.

6.1.1. Bound states

Let us examine the Green's function using as boundary condition the already discussed δ interaction in each vertex in the cube graph. To simplify lets use the same intensity γ for the δ in all vertices. Thus, all reflection coefficients are equal to $r = (2\gamma - (N-2)ik)/(Nik - 2\gamma)$ and the transmission coefficients are equal to $t = 2ik/(Nik - 2\gamma)$, with $N = 3$, the number of edges in each vertex. The bounded states are the poles of Green's function, i.e., the roots of $g = 0$. In the Table 1 we show the eigenvalues of the cube quantum graph for two values of γ (also for $\mu = \hbar = 1$).

	γ	
State	0.0	1.0
1	1.230959	1.094322
2	1.919633	1.642395
3	3.141593	2.190764
4	4.372552	3.141593
5	5.052226	3.516328
6	6.283185	5.177393
7	7.514145	6.283185
8	8.193819	7.602957
9	9.424778	8.273085
10	10.65574	9.424778

Table 1: The first ten numerically calculated k_n values (from $g = 0$, see Eq. (57)) for the cube quantum graph. All the vertices are assumed generalized δ interactions of strength $\gamma = 0.0$ (Neumann-Kirchhoff) and $\gamma = 1.0$.

In order to compare the eigenvalues found through the Green's function, we solve the Schrödinger equation to cube quantum graph. On each edge i the component of total wave function Ψ is the solution of one-dimensional Schrödinger equation

$$-\frac{d^2}{dx^2}\psi_i(x) = k^2\psi_i(x), \tag{62}$$

where $k = \sqrt{2\mu E}/\hbar$. The solutions have the form

$$\psi_i(x) = A_i \exp[ikx] + B_i \exp[-ikx], \tag{63}$$

with $i = 1, ..., 12$. The coefficients A_i and B_i are determined by the boundary condition on vertices. Considering all vertices with boundary condition the δ interaction we have $\psi_i(x_n) = \psi_j(x_n) = \psi_n$ ($x = x_n$ is the n vertex coordinate), for all i, j meeting the vertex n, and $\sum_i \psi_i'(x_n) = \gamma\psi_n$. So, using this boundary condition in the cube quantum graph in the Fig. 9 and setting the origin of edges in the vertices A, C, F and H we obtain a system of 24 equations. Solving this system we get the eigenfunctions and eigenvalues. Analyzing the solutions we found four groups of eigenfunctions. In the first group, with quantum numbers $\nu = (1 + 4m)$, $m = 0, 1, 2, ...$,the eigenfunctions are the same in all edges. The second group, with quantum number $\nu = (2 + 4m)$, $m = 0, 1, 2, ...$, have $\psi_1 = \psi_5$, $\psi_2 = \psi_{12}$, $\psi_3 = \psi_8$, $\psi_6 = \psi_9$ and $\psi_7 = \psi_{11}$. The third group, with quantum numbers $\nu = (3 + 4m)$, $m = 0, 1, 2, ...$, have too $\psi_1 = \psi_5$, $\psi_2 = \psi_{12}$, $\psi_3 = \psi_8$, $\psi_6 = \psi_9$ and $\psi_7 = \psi_{11}$, but the eigenfunctions are much more localized in the edges 2 and 12. Finally, the fourth group, with quantum numbers $\nu = (4 + 4m)$, $m = 0, 1, 2, ...$ have $\psi_1 = \psi_3 = \psi_5 = \psi_8$, $\psi_2 = \psi_{12}$, $\psi_6 = \psi_7 = \psi_8 = \psi_{11}$ and the $B_i = -A_i$, showing be sinusoidal eigenfunctions. The eigenvalues obtained are in complete agreement those obtained using the Green's function approach.

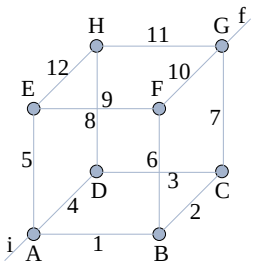

Figure 10: (Color online). The original closed cube quantum graph is attached to two leads (at the vertices A and G), thus becoming an open quantum graph structure.

6.1.2. *Scattering*

We can also calculate the transmission through cube quantum graph. In Fig. 10 we show one cube quantum graph connected to two external leads. The Green's function is given by

$$G_{fi}(x_f, x_i; k) = \frac{\mu}{i\hbar^2 k} T_{if} \exp[ik(x_f + x_i)]. \tag{64}$$

In the Fig. 11 we show the quantum probabilities for the cube quantum graph.

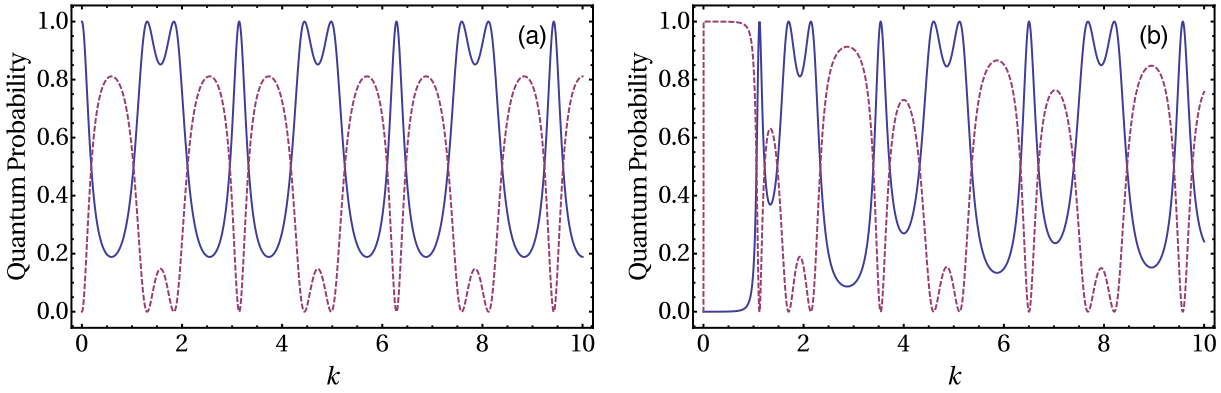

Figure 11: (Color online). The transmission $|T_{if}|^2$ (solid line) and reflection $|R_i|^2$ (dashed) probabilities for the open cube quantum graph of Fig. 10. All the vertices are generalized δ interactions of strength (a) $\gamma = 0.0$ and (b) $\gamma = 1.0$. Here also $\mu = \hbar = 1$.

6.2. *Binary tree*

The fact we can write the Green's function in terms of the general r and t coefficients allows one to use a recursive procedure to obtain the solution to more complicated graphs. The binary tree quantum graph in Fig. 12(c) is a good example of this. To show this let us first calculate the transmission and reflection coefficients for the simple graph in the Fig. 12(a). In fact, this was already done when calculate the $r_I^{(1)}$ and $t_I^{(1,11)}$ for the cube quantum graph. So, by grouping the four vertices A, B, C e D in a single vertex α the reflection coefficient R_α is given by

$$R_\alpha = r_A^{(i)} + t_A^{(i,1)} P_1 + t_A^{(i,2)} P_2 \tag{65}$$

where

$$\begin{cases} P_1 = r_B^{(1)} \exp[2ik\ell]\left(r_A^{(1)}P_1 + t_A^{(1,2)}P_2 + t_A^{(1,i)}\right) \\ \quad + t_B^{(1,3)} \exp[2ik\ell]\left(r_D^{(3)}P_3 + t_D^{(3,4)}P_4\right) \\ P_2 = r_C^{(2)} \exp[2ik\ell]\left(r_A^{(2)}P_2 + t_A^{(2,1)}P_1 + t_A^{(2,i)}\right) \\ \quad + t_C^{(2,4)} \exp[2ik\ell]\left(r_D^{(4)}P_4 + t_D^{(4,3)}P_3\right) \\ P_3 = t_B^{(3,1)} \exp[2ik\ell]\left(r_A^{(1)}P_1 + t_A^{(1,2)}P_2 + t_A^{(1,i)}\right) \\ \quad + r_B^{(3)} \exp[2ik\ell]\left(r_D^{(3)}P_3 + t_D^{(3,4)}P_4\right) \\ P_4 = t_C^{(4,2)} \exp[2ik\ell]\left(r_A^{(2)}P_2 + t_A^{(2,1)}P_1 + t_A^{(2,i)}\right) \\ \quad + r_C^{(4)} \exp[2ik\ell]\left(r_D^{(4)}P_4 + t_D^{(4,3)}P_3\right). \end{cases} \tag{66}$$

And the transmission coefficient, T_α, is

$$T_\alpha = t_A^{(i,1)}P_1 + t_A^{(i,2)}P_2. \tag{67}$$

The relations to determine the T_α coefficient are the same equations those in (66), with the exchange of indices $1 \leftrightarrow 3$, $2 \leftrightarrow 4$, $A \leftrightarrow D$ and $i \leftrightarrow f$. Solving the system (66) we get the expression to R_α and T_α. Now, we insert into vertices B and C another binary graph, like showed in the Fig. 12(a), resulting in the graph in Fig. 12(b). We use the solution of system (66), but now in the place of r_B and r_C we put R_α expression and for the t_B and t_C we put the T_α expression, obtaining the R_β and T_β coefficients. The final step is to insert again a binary graph into central vertices, generating the binary tree graph in Fig. 12(c). Again we use the solution of equation (66), but this time with R_β in the place of r_B and r_C and T_β in the place of t_B and t_C getting the R_γ and T_γ. Finally, we use the solution one more time, with the expression for R_γ in place of r_B and r_C and the expression for T_γ in place of t_B and t_C, obtaining the the R and T coefficients for the binary tree quantum graph of Fig. 12(d). This recursive process can be repeated until we obtain the final G, despite of graph topology.

As an example, consider all edges with the same length $\ell = 1.0$ and Dirac δ interaction with intensity $\gamma = 1.0$ as boundary condition in the vertices. For the vertices with two edges we have $r_B = \gamma/(ik-\gamma)$ and $t_B = ik/(ik-2\gamma)$ and for vertices with three edges $r_A = (2\gamma - ik)/(3ik - 2\gamma)$ and $t_A = 2ik/(3ik-2\gamma)$. In the Fig. 13 we show the transmission probabilities T_α, T_β, T_γ and T. We notice that increasing the complexity of the tree graph also increase the complexity of the transmission coefficients and in general the transmission probability decrease for a same k. This fact is natural once that occur a pronounced increase in a length of path to a particle leave the lead i and arrive the lead f and occur an increase in the number of vertices in the path, increasing the probability of reflection of particle.

6.3. Sierpiński-like graphs

One of the many reasons for the interest of physicists in self-similar lattices is that they can be used as models backbones of different physical systems [212]. In the previous section we already study the tree like quantum graph and the use of recursive procedure to obtain the Green's function. Here we will apply the same recursive procedure to obtain the Green's function to Sierpiński graph. The Sierpiński gasket was considered in [215, 216], where it is discussed the quantum scattering coefficients. However, the most general case of energy dependent quantum coefficients are not discussed and is not presented a schematically way to regroup the contributions of multiple scattering to calculate the Green's function. We fill this gap in the present section. The Sierpiński graph also was studied in terms of its relation to small-worlds networks in [217].

The Sierpiński graphs come from the Sierpiński gasket, the well-known fractal object introduced by Sierpiński in 1915 [213], and they can be recursively constructed from a basic building block. In the Fig. 14 we show three different stages Sierpiński graphs.

Because the Sierpiński graph of stage-n possesses three semi-infinite leads, the scattering matrix is of order 3, that we write as

$$S^{(n)}(k) = \begin{pmatrix} R_{11}^{(n)}(k) & T_{12}^{(n)}(k) & T_{13}^{(n)}(k) \\ T_{21}^{(n)}(k) & R_{22}^{(n)}(k) & T_{23}^{(n)}(k) \\ T_{31}^{(n)}(k) & T_{32}^{(n)}(k) & R_{33}^{(n)}(k) \end{pmatrix}. \tag{68}$$

Here we use a different notations for the quantum amplitudes as follow. Using the triangle symmetry, we can write $R_{ii}^{(n)}(k) = R_k^{(n)}$ for $i = 1, 2, 3$ and $T_{ij}^{(n)}(k) = T_k^{(n)}$ for $i, j = 1, 2, 3$, with $i \neq j$. The Green's function for the transmission

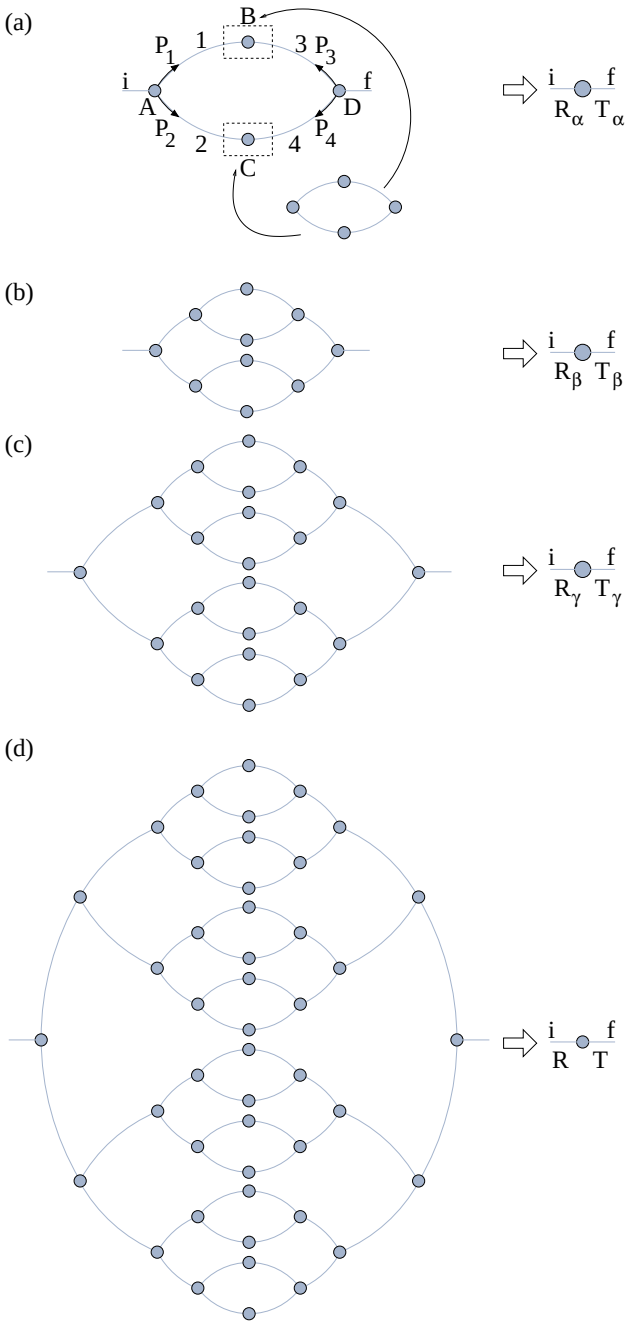

Figure 12: (Color online). Binary tree quantum graphs (attached to leads i and f) with different number of recursive compositions. By regrouping the structure, we end up with a simple graph comprising an unique effective vertex linked to two leads. At each level the rescaled system has the same global transmission T_ξ and reflection R_ξ amplitudes than the corresponding original graph. Here it is shown, (a) the initial basic topology, and (b) one, (c) two, and (d) three, insertions

.

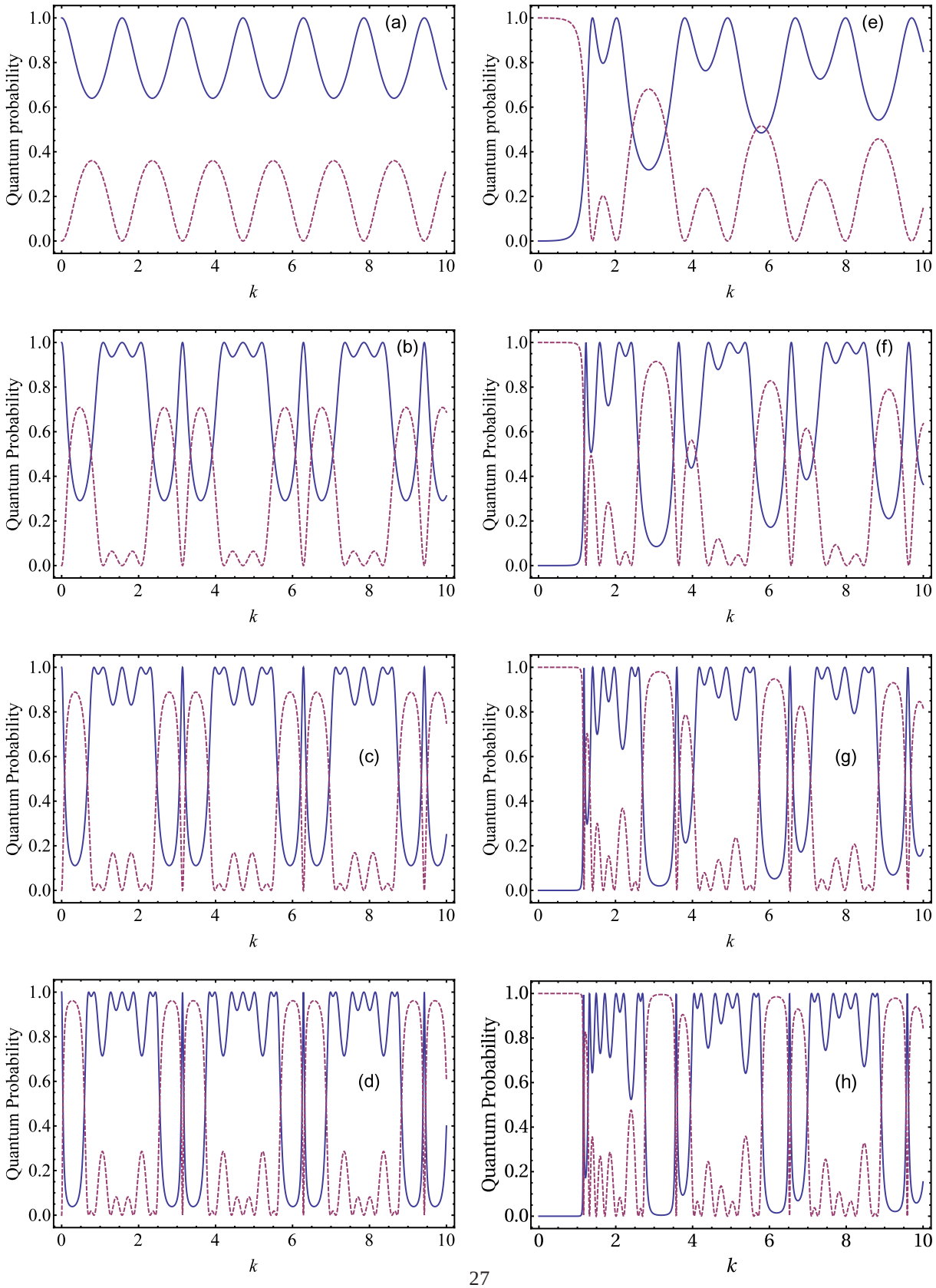

Figure 13: (Color online). The transmission $|T_\xi|^2$ (solid line) and reflection $|R_\xi|^2$ (dashed) probabilities for the binary trees of Fig. 12. All the vertices are generalized δ interactions of strength (a)-(d) $\gamma = 0.0$ and (e)-(h) $\gamma = 1.0$. All the edges have length $\ell = 1.0$. Here also $\mu = \hbar = 1$. The quantum probabilities for the graphs of Fig. 12 (a), (b), (c) and (d) are shown, respectively, in (a) and (e), (b) and (f), (c) and (g) and (d) and (h).

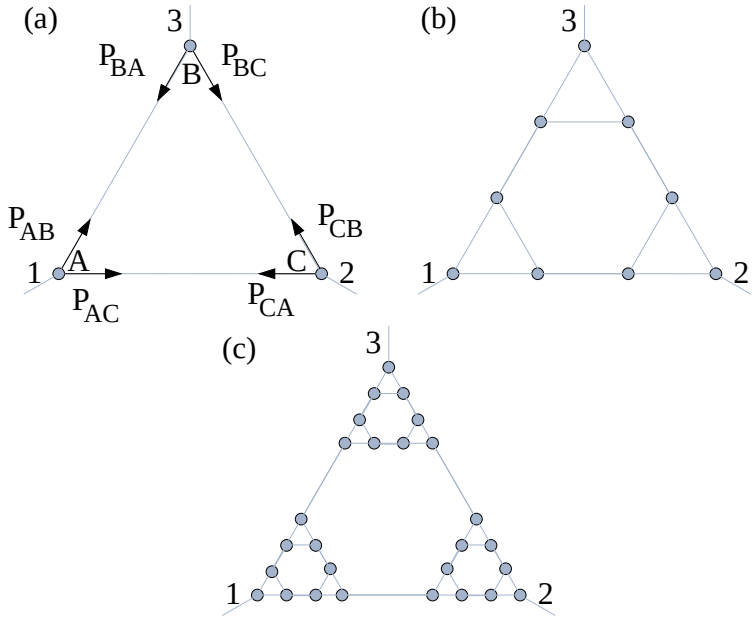

Figure 14: (Color online). Sierpiński-like finite graphs with different number of recursive stages: (a) stage-1 (SG_1), (b) stage-2 (SG_2), and (c) stage-3 (SG_3).

case of the Sierpiński graph is given by

$$G_{ij}(x_f, x_i; k) = \frac{\mu}{i\hbar^2 k} T_k^{(n)} \exp[ik(x_f + x_i)], \tag{69}$$

and

$$G_{ii}(x_f, x_i; k) = \frac{\mu}{i\hbar^2 k}\Big(\exp[ik|x_f - x_i|] + R_k^{(n)} \exp[ik(x_f + x_i)]\Big), \tag{70}$$

for the reflection case. To simplify our analysis, we assume that all the boundary condition at the vertices of graph are the same. For this reason, reflection and transmission coefficients are r_k and t_k (k denotes the energy dependency), respectively, and the width of each edge is ℓ. The quantum coefficients for the stage-1 of Sierpiński graph are obtained by the solution of the following system of equation,

$$\begin{cases} P_{AB} = \exp[ik\ell](r_k P_{BA} + t_k P_{BC}) \\ P_{AC} = \exp[ik\ell](r_k P_{CA} + t_k P_{CB} + t_k) \\ P_{BC} = \exp[ik\ell](r_k P_{CB} + t_k P_{CA} + t_k) \\ P_{BA} = \exp[ik\ell](r_k P_{AB} + t_k P_{AC}) \\ P_{CA} = \exp[ik\ell](r_k P_{AC} + t_k P_{AB}) \\ P_{CB} = \exp[ik\ell](r_k P_{BC} + t_k P_{BA}) \end{cases}, \tag{71}$$

with

$$T_k^{(1)} = t_k(P_{AB} + P_{AC}) \qquad \text{and} \qquad R_k^{(1)} = r_k + t_k(P_{CA} + P_{CB}). \tag{72}$$

Solving the system of equations in (71), we get the transmission and reflection coefficients to the stage-1 of Sierpiński graph, Fig. 14(a),

$$R_k^{(1)} = r_k + \frac{2t_k^2(r_k + (t_k^2 - r_k^2)\exp[ik\ell])\exp[2ik\ell]}{(1 - (r_k + t_k)\exp[ik\ell])(1 + t_k\exp[ik\ell] + (t_k^2 - r_k^2)\exp[2ik\ell])}, \tag{73}$$

and

$$T_k^{(1)} = \frac{t_k^2(1 + (t_k - r_k)\exp[ik\ell])\exp[ik\ell]}{(1 - (r_k + t_k)\exp[ik\ell])(1 + t_k\exp[ik\ell] + (t_k^2 - r_k^2)\exp[2ik\ell])}. \tag{74}$$

Given its recursive structure, the scattering coefficients to stage-n+1 are recursively obtained through the scattering coefficients of stage-n. We define

$$D_k^{(n)} = (1 - (R_k^{(n)} + T_k^{(n)}) \exp[ik\ell])(1 + T_k^{(n)} \exp[ik\ell] + ([T_k^{(n)}]^2 - [R_k^{(n)}]^2) \exp[2ik\ell]), \tag{75}$$

so

$$R_k^{(n+1)} = R_{k/3}^{(n)} + \frac{2[T_{k/3}^{(n)}]^2 (R_{k/3}^{(n)} + ([T_{k/3}^{(n)}]^2 - [R_{k/3}^{(n)}]^2) \exp[ik\ell/3]) \exp[2ik\ell/3]}{D_{k/3}^{(n)}}, \tag{76}$$

and

$$T_k^{(n+1)} = \frac{[T_{k/3}^{(n)}]^2 (1 + (T_{k/3}^{(n)} - R_{k/3}^{(n)}) \exp[ik\ell/3]) \exp[ik\ell/3]}{D_{k/3}^{(n)}}, \tag{77}$$

where we take a division by 3 of width of edge in each new stage of Sierpiński graph. In this way, using the expressions in (76) and (77), together with $R_k^{(1)}$ and $T_k^{(1)}$ in (73) and (74), we can get the scattering coefficients of Sierpiński graph of stage-n with general point interaction in each vertex.

Using the width of edge to stage-1 as $\ell = 1.0$ and a delta type point interaction with intensity $\gamma = 0.0$ and $\gamma = 1.0$ at each vertex, in the Fig. 15 and Fig. 16, respectively, we show the behavior of reflection and transmission coefficient, respectively, to the Sierpiński graph up to stage-5. We can note that at each stage for the Sierpiński graph the structure of quantum coefficients became more selective to what energies (k) can be transmitted. Also, this behavior is different of that one observed in the tree graph, Fig. 13, where we have an increase of the reflection amplitude, but without so much change in the original form. Here, at each new stage, the quantum coefficients have a change in its behavior as function of k in a very pronounced way.

7. Quasi-bound states in quantum graphs

As a last application for the Green's function approach reviewed in the previous sections, we shall consider a context not usually addressed for quantum graphs, namely, quasi-bound states (but see [183]). For a general treatment for such problems using G – however not discussing quantum graphs – we mention [218].

A quasi-bound state occurs when a particle move inside a system for a considerable period of time, leaving it when a fairly long time interval τ has elapsed [219], where τ is called lifetime of the quasi-bound state. The concept of quasi-bound states is a fundamental one, and has been applied in all areas of physics. They have been used to calculate tunneling ionization rates [220], to understand the phenomenon of diffraction in time [221], to describe the decay of cold atoms in quasi-one-dimensional traps [222], and are directly relevant to recent condensed-matter experiments [223].

Thus, let us begin our discussion considering the linear quantum graph depicted in Fig. 17. Suppose initially that we have a boundary condition with zero transmission amplitude in both vertices A and B. For instance, consider a Dirichlet boundary condition. This system is equivalent to an infinite square well, so it is possible for a particle to be trapped inside the graph in the edge between the vertices A and B, i.e., the system would have genuine bound states, with well definite energy

$$E = \frac{n^2\pi^2\hbar^2}{2\mu\ell_{AB}^2}. \tag{78}$$

They are genuine bound states in the sense that are eigenstates of the Hamiltonian with an infinite lifetime. From the Heisenberg uncertainty principle, $\Delta E \Delta t \approx \hbar$, so, if the energy possesses null uncertainty, the state's life time is infinity [224].

In the situation of a arbitrary boundary condition with non-zero transmission amplitude in both vertices the particle can be trapped, but it can not be trapped forever, as a consequence of quantum tunneling. The energy spectrum in this case will be quasi-discrete, and it consists of a series of broadened levels, whose width is represented by $\Gamma = \hbar/\tau$ [225], and the energy values are called quasi-energies. The situation become very interesting when we analyze the scattering of particles when the incident energy is close to the quasi-energy

$$E^{(\mathrm{inc})} \approx E^{(\mathrm{qb})}. \tag{79}$$

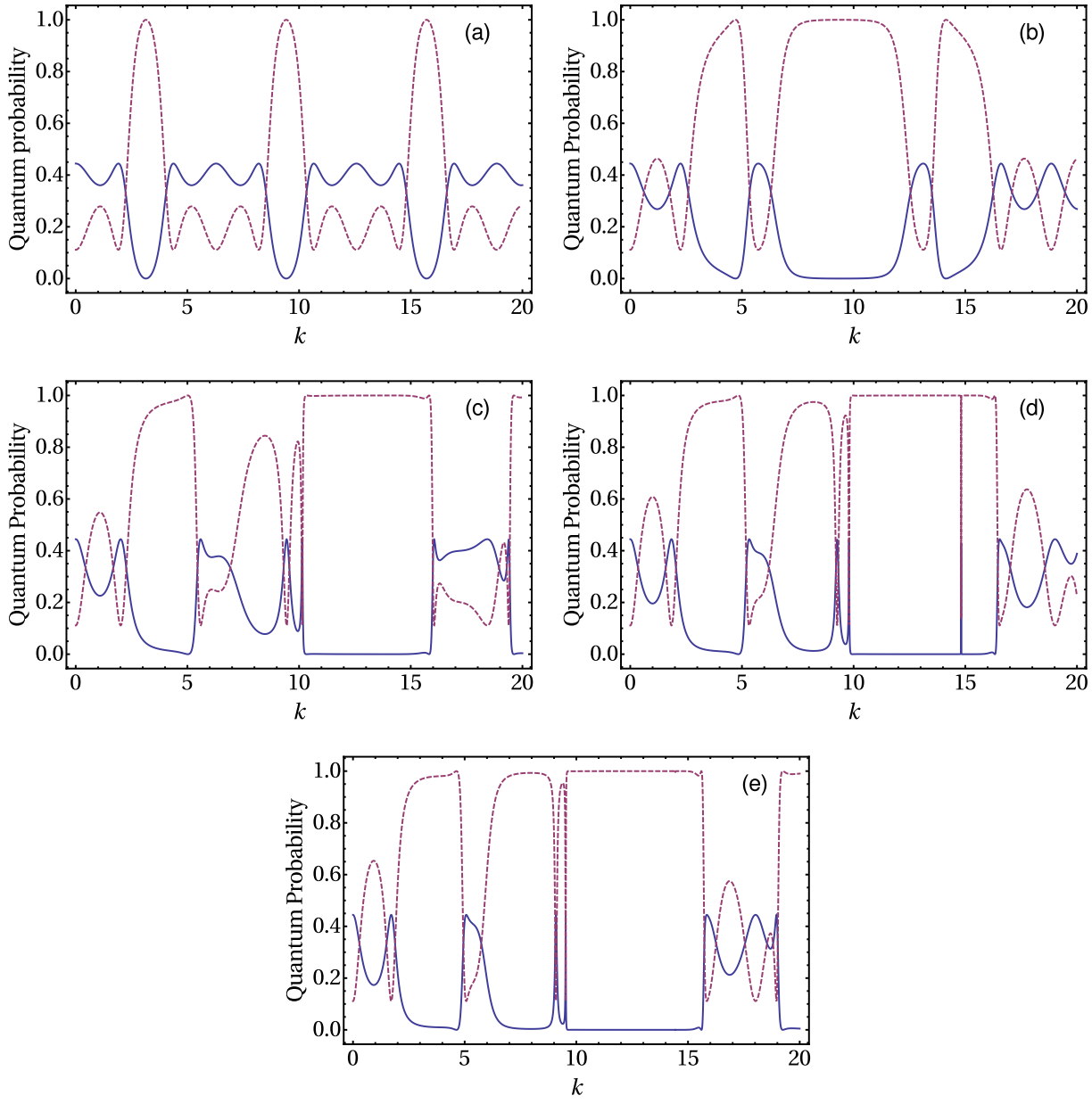

Figure 15: (Color online). The transmission $|T_n|^2$ (solid line) and reflection $|R_n|^2$ (dashed) probabilities for the stage-n of the Sierpiński graph, Fig. 14. All the edges have $\ell = 1.0$ and $\mu = \hbar = 1$. At any edge we have a δ interaction of strength $\gamma = 0.0$. The cases $n = 1$, $n = 2$, $n = 3$, $n = 4$, and $n = 5$, are displayed, respectively, in (a), (b), (c), (d) and (e).

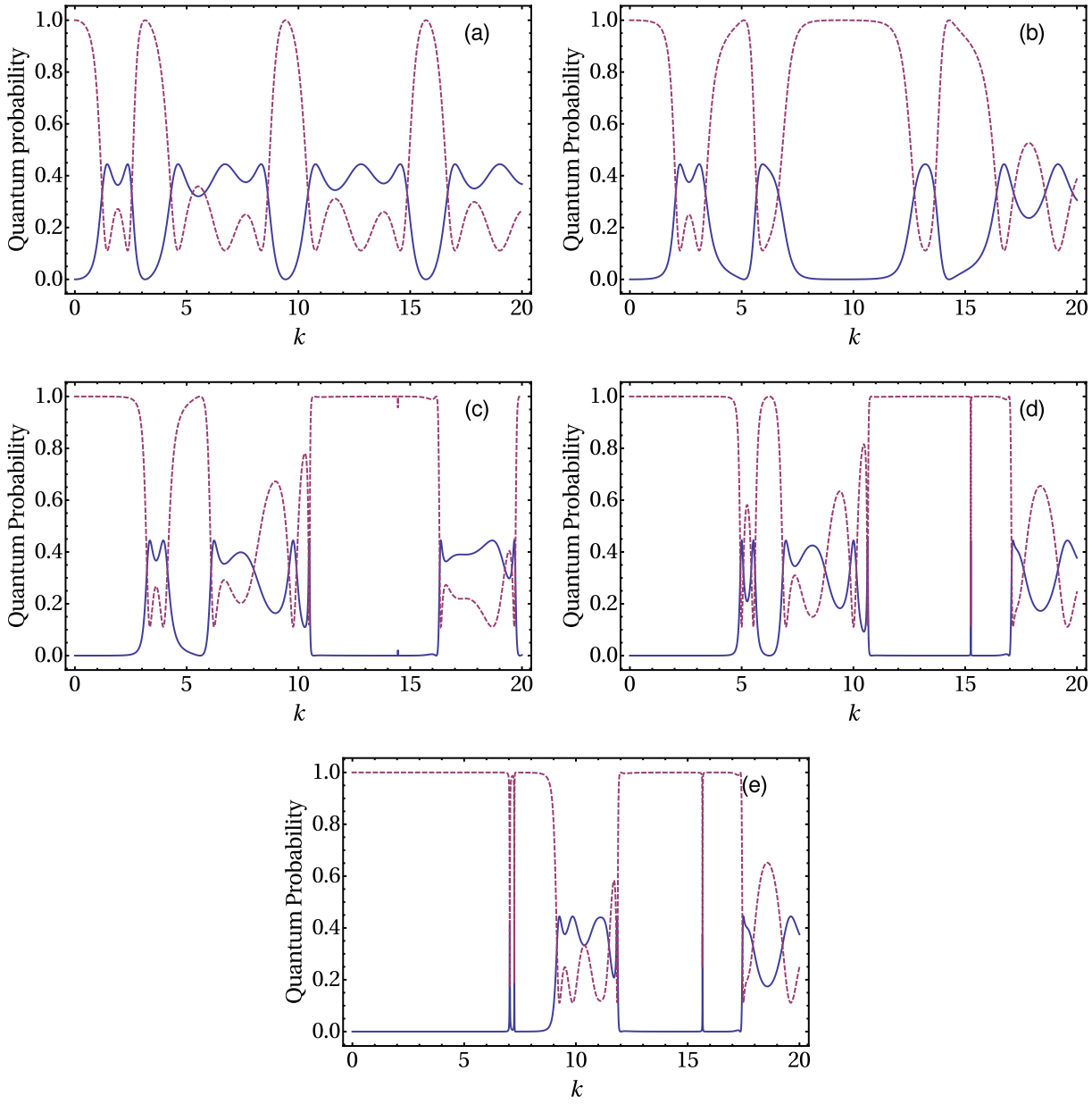

Figure 16: (Color online). The same as in Fig. 15, but for the vertices being δ interaction of strength $\gamma = 1.0$.

Figure 17: (Color online). An open quantum graph with two vertices, one edge and two leads (similar to that studied in Sec. 4.1).

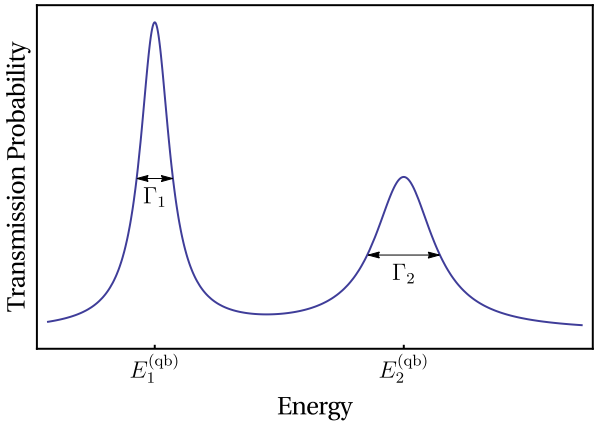

Figure 18: (Color online). Typical profile of the transmission probability as function of energy for a potential displaying two quasi-bound states at energies $E_1^{(qb)}$ and $E_2^{(qb)}$. The quasi-bound states widths, Γ_1 and Γ_2, can usually be obtained from such a plot.

In this energy interval, the square module of transmission amplitude exhibits pronounced peaks, and this is called resonant scattering [224]. This behavior was already observed in the previous sections, and in Fig. 18 it is depicted the typical transmission probability as a function of the incident energy for a scattering of a system which supports quasi-bound states. The width of this quasi-bound states Γ is defined as half height width of peak of the transmission coefficient, as depicted in Fig. 18.

Now, let us consider an intermediate situation where the vertex B has a boundary condition with zero transmission amplitude and an arbitrary boundary condition with a non-zero transmission amplitude in the vertex A. In this situation, the system can also has quasi-bound states, due the tunneling through the vertex A. The scattering solution for a particle incident from the left is given by

$$\psi(x) \approx \frac{1}{\sqrt{2\pi}} \left\{ \exp\left[ikx\right] + R_{AB}^{(+)} \exp\left[-ikx\right] \right\}, \qquad x \to -\infty. \tag{80}$$

where $R_{AB}^{(+)}$ is the reflection amplitude for the whole graph

$$R_{AB}^{(+)} = r_A^{(+)} + \frac{r_B^{(-)} t_A^{(-)} t_A^{(+)} \exp\left[ik\ell_{AB}\right]}{1 - r_A^{(-)} r_B^{(+)} \exp\left[2ik\ell_{AB}\right]}. \tag{81}$$

By analogy with the previous case, we can try to extract the information about quasi-bound states from the square modules of reflection amplitude $\left|R_{AB}^{(+)}\right|^2$. Unfortunately, because the boundary condition in the vertex B, $\left|R_{AB}^{(+)}\right|^2 = 1$ for all range of energies. So, we can not obtain information about quasi-bound states for this situation by the above method. So, we propose a Green's function approach to extract information about quasi-bound states for this kind of situation, as we explain below.

Consider the open quantum graph in Fig. 19. As we explain below, here we use a slightly different notation for the quantum coefficients. Using the simplification procedures of Sec. 4.2 we can get the Green's function straightforwardly. In this manner, the Green's function for the case where $x_i < y_1$ is in the semi-infinity lead i and x_f is in the edge j between the vertices y_j and y_{j+1} is given by

$$G_{ij}(x_f, x_i; k) = \frac{\mu}{i\hbar^2 k} \frac{T_{(1,j)}^{(+)} \exp\left[ik(x_f - x_i + y_j - y_1)\right]}{1 - R_{(1,j)}^{(-)} R_{(j+1,N)}^{(+)} \exp\left[ik(y_{j+1} - y_j)\right]}, \tag{82}$$

where $T_{(1,j)}^{(+)}$ is the transmission coefficient to the left $(+)$ of block $(1, j)$ comprising all vertices between y_1 and y_j, $R_{(1,j)}^{(-)}$ is the reflection coefficient to the right $(-)$ of block $(1, j)$ comprising all the vertices between y_j and y_1 and $R_{(j+1,N)}^{(+)}$ is the reflection coefficient to the left $(+)$ of block $(1, j)$ comprising all the vertices at right of y_{j+1}.

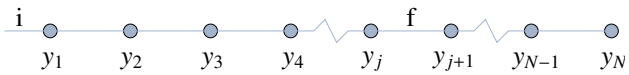

Figure 19: (Color online). A semi-infinite lead attached to a series of N simply connected vertices. This structure allows quasi-bound states.

7.1. Recurrence formulas for the reflection and transmission coefficients

The global reflection and transmission coefficients are obtained recursively in terms of reflection and transmission coefficients of each individual vertex. To understand this construction consider the graph composed only with two vertices at y_l and y_{l+1}, and that both $x_i, x_f < y_l < y_{l+1}$, with x_i and x_f in the same semi-infinity lead i, Fig. 20(a).

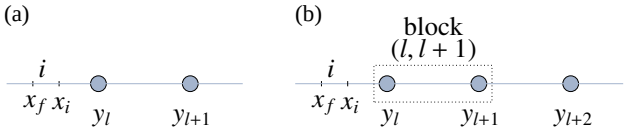

Figure 20: (Color online). (a) Two and (b) three simply connected vertices attached to two semi-infinite leads. In (b) it is exemplified the construction process of block structures.

Performing the sum over all scattering paths, the Green's function to the graph in Fig. 20(a) is given by

$$G_{ii}(x_f, x_i; k) = \frac{\mu}{i\hbar^2 k}\Bigg\{\exp[ik|x_f - x_i|] + r_l^{(+)}\exp[-ik(x_f + x_i - 2y_l)] + \frac{r_{l+1}^{(+)}t_l^{(+)}t_l^{(-)}\exp[2ik(y_{l+1} - y_l)]\exp[-ik(x_f + x_i - 2y_l)]}{1 - r_l^{(-)}r_{l+1}^{(+)}\exp[2ik(y_{l+1} - y_l)]}\Bigg\}. \tag{83}$$

In the above expression a global reflection coefficient to the right of block $(l, l+1)$, $R_{(l,l+1)}^{(-)}$, comprising of two vertices y_l and y_{l+1} as

$$R_{(l,l+1)}^{(+)} = r_l^{(+)} + \frac{r_{l+1}^{(+)}t_l^{(+)}t_l^{(-)}\exp[2ik(y_{l+1} - y_l)]}{1 - r_l^{(-)}r_{l+1}^{(+)}\exp[2ik(y_{l+1} - y_l)]}. \tag{84}$$

In an analogous way, calculating the G for $x_i, x_f > y_l > y_{l+1}$ we can associate a global reflection coefficient at the left of block $(l, l+1)$, $R_{(l,l+1)}^{(-)}$, its is given by

$$R_{(l,l+1)}^{(-)} = r_{l+1}^{(-)} + \frac{r_l^{(-)}t_{l+1}^{(-)}t_{l+n}^{(+)}\exp[2ik(y_{l+1} - y_l)]}{1 - r_l^{(-)}r_{l+1}^{(+)}\exp[2ik(y_{l+1} - y_l)]}. \tag{85}$$

Now, considering the case where $x_i < y_l < y_{l+1} < x_f$, the Green's function is given by

$$G_{i\,l+1}(x_f, x_i; k) = \frac{\mu}{i\hbar^2 k}\frac{t_l^{(+)}t_{l+1}^{(+)}\exp[ik(y_{l+1} - y_l)]}{1 - r_l^{(-)}r_{l+1}^{(+)}\exp[2ik(y_{l+1} - y_l)]}\exp[ik(x_f - x_i - (y_{l+1} - y_l))], \tag{86}$$

and again we can associate a global transmission coefficient at the left of block $(l, l+1)$, $T_{(l,l+1)}^{(+)}$, as

$$T_{(l,l+1)}^{(+)} = \frac{t_l^{(+)}t_{l+1}^{(+)}\exp[ik(y_{l+1} - y_l)]}{1 - r_l^{(-)}r_{l+1}^{(+)}\exp[2ik(y_{l+1} - y_l)]}. \tag{87}$$

And calculating the G for $x_i > y_{l+1} > y_l > x_f$ we get the transmission coefficient at right of block $(l, l+1)$, $T_{(l,l+1)}^{(-)}$, and is given by

$$T_{(l,l+1)}^{(-)} = \frac{t_l^{(-)}t_{l+1}^{(-)}\exp[ik(y_{l+1} - y_l)]}{1 - r_l^{(-)}r_{l+1}^{(+)}\exp[2ik(y_{l+1} - y_l)]}. \tag{88}$$

To get recurrence formulas for the reflection and transmission coefficients, consider a third vertex, in the position y_{l+2}, like the one shown in Fig. 20(b). Let the reflection and transmission coefficients, where $x_i, x_f < y_l < y_{l+1} < y_{l+2}$, be $R^{(\pm)}_{(l,l+1)}$ and $T^{(\pm)}_{(l,l+1)}$ the reflection and transmission coefficients of block $(l, l+1)$, respectively. Again, using the simplification procedures of section 4.2 and by inspection of Eq. (84) we can infer the reflection coefficient for the block $(l, l+2)$ formed by the vertices y_l, y_{l+1} and y_{l+2}, $R^{(+)}_{(l,l+2)}$, as

$$R^{(+)}_{(l,l+2)} = R^{(+)}_{(l,l+1)} + \frac{T^{(+)}_{(l,l+1)} T^{(-)}_{(l,l+1)} r^{(+)}_{l+2} \exp[2ik(y_{l+2} - y_{l+1})]}{1 - R^{(-)}_{(l,l+1)} r^{(+)}_{l+2} \exp[2ik(y_{l+2} - y_{l+1})]}. \tag{89}$$

Based in the above two cases, we can generalize for a block $(l, l+n)$ with $n+1$ vertices. Here we write the final results. So, the reflection coefficient at right of block $(l, l+n)$ is given by

$$R^{(+)}_{(l,l+n)} = R^{(+)}_{(l,l+n-1)} + \frac{T^{(+)}_{(l,l+n-1)} T^{(-)}_{(l,l+n-1)} r^{(+)}_{l+n} \exp[2ik(y_{l+n} - y_{l+n-1})]}{1 - R^{(-)}_{(l,l+n-1)} r^{(+)}_{l+n} \exp[2ik(y_{l+n} - y_{l+n-1})]}. \tag{90}$$

and the reflection coefficient at left of block $(l, l+n)$, $R^{(-)}_{(l,l+1)}$, is given by

$$R^{(-)}_{(l,l+n)} = r^{(-)}_n + \frac{t^{(+)}_n t^{(-)}_n R^{(-)}_{(l,l+n-1)} \exp[2ik(y_{l+n} - y_{l+n-1})]}{1 - R^{(-)}_{(l,l+n-1)} r^{(+)}_{l+n} \exp[2ik(y_n - y_{n-1})]}. \tag{91}$$

In an analogous way the transmission coefficient at left, $T^{(+)}_{(l,l+n)}$, and at right, $T^{(-)}_{(l,l+n)}$, of block $(l, l+n)$ can be obtained, and are given by

$$T^{(+)}_{(l,l+n)} = \frac{T^{(+)}_{(l,l+n-1)} t^{(+)}_{l+n} \exp[ik(y_{l+n} - y_{l+n-1})]}{1 - R^{(-)}_{(l,l+n-1)} r^{(+)}_{l+n} \exp[2ik(y_{l+n} - y_{l+n-1})]} \tag{92}$$

and

$$T^{(-)}_{(l,l+n)} = \frac{T^{(-)}_{(l,l+n)} t^{(-)}_{l+1} \exp[ik(y_{l+n} - y_{l+n-1})]}{1 - R^{(-)}_{(l,l+n-1)} r^{(+)}_{l+n} \exp[2ik(y_{l+n} - y_{l+n-1})]}. \tag{93}$$

7.2. Green's function as a probability amplitude

Once obtained the recurrence formulas for the quantum coefficients, consider again the Green's function in (82). The Green's function for a quantum system could be interpreted as the probability amplitude for a particle initially in the point x_i arrive the point x_f with fixed energy E [181]. So, in Eq. (82), the amplitude

$$\mathcal{A}_{i,j} = \frac{T^{(+)}_{1,j}}{1 - R^{(-)}_{1,j} R^{(+)}_{j+1,N} \exp\left[ik(y_{j+1} - y_j)\right]}, \tag{94}$$

can be interpreted as a probability amplitude for a particle leaving the point x_i in the semi-infinity lead i and arriving at the point x_f in the edge j with energy E. If the graph support at least one quasi-bound state, an incident wave with energy E close to the quasi-bound state energy have a great probability to tunnel, entering in the confinement region. In this way, plotting $|\mathcal{A}_{i,j}|^2$ against E, we have peaks at each time that the energy E was close to $E^{(\mathrm{qb})}$, like in Fig. 18. With this we can extract information about the energy values of quasi-bound states and its respective widths. Here a little technical detail. The amplitude $|\mathcal{A}_{i,j}|^2$ is not normalized, but it is not a problem, because we are interested in the energy and width of each quasi-bound state.

An interesting characteristic of the Green's function approach to study quasi-bound states on graphs is the possibility to calculate directly, localized quasi-bound states in a specific edge. Besides, it is also possible to analyze the influence of different point interactions — implemented through boundary conditions — on the width and the energy of a quasi-bound state. As an example, consider a graph with six vertices like that in the Fig. 21. Let $\mu = \hbar = 1$ and the lengths of edges all equals to $\ell = 1.0$. In each vertex we use delta type interaction with γ, but in the vertex y_6,

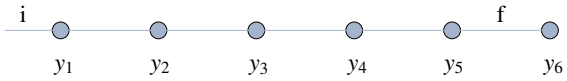

Figure 21: (Color online). The example of Fig. 20 with $N = 6$. In the vertex y_6 we consider both Dirichlet and Neumann boundary conditions.

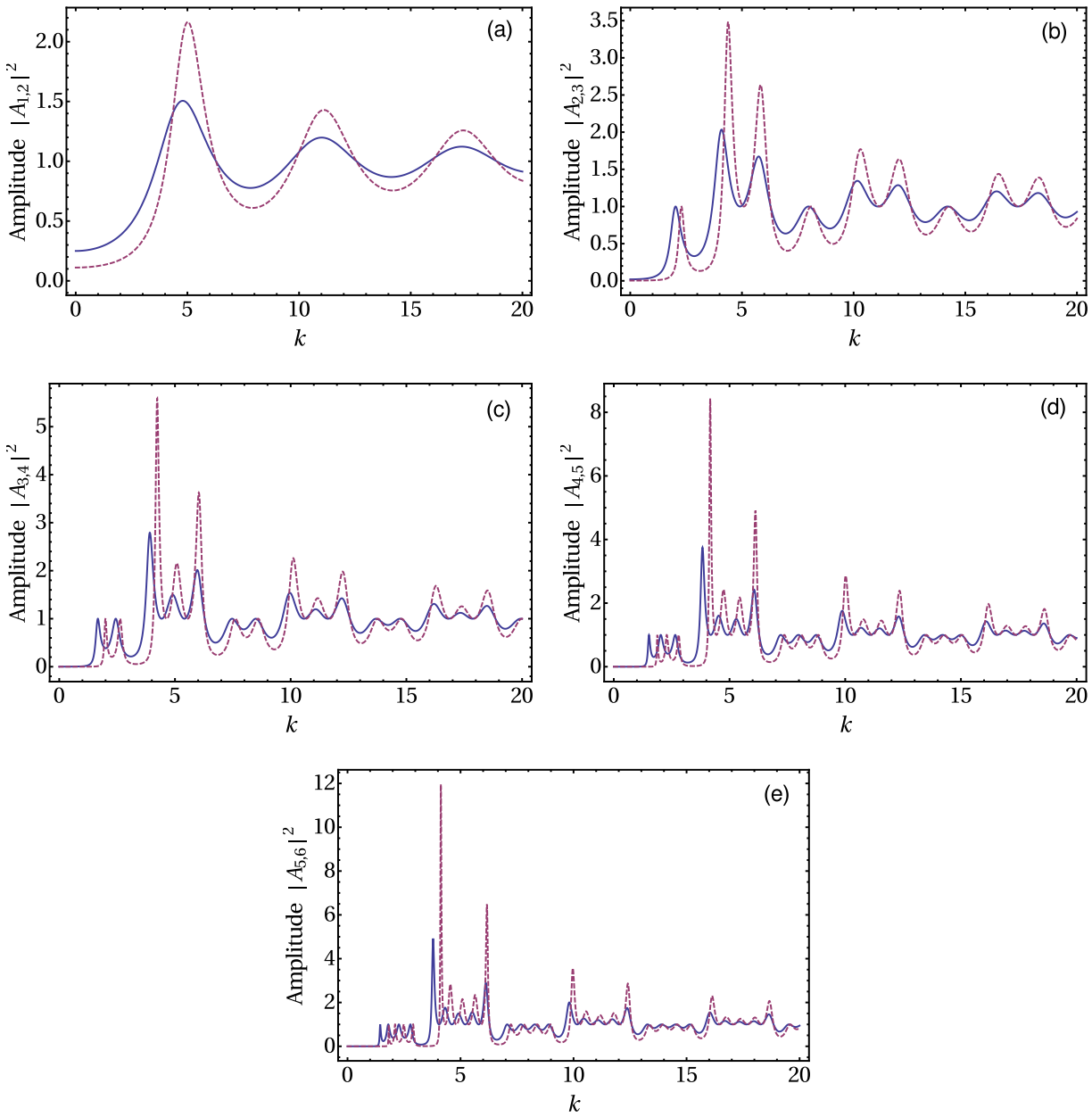

Figure 22: (Color online). Behavior of $\mathcal{A}_{i,j}$ as a function of energy using Dirichlet boundary condition ($r_6 = -1$) at the vertex y_6 of Fig. 21. The amplitudes for the quasi-bound states localized in the edge between the vertices: (a) 1 and 2, (b) 2 and 3, (c) 3 and 4, (d) 4 and 5 and (e) 5 and 6. The solid line is for $\gamma = 1.0$ and the dashed line is for $\gamma = 2.0$.

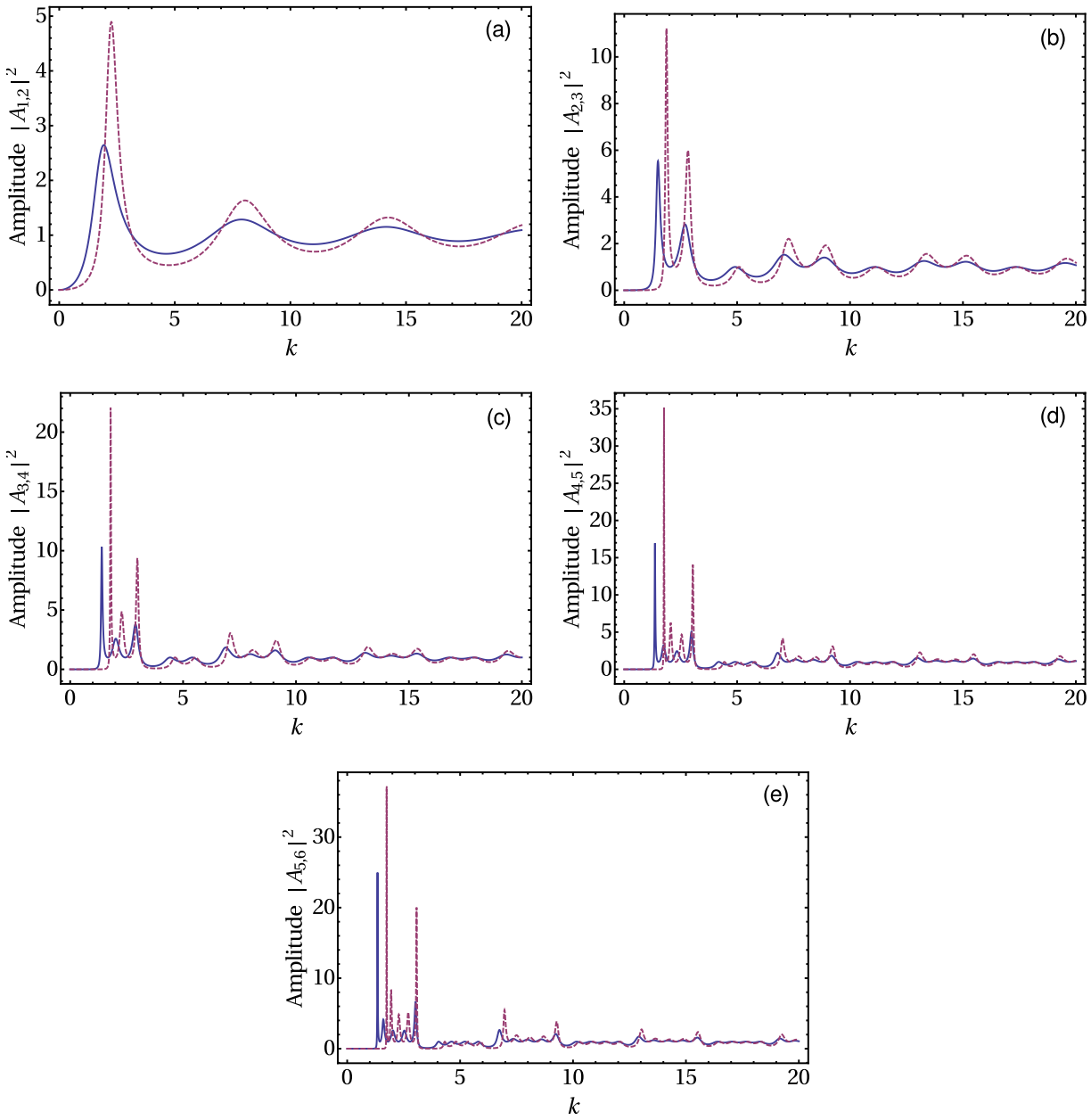

Figure 23: (Color online). Behavior of $\mathcal{A}_{i,j}$ as a function of energy using Neumann boundary condition ($r_6 = 1$) in the vertex y_6 of Fig. 21. The amplitudes for the quasi-bound states localized in the edge between the vertices: (a) 1 and 2, (b) 2 and 3, (c) 3 and 4, (d) 4 and 5 and (e) 5 and 6. The solid line is for $\gamma = 1.0$ and the dashed line is for $\gamma = 2.0$.

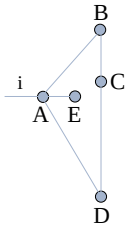

Figure 24: (Color online). Example of an open quantum graph, whose a slight modified version has been studied in [137] to transmit information using quantum protocols.

where we use either Dirichlet, $r_6 = -1.0$ or Neumann, $r_6 = 1.0$, boundary condition. In the Figs. 22 and 23 we show $\mathcal{A}_{i,j}$ for the Dirichlet and Neumann boundary conditions, respectively.

The analysis of figures make it clear the presence of quasi-bound state as a function of energy. Also, it is evident the influence of the boundary condition utilized on the vertex y_6 in the quasi-energies and in the width of quasi-bound state. The quasi-energies of quasi-bound state in the Neumann case have lower energies and widths when compared with the quasi-energies of Dirichlet one. Another observation is the increase in the number of quasi-bound states when the final point x_f is near of vertex y_6. In this later case, escaping the graph become mode difficult because of multiple reflections and interference along its edges. In fact, there is a narrowing the half height width, Γ, and consequently an increase in the lifetime of quasi-state.

7.3. Quasi-bound state in arbitrary graphs

Observing the form of $\mathcal{A}_{i,j}$ in Eq. (94), we can note that the amplitude $\mathcal{A}_{i,j}$ is giving by the quotient of transmission coefficient from the initial point x_i to final point x_f in the numerator and a term what is 1 minus the product of the reflections coefficients at left and at right of edge and of complex exponential of length of edge where is situated the final point x_f in denominator. This term in the denominator are associated with the energy eigenvalues [152, 226], given by the sum of possible periodic orbits in the edge where is the final point [137]. In general, the amplitude to localized quasi-bound state between two vertices I and J of arbitrary graph is given by

$$\mathcal{A}_{I,J} = \frac{T_{I,J}}{1 - R_{I,J}\, R_{J,I}\, \exp[2ik\ell_{I,J}]}, \tag{95}$$

with $T_{I,J}$ is the global transmission coefficient for the particle be transmitted to the edge between the vertices I and J, $R_{I,J}$ is the global reflection coefficient at the vertex I and $R_{J,I}$ is the global reflection coefficient at the vertex J.

As an example of arbitrary graph and the use of Eq. (95), consider the graph in Fig. 24. We can use different boundary conditions in each version and lengths of each edges, but here we use delta type point interactions in each vertex with intensity $\gamma = 1.0$, but in vertex E we use Dirichlet or Neumann boundary condition. All the edges have the same length $\ell = 1.0$. So, with all edges with the same length, due the symmetry, we have three different edges where we can calculate the quasi-bound state between the vertices AE, AB and BC. In the Fig. 25 we show the behavior for the three above cases using the Dirichlet and Neumann condition, respectively. Again, we note the strong influence of boundary condition in vertex E in the widths and quasi-energies. Also, the influence of position of quasi-state is observed. This influence also was observed in this same graph for the transmission coefficient in [137]. As expected, because complexity of graph, in this case the profile is more complicated than those o linear graph shown in the shown previously.

8. Conclusion

The quantum graphs are very interesting because they can modeling waves in a large variety of systems, having applications going from nanotechnology to medicine. They are very simple system, nonetheless, it is not easy to obtain the Green's function for general quantum graphs by means of standard procedures, being necessary for instance to modify the Krein's resolvent formula [138] or by doing some complicated calculations [139]. In this contribution, we have shown a physically motivated construction for the exact Green's function for arbitrary quantum graphs of any

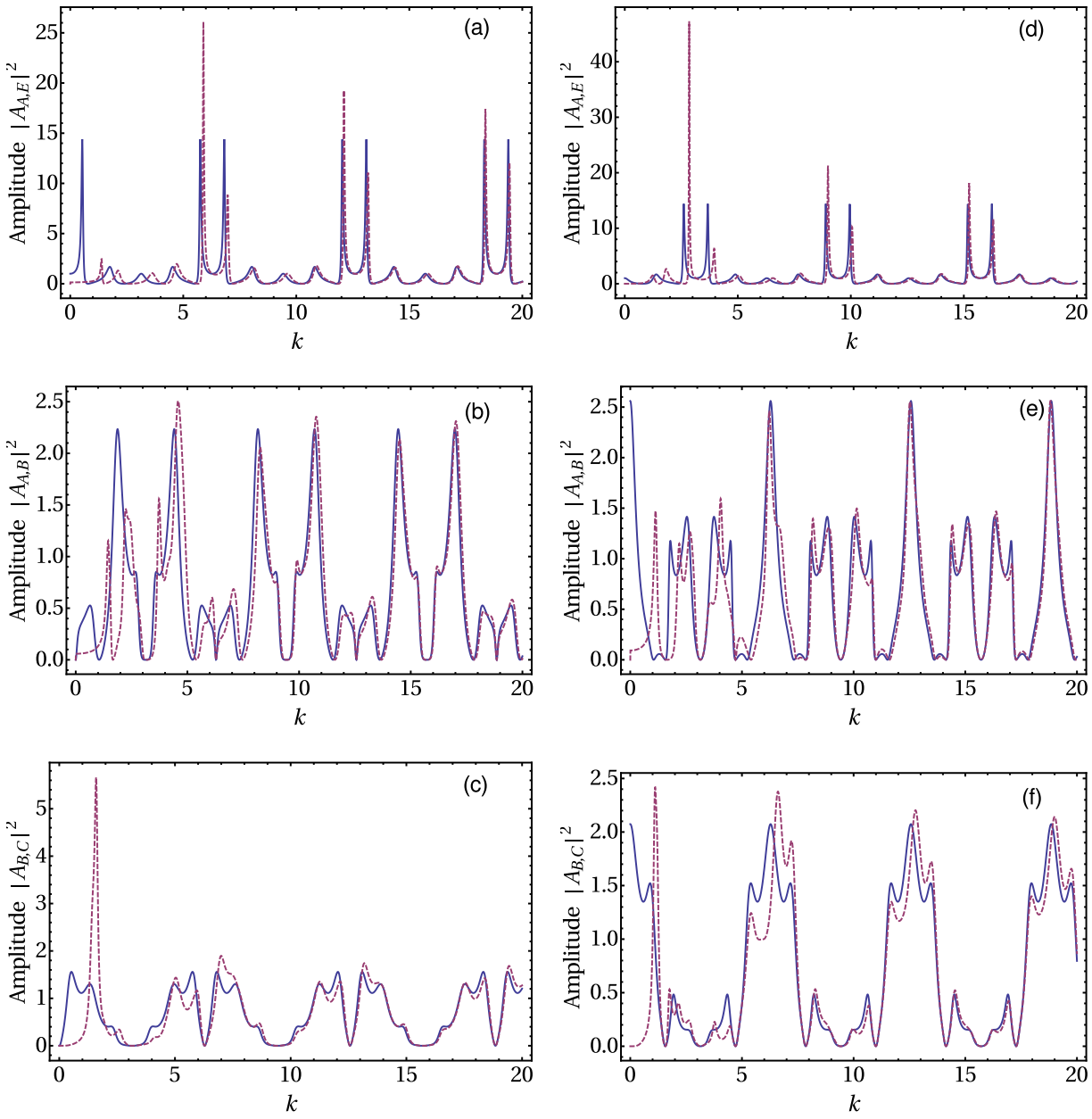

Figure 25: (Color online). Behavior of amplitude $\mathcal{A}_{I,J}$ as function of energy using the Dirichlet ($r_E = -1$) or Neumann ($r_E = 1$) boundary condition on vertex E of graph in the Fig. 23. The figures in (a)-(c) are using Dirichlet boundary condition and in (d)-(f) are using Neumann boundary condition, for quasi-bound state localized in the edges between vertices (a) and (d) A and E, (b) and (e) A and B and (c) and (f) B and C. The solid line is for $\gamma = 0.0$ and the dashed line is for $\gamma = 1.0$.

topology, avoiding those complicated calculations. The exact Green's function is given by a sum over classical paths, taking into account local quantum effects through the quantum amplitudes defined through the boundary conditions on each vertex of the graph. This result is very important because it allows one to solve problems in a recursive way, a key factor in the solution of quantum graphs of arbitrary topologies.

In order to construct the exact Green's function we developed two simplification procedures: the regrouping of infinity paths in finite classes of paths and the separation of a large graph into small ones. Using this two simplification procedures, the exact Green's function for open and closed quantum graphs was obtained. Several concrete examples was considered, like cube, binary tree and Sierpiński-like quantum graphs. From the poles and residues of the Green's functions the bound state eigenenergies and eigenfunctions were obtained with the correct normalization constant. I worth to comment that the wave function normalization constant often involves a difficult integral in the other methods. The method outlined here can also be applied for dressed quantum graphs if the potentials along the edges decay at least exponentially, and very good analytical approximation for the Green's function can be obtained. But in this case it is necessary to include the quantum amplitudes of the potentials and calculate the classical action of the quantum particle under the action of the potential. Finally, a very interesting application of Green's function approach was done to extract information about quasi-bound states in open quantum graphs. The method allows us to extract information of localized quasi-bound state and the influence of different boundary conditions in the energy and width of quasi-bound state.

Our analysis generalizes the quantum version of the Kirchhoff's rules discussed in Ref. [134], because we construct the scattering matrix in a systematic and very general way, and also generalizes the results of Ref. [35], where was studied only open quantum graphs and was not showed how to classify and sum up all the classical trajectories. We illustrate our method by some concrete examples like binary tree, cube and Sierpiński-like quantum graphs, obtaining the transmission (as well the reflection) amplitudes as functions of wave number of incident plane waves, by using k-dependent boundary conditions.

The approach developed here can be also applied to study a close related class of systems, namely, scattering quantum walks as addressed in [77, 78]. The advantage of the present approach to study scattering quantum walks lies in the easily to obtain the Green's function for general quantum graphs and in the possibility to explore specific paths and obtain the contribution of each path to the interference phenomena responsible for the superdifusivity of quantum walks.

We hope that all these technical aspects developed in this work can contribute to a better understanding of quantum graphs.

9. Acknowledgments

FMA would like to thank Simone Severini and Sougato Bose at University College London for the hospitality extended during the period this manuscript was prepared. Support is acknowledge from CNPq for researcher grants. FMA also thanks CNPq for grants No. 460404/2014-8 (Universal) and 206224/2014-1 (PDE).

A. The most general point interaction conserving probability flux as a quantum graph vertex

A.1. The usual case: the line

The probability density flux in the usual 1D quantum mechanics reads

$$j(x) = \frac{1}{2i}[\psi^*(x)\psi'(x) - \psi(x)\psi'^*(x)]. \tag{A.1}$$

Thus, if we define ($\psi'(x) \equiv d\psi(x)/dx$)

$$\Phi(x) = \begin{pmatrix} \psi(x) \\ \psi'(x) \end{pmatrix}, \tag{A.2}$$

and

$$J = \begin{pmatrix} 0 & 1 \\ -1 & 0 \end{pmatrix}, \tag{A.3}$$

$j(x)$ can be written in a complex sympletic-like form as

$$j(x) = \frac{1}{2i}\Phi^{\dagger}(x)\, J\, \Phi(x). \tag{A.4}$$

Now, suppose a free particle of energy $E = k^2/2$ on the line $(-\infty < x < +\infty)$, obeying to $-d^2\psi(x)/dx^2 = k^2\psi(x)$ for $x \neq 0$. At $x = 0$ we assume a point interaction. Since, by definition, the range of action of such kind of potential is zero, its only effect is to set a specific BC for the wave function $\psi(x)$ at $x = 0$. Thus, the most general point potential corresponds to the most general linear boundary condition, represented by

$$\Phi(0^+) = \Gamma\, \Phi(0^-), \tag{A.5}$$

with

$$\Gamma = \omega \begin{pmatrix} a & b \\ c & d \end{pmatrix}. \tag{A.6}$$

For example, for the common delta function potential $\gamma\,\delta(x)$ (of strength γ), the parameters are $a = d = \omega = 1$, $b = 0$, and $c = \gamma$.

Using the Eqs. (A.4) and (A.5), we have

$$j(0^+) = \frac{1}{2i}\Phi^{\dagger}(0^-)\,\Gamma^{\dagger}\, J\,\Gamma\,\Phi(0^-). \tag{A.7}$$

If we impose $j(0^+) = j(0^-)$, it follows that $\Gamma^{\dagger}\, J\,\Gamma = J$, yielding

$$ad - bc = 1,\ \ a, b, c, d \text{ real numbers and } |\omega| = 1. \tag{A.8}$$

Therefore, the most general point interaction consistent with flux conservation is characterized by Eq. (A.5), with Γ given by Eqs. (A.6) and (A.8).

Next, to consider a $\mathcal{S}$ matrix formalism [194], suppose typical plane wave scattering solutions characterized by k. The incoming and outgoing parts of the state are then connected by

$$\begin{pmatrix} \psi_k^{(\text{out})}(0^-) \\ \psi_k^{(\text{out})}(0^+) \end{pmatrix} = \mathcal{S}(k) \begin{pmatrix} \psi_k^{(\text{in})}(0^-) \\ \psi_k^{(\text{in})}(0^+) \end{pmatrix}. \tag{A.9}$$

Probability conservation at the origin,

$$|\psi_k^{(\text{in})}(0^-)|^2 + |\psi_k^{(\text{in})}(0^+)|^2 = |\psi_k^{(\text{out})}(0^-)|^2 + |\psi_k^{(\text{out})}(0^+)|^2, \tag{A.10}$$

inserted into Eq. (A.9) leads to $\mathcal{S}(k)\mathcal{S}^{\dagger}(k) = \mathcal{S}^{\dagger}(k)\mathcal{S}(k) = \mathbf{1}$, i.e., $\mathcal{S}$ is unitary. Furthermore, making in Eq. (A.9) the substitution $k \to -k$, we can write

$$\begin{pmatrix} \psi_{-k}^{(\text{in})}(0^-) \\ \psi_{-k}^{(\text{in})}(0^+) \end{pmatrix} = \mathcal{S}^{\dagger}(-k) \begin{pmatrix} \psi_{-k}^{(\text{out})}(0^-) \\ \psi_{-k}^{(\text{out})}(0^+) \end{pmatrix}. \tag{A.11}$$

But $k \to -k$ inverts the flux direction, physically implying in $\psi^{(\text{in})} \leftrightarrow \psi^{(\text{out})}$. So, given such in-out exchange in Eq. (A.11) and once the relation between incoming and outgoing wave function components is always set in the form of Eq. (A.9), we must have $\mathcal{S}(k) = \mathcal{S}^{\dagger}(-k)$.

For any arbitrary point interaction, we can write the scattering solutions $\psi_k^{(\pm)}(x)$ assuming a plane wave, of wave number k, incident either from the left $(+)$ or right $(-)$, so that $(N_k = 1/\sqrt{2\pi})$

$$\psi_k^{(\pm)}(x) = N_k \times \begin{cases} \exp[\pm ikx] + R^{(\pm)}(k)\exp[\mp ikx], & x \lesseqgtr 0 \\ T^{(\pm)}(k)\exp[\pm ikx], & x \gtreqless 0. \end{cases} \tag{A.12}$$

Observing that $\exp[\pm ikx]$ are the incoming and the terms involving R and T are the outgoing parts of the above full scattering states, one gets that arbitrary linear combinations of $\psi_k^{(+)}$ and $\psi_k^{(-)}$ results, from Eq. (A.9), in

$$\mathcal{S}(k) = \begin{pmatrix} R^{(+)}(k) & T^{(-)}(k) \\ T^{(+)}(k) & R^{(-)}(k) \end{pmatrix}. \tag{A.13}$$

Now, imposing $\mathcal{S}\mathcal{S}^\dagger = \mathcal{S}^\dagger\mathcal{S} = \mathbf{1}$ and $\mathcal{S}(k) = \mathcal{S}^\dagger(-k)$ to Eq. (A.13), ones finds that

$$|R|^2 + |T|^2 = 1, \qquad R^{(+)^*}T^{(\pm)} + T^{(\mp)^*}R^{(-)} = 0,$$
$$R^{(\pm)^*}(k) = R^{(\pm)}(-k), \qquad T^{(\pm)^*}(k) = T^{(\mp)}(-k). \tag{A.14}$$

These are the basic conditions to assure proper features for the scattering solutions in quantum mechanics [194], e.g., orthonormalization, flux conservation, and the existence of the scattering inverse problem. If, furthermore, one also requires time-reverse invariance – what we are not imposing in this work – then $T^{(+)} = T^{(-)}$.

Finally, to establish a full correspondence between the two approaches, the boundary condition treatment and the $\mathcal{S}$ matrix formalism, let us assume Eq. (A.5) for the states in Eq. (A.12). Thus [192]

$$R^{(\pm)}(k) = \frac{c \pm ik(d-a) + bk^2}{-c + ik(d+a) + bk^2}, \quad T^{(\pm)}(k) = \frac{2ik\omega^{\pm 1}}{-c + ik(d+a) + bk^2}. \tag{A.15}$$

It is easy to verify that the quantum amplitudes in Eq. (A.15) satisfies *all* the fundamental requirements in Eq. (A.14) [192]. Hence, up to a global phase ω, the problem is likewise specified from the parameters a, b, c and d or from the coefficients $R^{(\pm)}$ and $T^{(\pm)}$. Thus, the two approaches are completely equivalent and arbitrary point interactions can be defined entirely in terms of their $\mathcal{S}$ matrix (for a more detailed analysis, see, e.g., [187]).

A.2. A point interaction in 1D for multiple directions: a star graph topology

The above prescription for the line is directly extendable to the more general case. To see how, first note that in the 1D case, a zero-range potential at the origin divides the interval $-\infty < x < +\infty$ into two semi-infinite lines. Thus, from the identification $x_1 = -x$ and $x_2 = +x$, the left ($-\infty < x < 0$) and right ($0 < x < +\infty$) regions could be represented by $0 \le x_1 \le +\infty$ and $0 \le x_2 \le +\infty$. Hence, in a quantum graph framework, the system topology is that of a single vertex joining two leads. Also, the original nomenclature 0^+ (0^-) now becomes $x_2 = 0$ ($x_1 = 0$), indicating that we are considering the vertex but from the right (left) side, i.e., at the beginning of lead 2 (1).

A zero-range potential located at 0 and attached to $N = E$ semi-infinite lines constitutes a star graph-like topology, depicted in Figure 1(c). Along each lead n (with $n = 1, 2, \ldots, N$) the spatial coordinate x_n ranges from 0 to ∞ and $\psi_k^{(\text{in})}(x_n)$ and $\psi_k^{(\text{out})}(x_n)$ denote, respectively, incoming and outgoing k plane wave states. In this case, the equivalent of Eqs. (A.9) and (A.11) read

$$\Psi_k^{(\text{out})}(0) = \mathcal{S}(k)\,\Psi_k^{(\text{in})}(0) \;\text{ and }\; \Psi_{-k}^{(\text{in})}(0) = \mathcal{S}^\dagger(-k)\,\Psi_{-k}^{(\text{out})}(0), \tag{A.16}$$

with Ψ a N-components column vector (naturally extending the 2-components for the line) and $\mathcal{S}(k)$ a $N\times N$ scattering matrix, whose element $\mathcal{S}_{nl}(k)$ yield the quantum transition amplitude to go from lead n to lead l for a state of wave number k. Probability conservation and moment inversion reciprocity, namely,

$$\Psi_k^{(\text{out})}(0)^\dagger\,\Psi_k^{(\text{out})}(0) = \Psi_k^{(\text{in})}(0)^\dagger\,\Psi_k^{(\text{in})}(0) \text{ and } k \leftrightarrow -k \iff \Psi^{(\text{out})} \leftrightarrow \Psi^{(\text{in})}, \tag{A.17}$$

demand $\mathcal{S}(k)$ to be unitary and $\mathcal{S}(k) = \mathcal{S}^\dagger(-k)$, exactly as in Sec. A.1. Therefore, any $N \times N$ matrix satisfying these two conditions will represent a proper zero-range interaction, resulting in a well-behaved quantum dynamics on a N star graph. Furthermore, the scattering states follow from a direct generalization of Eq. (A.12), where the amplitudes are given by the corresponding matrix elements of $\mathcal{S}(k)$ (cf., Sec. 2).

Finally, the BC approach in [134, 153] can be put in a direct relation with the above $\mathcal{S}$ formalism through an one-to-one correspondence between the N^2 independent real parameters defining the BC at the vertex (see Sec. 2.1) and the matrix elements of $\mathcal{S}$, likewise parameterizable by N^2 independent real constants [227].

A.3. A general graph

To conclude the analysis, we note that in an arbitrary undressed graph, the region around each vertex n is basically a star structure. The difference is that instead of going from 0 to ∞, some (or all) edges can be finite, ending up in another vertex m. Due to the superposition principle – which holds true for any linear wave-like differential equation (here Helmholtz) – the global state for an spatially extended problem can be construct in terms of a multiple scattering process [228]. In other words, a proper sum of the locally scattered waves (entirely determined by $\mathcal{S}^{(n)}(k)$) results in the full exact solution. This is the case even if the system is closed (the graph has no leads)[9].

[9] A trivial example is that of an infinite square well (a graph with two vertices and one edge), whose typical bounded $\psi_n(x) \propto \sin[k_n x]$ (with $k_n = n\pi/L$) is given as the linear combination of the plane waves scattered off by each wall (vertex), at $x = 0$ and $x = L$.

In this way, a legitimate and univocal quantum dynamics for any open or closed graph is utterly obtained by associating to each vertex n a corresponding scattering matrix $\mathcal{S}^{(n)}(k)$ (for $\mathcal{S}^{(n)}(k)$ as described in Sec. A.2). Then, it also directly follows that the BC prescription and the $\mathcal{S}$ scheme are totally equivalent regardless the graph topology.

B. The exact Green's function for quantum graphs: the generalized semiclassical formula

Here we shall just outline the main steps necessary to demonstrate that the exact Green's function for quantum graphs can be written in the same functional form of Eq. (13), i.e., as generalized semiclassical formula.

B.1. Reviewing a simple case, the Green's function for a point interaction on the line

Suppose the usual infinite line and an arbitrary point interaction at the origin ($x = 0$), for which the reflection and transmission coefficients are $R^{(\pm)}$ and $T^{(\pm)}$ (see Appendix A.1). It is worth recalling that this example corresponds to a quantum graph with one vertex and two leads. From [150], we can readily write down its exact Green's function. Defining G_{+-} for $x_f > 0 > x_i$, G_{-+} for $x_i > 0 > x_f$, G_{++} for $x_f,\ x_i > 0$ and G_{--} for $x_f,\ x_i < 0$, one finds

$$\begin{aligned} G_{\pm\mp}(x_f, x_i; k) &= \frac{\mu}{i\hbar^2 k} T^{(\pm)} \exp[ik|x_f - x_i|], \\ G_{\pm\pm}(x_f, x_i; k) &= \frac{\mu}{i\hbar^2 k} \Big[\exp[ik|x_f - x_i|] + R^{(\pm)} \exp[ik(|x_f| + |x_i|)]\Big], \end{aligned} \tag{B.1}$$

which have the structure of Eq. (13). In fact, for $\pm\mp$ there is only one sp leaving x_i, crossing the origin, and finally arriving at x_f. In this case, the classical-like action reads $S_{sp} = pL_{sp}/\hbar = k|x_f - x_i|$, whereas the quantum weight is given by $W_{sp} = T^{(\pm)}$ (just the amplitude gained in this scattering process, a transmission). For $\pm\pm$, both end points are at the same side of the zero range potential. Therefore, we have (i) a direct sp, going straight from x_i to x_f, so with $W_{sp} = 1$ and $S_{sp} = k|x_f - x_i|$, and (ii) an indirect sp, along which there is a single reflection (at $x = 0$), thus $W_{sp} = R^{(\pm)}$ and $S_{sp} = k(|x_f| + |x_i|)$.

B.2. Green's function for a star graph

Similarly to what has been done in the Appendix A.2, to see why G for quantum graphs can be written in the general form of Eq. (13), we can start considering the basic (building block) star shape depicted in Figure 1(c). The vertex V (assumed to be at the origin of all leads, in a total of $N = E$) is interpreted as an arbitrary scattering center, so a general point interaction.

Suppose $\{\Psi^{(\kappa)}, \Psi^{(\sigma)}(k)\}$ to represent the complete full set of solutions for the Schrödinger equation for this graph, where $\Psi^{(\sigma)}(k) = (\psi_1^{(\sigma)}(x_1; k), \ldots, \psi_N^{(\sigma)}(x_N; k))^T$ and $\Psi^{(\kappa)} = (\psi_1^{(\kappa)}(x_1), \ldots, \psi_N^{(\kappa)}(x_N))^T$ are, respectively, the scattering and bound states with energy $E = \hbar^2 k^2/2\mu$ and E_κ. We also observe that for each wave number k, we have a scattering state σ, labeling through which initial lead σ the plane wave is incident to the vertex. This is equivalent to the 1D problem where one has two leads and so two solutions ($\sigma = \pm$), one incoming from the left and other from the right of the origin [150–152] (cf, Eq. (A.12) in Appendix A.1).

From the Green's function spectral decomposition property, we can write [135] (for x_f and x_i in the edges l and n, respectively)

$$G_{ln}(x_f, x_i; E) = G_{ln}^{(\text{b.s.})}(x_f, x_i; E) + G_{ln}^{(\text{s.s.})}(x_f, x_i; E), \tag{B.2}$$

$$G_{ln}^{(\text{b.s.})}(x_f, x_i; E) = \sum_\kappa \frac{\psi_l^{(\kappa)}(x_f)\, \psi_n^{(\kappa)*}(x_i)}{E - E_\kappa}, \tag{B.3}$$

$$G_{ln}^{(\text{s.s.})}(x_f, x_i; E) = \int_0^\infty dk \sum_{\sigma=1}^{N} \frac{\psi_l^{(\sigma)}(x_f; k)\, \psi_n^{(\sigma)*}(x_i; k)}{E - \hbar^2 k^2/(2\mu)}. \tag{B.4}$$

The scattering solution for a plane wave of energy $E = \hbar^2 k^2/2\mu$, incoming from lead σ towards the vertex, is given by (with x in l, for $l = 1, \ldots, N$)

$$\psi_l^{(\sigma)}(x; k) = \frac{1}{\sqrt{2\pi}} \Big(\delta_{l\sigma} \exp[-ikx] + S_{\sigma l}(k) \exp[ikx]\Big), \tag{B.5}$$

By inserting (B.5) into (B.4), then ($E = \hbar^2\lambda^2/(2\mu)$)

$$G_{ln}(x_f, x_i; \lambda) = G_{ln}^{(\text{b.s.})}(x_f, x_i; E) + \frac{2\mu}{\hbar^2}\frac{1}{2\pi}\int_0^\infty \frac{dk}{\lambda^2 - k^2} \times \Big\{\delta_{nl}\exp[-ik(x_f - x_i)] + S_{nl}(k)\exp[ik(x_f + x_i)] + {S_{ln}}^*(k)\exp[-ik(x_f + x_i)] + \sum_{\sigma=1}^{N} S_{\sigma l}(k)\,{S_{\sigma n}}^*(k)\exp[ik(x_f - x_i)]\Big\}. \tag{B.6}$$

Using the relations in Eq. (8), the above equation can be written as

$$G_{ln}(x_f, x_i; \lambda) = G_{ln}^{(\text{b.s.})}(x_f, x_i; E) + \frac{2\mu}{\hbar^2}\frac{1}{2\pi}\int_{-\infty}^\infty \frac{dk}{\lambda^2 - k^2}\Big\{\delta_{nl}\exp[-ik(x_f - x_i)] + S_{nl}(k)\exp[ik(x_f + x_i)]\Big\}. \tag{B.7}$$

Above, the integral involving $\exp[-ik(x_f - x_i)]$ leads to the free particle Green's function. For the other integral, we consider a contour integration along the real axis closed by a infinite semicircle in the upper half of the complex plane. The pole contributions are due the denominator $\lambda^2 - k^2$ and possible singularities of $S_{nl}(k)$. If the vertex V (a zero range potential) does not allow bounded states, $G^{(\text{b.s.})} = 0$ and $S_{nl}(k)$ does not have poles. On the other hand, for a very large number of situations the terms in the integration resulting from the bound energy poles exactly cancel out with $G^{(\text{b.s.})}$ [196, 229, 230]. This is precisely what takes place for general point interactions [187]. Putting all this together, the remaining steps in evaluating Eq (B.7) are straightforward. Thus, reverting to the notation k for the wave number variable, we finally get

$$G_{ln}(x_f, x_i; k) = \frac{\mu}{i\hbar^2 k}\Big\{\delta_{nl}\exp[ik|x_f - x_i|] + S_{nl}(k)\exp[ik(x_f + x_i)]\Big\}. \tag{B.8}$$

Now, notice that Eq. B.8 would readily follow from the sum over scattering paths prescription. In fact, for a particle with x_i in lead n, arriving at x_f in lead l, we have two possibilities. (i) The leads n and l are the same, so there are two scattering paths: straight propagation from x_i to x_f, corresponding to $\exp[ik|x_f - x_i|]$ and $W = 1$; and propagation from x_i to the vertex V, reflection (gaining a factor $S_{nn}(k)$) and then propagation to x_f, in this case yielding $\exp[ik(x_f + x_i)]$ and an amplitude $S_{nn}(k)$ (i.e., the reflection coefficient from n to n). These contributions result in $G_{nn}^{(\text{semicl gen})}(x_f, x_i; k) = (\mu/(i\hbar^2 k))\{\exp[-ik|x_f - x_i|] + S_{nn}(k)\exp[ik(x_f + x_i)]\}$. (ii) The leads are distinct, thus there is only one scattering path: propagation from x_i to the vertex, a transmission through it (gaining a factor $S_{nl}(k)$), and finally propagation to x_f. So, $G_{ln}^{(\text{semicl gen})}(x_f, x_i; k) = (\mu/(i\hbar^2 k))\{S_{nl}(k)\exp[ik(x_f + x_i)]\}$. These two possibilities are exactly summarized by Eq. (B.8).

B.3. The Green's function for an arbitrary graph

Lastly, for an arbitrary case the reasoning resembles that in the Appendix A.3. For the star graph, the exact G is written in terms of a (finite) sum of scattering paths. Extending for any topology (as considered in this work), the local scattering – around each vertex, so in a star-like configuration – can be associated to a stretch of a much larger sp, leaving from x_i, running across the totality or segments of the whole graph, and finally arriving at x_f. This is just the usual multiple scattering process, valid to describe any wave propagation in the linear context. Along the way, the W_{sp} are built from the quantum amplitudes gained through the successive scattering at the vertices. On its turn $S_{sp} = kL_{sp}$, for L_{sp} the sp total classical distance traveled between the end points. Of course, generally the number of sp can be infinite (thus demanding the techniques of Sec. 4 for explicit calculations). But the main point is that Eq. (13) represents the exact construction for the Green's function of any quantum graph.

References

References

[1] P. Kuchment, Quantum graphs, Waves Random Complex Media 14 (1) (2004) S3. doi:10.1088/0959-7174/14/1/007.

[2] G. Berkolaiko, R. Carlson, S. A. Fulling, P. Kuchment (Eds.), Quantum Graphs and Their Applications, Vol. 415 of Contemp. Maths., American Mathematical Society, Providence, RI, 2006.
[3] A. Hussein, D. Mugnolo, Quantum graphs with mixed dynamics: the transport/diffusion case, J. Phys. A 46 (23) (2013) 235202–. doi:10.1088/1751-8113/46/23/235202.
[4] L. Pauling, The diamagnetic anisotropy of aromatic molecules, J. Chem. Phys. 4 (1936) 673. doi:10.1063/1.1749766.
[5] H. Kuhn, Elektronengasmodell zur quantitativen deutung der lichtabsorption von organischen farbstoffen i, Helv. Chim. Acta 31 (6) (1948) 1441–1455. doi:10.1002/hlca.19480310602.
[6] J. R. Platt, Classification of spectra of cata-condensed hydrocarbons, J. Chem. Phys. 17 (1949) 484. doi:10.1063/1.1747293.
[7] K. Ruedenberg, C. W. Scherr, Free-electron network model for conjugated systems. i. theory, J. Chem. Phys. 21 (1953) 1565. doi:10.1063/1.1699299.
[8] C. A. Coulson, Note on the applicability of the free-electron network model to metals, Proc. Phys. Soc. A 67 (1954) 608. doi:10.1088/0370-1298/67/7/305.
[9] E. W. Montroll, Quantum theory on a network. i. a solvable model whose wavefunctions are elementary functions, J. Math. Phys. 11 (1970) 635. doi:10.1063/1.1665178.
[10] M. J. Richardson, N. L. Balazs, On the network model of molecules and solids, Ann. Phys. (NY) 73 (1972) 308. doi:10.1016/0003-4916(72)90285-0.
[11] J. E. Avron, A. Raveh, B. Zur, Adiabatic quantum transport in multiply connected systems, Rev. Mod. Phys. 60 (4) (1988) 873–915. doi:10.1103/RevModPhys.60.873.
[12] D. N. Beratran, J. N. Betts, J. N. Onuchic, Protein electron transfer rates set by the bridging secondary and tertiary structure, Science 252 (1991) 1285. doi:10.1126/SCIENCE.1656523.
[13] L. Pogliani, From molecular connectivity indices to semiempirical connectivity terms: Recent trends in graph theoretical descriptors, Chem. Rev. 100 (10) (2000) 3827. doi:10.1021/cr0004456.
[14] R. Garcia-Domenech, J. Galvez, J. V. de Julian-Ortiz, L. Pogliani, Some new trends in chemical graph theory, Chem. Rev. 108 (3) (2008) 1127. doi:10.1021/cr0780006.
[15] K. C. Kao, W. Hwang, Electrical Transport in Solids, Oxford: Pergamon, Oxford, 1981.
[16] M. N. Kobrak, E. R. Bittner, Quantum molecular dynamics study of polaron recombination in conjugate polymers, Phys. Rev. B 62 (17) (2000) 11473. doi:10.1103/PhysRevB.62.11473.
[17] J. A. Freire, M. G. E. da Luz, D. Ma, I. A. Hummelgen, The current–voltage dependence of nominally undoped thin conjugated polymer films, Appl. Phys. Lett. 77 (2000) 693. doi:10.1063/1.127088.
[18] M. Koehler, C. D. Canestraro, M. C. Schinitzler, M. M. Oliveira, A. J. G. Zarbin, L. Roman, M. G. E. Luz, Evidence of fractal structure for charge transport in carbon-nanotube/conjugated-polymer composites., Europhys. Lett. 79 (2007) 47011. doi:10.1209/0295-5075/79/47011.
[19] S. Alexander, Superconductivity of networks. a percolation approach to the effects of disorder, Phys. Rev. B 27 (3) (1983) 1541. doi:10.1103/PhysRevB.27.1541.
[20] P. W. Anderson, New method for scaling theory of localization. ii. multichannel theory of a "wire"and possible expansion to higher dimensionality, Phys. Rev. B 23 (10) (1981) 4828. doi:10.1103/PhysRevB.23.4828.
[21] B. Shapiro, Renormalization-group transformation for the anderson transition, Phys. Rev. Lett. 48 (12) (1982) 823. doi:10.1103/PhysRevLett.48.823.
[22] R. Klesse, M. Metzler, Spectral compressibility at the metal-insulator transition of the quantum hall effect, Phys. Rev. Lett. 79 (4) (1997) 721. doi:10.1103/PhysRevLett.79.721.
[23] J. Vidal, G. Montambaux, B. Doucot, Transmission through quantum networks, Phys. Rev. B 62 (24) (2000) R16294. doi:10.1103/PhysRevB.62.R16294.
[24] P. Exner, Contact interactions on graph superlattices, J. Phys. A 29 (1996) 87. doi:10.1088/0305-4470/29/1/011.
[25] D. Kowal, U. Sivan, O. Entin-Wohlman, Y. Imry, Transmission through multiply-connected wire systems, Phys. Rev. B 42 (14) (1990) 9009. doi:10.1103/PhysRevB.42.9009.
[26] C. Texier, G. Montambaux, Weak localization in multiterminal networks of diffusive wires, Phys. Rev. Lett. 92 (18) (2004) 186801. doi:10.1103/PhysRevLett.92.186801.
[27] C. Texier, G. Montambaux, Dephasing due to electron-electron interaction in a diffusive ring, Phys. Rev. B 72 (11) (2005) 115327. doi:10.1103/PhysRevB.72.115327.
[28] C. Texier, G. Montambaux, Quantum oscillations in mesoscopic rings and anomalous diffusion, J. Phys. A 38 (2005) 3455. doi:10.1088/0305-4470/38/15/015.
[29] A. Bondarenko, V. Dedok, Inverse scattering problem on quantum graphs in optical tomography technology, in: Science and Technology, 2003. Proceedings KORUS 2003. The 7th Korea-Russia International Symposium on, Vol. 3, 2003, p. 105.
[30] P. Exner, Lattice kronig-penney models, Phys. Rev. Lett. 74 (18) (1995) 3503. doi:10.1103/PhysRevLett.74.3503.
[31] J. Kuipers, Q. Hummel, K. Richter, Quantum graphs whose spectra mimic the zeros of the riemann zeta function, Phys. Rev. Lett. 112 (7) (2014) 070406–. doi:10.1103/PhysRevLett.112.070406.
[32] H. Schanz, U. Smilansky, Periodic-orbit theory of anderson localization on graphs, Phys. Rev. Lett. 84 (7) (2000) 1427. doi:10.1103/PhysRevLett.84.1427.
[33] V. Caudrelier, M. Mintchev, E. Ragoucy, Exact scattering matrix of graphs in magnetic field and quantum noise, J. Math. Phys. 55 (8) (2014) 083524. doi:10.1063/1.4893354.
[34] T. Kottos, U. Smilansky, Chaotic scattering on graphs, Phys. Rev. Lett. 85 (5) (2000) 968. doi:10.1103/PhysRevLett.85.968.
[35] F. Barra, P. Gaspard, Transport and dynamics on open quantum graphs, Phys. Rev. E 65 (1) (2001) 016205. doi:10.1103/PhysRevE.65.016205.
[36] B. Bellazzini, M. Mintchev, P. Sorba, Quantum wire junctions breaking time-reversal invariance, Phys. Rev. B 80 (24) (2009) 245441–. doi:10.1103/PhysRevB.80.245441.

[37] Z. Pluhař, H. A. Weidenmüller, Universal quantum graphs, Phys. Rev. Lett. 112 (14) (2014) 144102–. doi:10.1103/PhysRevLett.112.144102.
[38] T. Kottos, U. Smilansky, Quantum chaos on graphs, Phys. Rev. Lett. 79 (1997) 4794. doi:10.1103/PhysRevLett.79.4794.
[39] T. Kottos, U. Smilansky, Periodic orbit theory and spectral statistics for quantum graphs, Ann. Phys. (NY) 274 (1999) 76. doi:10.1006/aphy.1999.5904.
[40] M. L. Mehta, Random Matrices, 3nd Ed., Elsevier Academic Press, Amsterdam, 2004.
[41] M. C. Gutzwiller, Chaos in Classical and Quantum Mechanics, Springer-Verlag, New York, 1990.
[42] M. C. Gutzwiller, Periodic orbits and classical quantization conditions, J. Math. Phys. 12 (1971) 343. doi:10.1063/1.1665596.
[43] R. Blümel, Y. Dabaghian, R. V. Jensen, Explicitly solvable cases of one-dimensional quantum chaos, Phys. Rev. Lett. 88 (4) (2002) 044101. doi:10.1103/PhysRevLett.88.044101.
[44] R. Blümel, Y. Dabaghian, R. V. Jensen, Exact, convergent periodic-orbit expansions of individual energy eigenvalues of regular quantum graphs, Phys. Rev. E 65 (4) (2002) 046222. doi:10.1103/PhysRevE.65.046222.
[45] T. Kottos, H. Schanz, Quantum graphs: a model for quantum chaos, Physica E 9 (3) (2001) 523. doi:10.1016/S1386-9477(00)00257-5.
[46] L. Kaplan, Eigenstate structure in graphs and disordered lattices, Phys. Rev. E 64 (3) (2001) 036225. doi:10.1103/PhysRevE.64.036225.
[47] S. Gnutzmann, U. Smilansky, Quantum graphs: Applications to quantum chaos and universal spectral statistics, Adv. Phys. 55 (2006) 527. doi:10.1080/00018730600908042.
[48] M. A. Nielsen, I. I. Chuang, Quantum computation and quantum information, Cambridge Univ. Press, 2010.
[49] V. Kostrykin, R. Schrader, Kirchhoff's rule for quantum wires. ii: The inverse problem with possible applications to quantum computers, Fortschr. Phys. 48 (8) (2000) 703–716. doi:10.1002/1521-3978(200008)48:8<703::AID-PROP703>3.0.CO;2-0.
[50] T. Cheon, I. Tsutsui, T. Fülöp, Quantum abacus, Physics Letters A 330 (5) (2004) 338–342. doi:10.1016/j.physleta.2004.08.011.
[51] R. Raussendorf, P. Hoyer, M. Mosca, D. Feder, S. Severini, Quantum information and graph theory - introduction, in: Quantum Information and Graph Theory: emerging connections, 2008, p. 1.
URL http://pirsa.org/08040074/
[52] P. Kuchment, Quantum graphs: Ii. some spectral properties of quantum and combinatorial graphs, J. Phys. A 38 (22) (2005) 4887. doi:10.1088/0305-4470/38/22/013.
[53] H. J. Briegel, R. Raussendorf, Persistent entanglement in arrays of interacting particles, Phys. Rev. Lett. 86 (5) (2001) 910–913. doi:10.1103/PhysRevLett.86.910.
[54] R. Raussendorf, H. J. Briegel, A one-way quantum computer, Phys. Rev. Lett. 86 (22) (2001) 5188–5191. doi:10.1103/PhysRevLett.86.5188.
[55] R. Raussendorf, D. E. Browne, H. J. Briegel, Measurement-based quantum computation on cluster states, Phys. Rev. A 68 (2) (2003) 022312–. doi:10.1103/PhysRevA.68.022312.
[56] M. Hein, W. Dür, J. Eisert, R. Raussendorf, M. V. den Nest, H.-J. Briegel, Entanglement in graph states and its applications, in: G. Casati, D. L. Shepelyansky, P. Zoller, G. Benenti (Eds.), Proceedings of the International School of Physics "Enrico Fermi", 2006, pp. 115–218. arXiv:quant-ph/0602096, doi:10.3254/978-1-61499-018-5-115.
[57] B. Antonio, D. Markham, J. Anders, Adiabatic graph-state quantum computation, New J. Phys. 16 (11) (2014) 113070. doi:10.1088/1367-2630/16/11/113070.
URL http://stacks.iop.org/1367-2630/16/i=11/a=113070
[58] J.-Y. Wu, M. Rossi, H. Kampermann, S. Severini, L. C. Kwek, C. Macchiavello, D. Bruß, Randomized graph states and their entanglement properties, Phys. Rev. A 89 (5) (2014) 052335–. doi:10.1103/PhysRevA.89.052335.
[59] D. Feder, Graphs in quantum information theory, in: Sixth Canadian Summer School on Quantum Information Processing, University of Calgary, 2006, p. 1.
[60] D. Bacon, S. T. Flammia, Adiabatic cluster-state quantum computing, Phys. Rev. A 82 (2010) 030303. doi:10.1103/PhysRevA.82.030303.
URL http://link.aps.org/doi/10.1103/PhysRevA.82.030303
[61] D. Leung, L. Mancinska, W. Matthews, M. Ozols, A. Roy, Entanglement can increase asymptotic rates of zero-error classical communication over classical channels, Commun. Math. Phys. 311 (1) (2012) 97–111. doi:10.1007/s00220-012-1451-x.
URL http://dx.doi.org/10.1007/s00220-012-1451-x
[62] J. Briët, H. Buhrman, D. Gijswijt, Violating the Shannon capacity of metric graphs with entanglement., Proc. Natl. Acad. Sci. USA 110 (7) (2012) 15. arXiv:1207.1779, doi:10.1073/pnas.1203857110.
URL http://www.ncbi.nlm.nih.gov/pubmed/23267109
[63] Y. Aharonov, I. Davidovich, N. Zagury, Quantum random walks, Phys. Rev. A 48 (2) (1993) 1687. doi:10.1103/PhysRevA.48.1687.
[64] J. Kempe, Quantum random walks: an introductory overview, Contemp. Phys. 44 (2003) 307. doi:10.1080/0010715103100011077 6.
[65] S. E. Venegas-Andraca, Quantum walks: a comprehensive review, Quantum Inf. Process. 11 (5) (2012) 1015–1106. doi:10.1007/s11128-012-0432-5.
[66] A. M. Childs, Universal computation by quantum walk, Phys. Rev. Lett. 102 (18) (2009) 180501. arXiv:0806.1972, doi:10.1088/1751-8113/41/7/075303.
[67] N. B. Lovett, S. Cooper, M. Everitt, M. Trevers, V. Kendon, Universal quantum computation using the discrete-time quantum walk, Phys. Rev. A 81 (4) (2010) 042330. doi:10.1103/PhysRevA.81.042330.
[68] A. M. Childs, D. Gosset, Z. Webb, Universal computation by multiparticle quantum walk, Science 339 (6121) (2013) 791–794. doi:10.1126/science.1229957.
[69] V. M. Kendon, A random walk approach to quantum algorithms, Phil. Trans. R. Soc. A 364 (2006) 3407. doi:10.1098/RSTA.2006.1901.
[70] M. Mosca, Quantum algorithms, in: R. A. Meyers (Ed.), Encyclopedia of Complexity and Systems Science, Springer New York, 2009, pp. 7088–7118. doi:10.1007/978-0-387-30440-3_423.
[71] R. Portugal, Quantum Walks and Search Algorithms, Springer New York, 2013. doi:10.1007/978-1-4614-6336-8.

[72] G. K. Tanner, Non-Linear Dynamics and Fundamental Interactions, Vol. 213, Springer Netherlands, 2006, Ch. From quantum graphs to quantum random walks, p. 69. doi:10.1007/1-4020-3949-2.
[73] V. Kendon, Quantum walks on general graphs, Int. J. Quantum Inf. 4 (2006) 791–805. doi:10.1142/S0219749906002195.
[74] S. Severini, G. Tanner, Regular quantum graphs, J. Phys. A 37 (26) (2004) 6675. doi:10.1088/0305-4470/37/26/005.
[75] V. Kostrykin, R. Schrader, Generating functions of random walks on graphs, arXiv:math/0404467arXiv:math/0404467.
[76] F. M. Andrade, M. G. E. da Luz, Equivalence between discrete quantum walk models in arbitrary topologies, Phys. Rev. A 80 (5) (2009) 052301. doi:10.1103/PhysRevA.80.052301.
[77] F. M. Andrade, M. G. E. da Luz, Green-function approach for scattering quantum walks, Phys. Rev. A 84 (4) (2011) 042343–. doi:10.1103/PhysRevA.84.042343.
[78] F. M. Andrade, M. G. E. da Luz, Superdiffusivity of quantum walks: A feynman sum-over-paths description, Phys. Rev. A 86 (4) (2012) 042309–. doi:10.1103/PhysRevA.86.042309.
[79] F. M. Andrade, Métodos de função de green na análise de grafos quânticos e caminhadas quânticas, Ph.D. thesis, Universidade Federal do Paraná (UFPR) (2009).
URL http://hdl.handle.net/1884/21922
[80] O. Hul, S. Bauch, P. Pakoński, N. Savytskyy, K. Życzkowski, L. Sirko, Experimental simulation of quantum graphs by microwave networks, Phys. Rev. E 69 (5) (2004) 056205–. doi:10.1103/PhysRevE.69.056205.
[81] B. Dietz, A. Richter, R. Samajdar, Cross-section fluctuations in open microwave billiards and quantum graphs: The counting-of-maxima method revisited, Phys. Rev. E 92 (2015) 022904. doi:10.1103/PhysRevE.92.022904.
[82] M. Ławniczak, A. Sawicki, S. Bauch, M. Kuś, L. Sirko, Resonances and poles in isoscattering microwave networks and graphs, Phys. Rev. E 89 (3) (2014) 032911–. doi:10.1103/PhysRevE.89.032911.
[83] M. Ławniczak, A. Nicolau-Kuklińska, S. Bauch, L. Sirko, Experimental investigation of the scattering fidelity in microwave networks simulating quantum graphs, Phys. Scr. 2014 (T160) (2014) 014025–. doi:10.1088/0031-8949/2014/T160/014025.
[84] O. Hul, How to hear the shape of isoscattering networks, Phys. Rev. E 87 (6) (2013) 062915–. doi:10.1103/PhysRevE.87.062915.
[85] M. Ławniczak, S. Bauch, A. Sawicki, M. Kus, L. Sirko, Isoscattering microwave networks - the role of the boundary conditions, Acta. Phys. Pol. A 124 (6) (2013) 1078–1081. doi:10.12693/APhysPolA.124.1078.
[86] A. Mouadili, E. H. El Boudouti, A. Soltani, A. Talbi, A. Akjouj, B. Djafari-Rouhani, Theoretical and experimental evidence of fano-like resonances in simple monomode photonic circuits, J. Appl. Phys. 113 (16) (2013) 164101. doi:10.1063/1.4802695.
[87] M. Ławniczak, A. Nicolau-Kuklińska, O. Hul, P. Masiak, S. Bauch, L. Sirko, Experimental and numerical determination of the correlation function of level velocities for microwave networks simulating quantum graphs, Phys. Scr. 2013 (T153) (2013) 014041–. doi:10.1088/0031-8949/2013/T153/014041.
[88] O. Hul, M. Ławniczak, S. Bauch, A. Sawicki, M. Kuś, L. Sirko, Are scattering properties of graphs uniquely connected to their shapes?, Phys. Rev. Lett. 109 (4) (2012) 040402–. doi:10.1103/PhysRevLett.109.040402.
[89] M. Ławniczak, S. Bauch, O. Hul, L. Sirko, Experimental investigation of microwave networks simulating quantum chaotic systems: the role of direct processes, Phys. Scr. 2012 (T147) (2012) 014018–.
URL http://stacks.iop.org/1402-4896/2012/i=T147/a=014018
[90] M. Ławniczak, S. Bauch, O. Hul, L. Sirko, Experimental investigation of the enhancement factor for irregular undirected and directed microwave graphs, in: Chaos Theory, WORLD SCIENTIFIC, 2011, p. 265. doi:10.1142/9789814350341_0031.
[91] O. Hul, L. Sirko, Parameter-dependent spectral statistics of chaotic quantum graphs: Neumann versus circular orthogonal ensemble boundary conditions, Phys. Rev. E 83 (6) (2011) 066204–. doi:10.1103/PhysRevE.83.066204.
[92] Michał Ławniczak, S. Bauch, O. Hul, L. Sirko, Experimental investigation of the enhancement factor and the cross-correlation function for graphs with and without time-reversal symmetry: the open system case, Phys. Scr. 2011 (T143) (2011) 014014–. doi:10.1088/0031-8949/2011/T143/014014.
[93] M. Ławniczak, A. Borkowska, O. Hul, S. Bauch, L. Sirko, Experimental determination of the autocorrelation function of level velocities for microwave networks simulating quantum graphs, Acta. Phys. Pol. A 120 (2011) 185.
[94] M. Ławniczak, O. Hul, S. Bauch, L. Sirko, Experimental simulation of quantum graphs by microwave networks - closed and open systems, Chaotic Modeling and Simulation 1 (2011) 105.
[95] M. Ławniczak, M.awniczak, S. Bauch, O. Hul, L. Sirko, Experimental investigation of the enhancement factor for microwave irregular networks with preserved and broken time reversal symmetry in the presence of absorption, Phys. Rev. E 81 (4) (2010) 046204–. doi:10.1103/PhysRevE.81.046204.
[96] M. Ławniczak, S. Bauch, O. Hul, L. Sirko, Experimental investigation of properties of hexagon networks with and without time reversal symmetry, Phys. Scr. 2009 (T135) (2009) 014050–. doi:10.1088/0031-8949/2009/135/014050.
[97] M. Ławniczak, O. Hul, S. Bauch, L. Sirko, Experimental and numerical studies of one dimensional and three dimensional chaotic open systems, Acta. Phys. Pol. A 116 (2009) 749.
[98] M. Ławniczak, O. Hul, S. Bauch, P. Seba, L. Sirko, Experimental and numerical investigation of the reflection coefficient and the distributions of wigner's reaction matrix for irregular graphs with absorption, Phys. Rev. E 77 (5) (2008) 056210–. doi:10.1103/PhysRevE.77.056210.
[99] O. Hul, M. Ławniczak, S. Bauch, L. Sirko, Simulation of quantum graphs by microwave networks, in: P. Exner, J. P. Keating, P. Kuchment, T. Sunada, A. Teplyaev (Eds.), Proceedings of Symposia in Pure Mathematics, Vol. 77, American Mathematical Society, 2008, pp. 595–615–. doi:10.1090/pspum/077/2459892.
[100] O. Hul, S. Bauch, M. Ławniczak, L. Sirko, Experimental investigation of reflection coefficient and wigner's reaction matrix for microwave graphs, Acta. Phys. Pol. A 112 (4) (2007) 655–664.
[101] O. Hul, O. Tymoshchuk, S. Bauch, P. M. Koch, L. Sirko, Experimental investigation of wigner's reaction matrix for irregular graphs with absorption, J. Phys. A 38 (49) (2005) 10489–. doi:10.1088/0305-4470/38/49/003.
[102] N. Goldman, Quantum transport in lattices subjected to external gauge fields: The quantum Hall effect in optical lattices and quantum graphs, VDM Verlag, Saarbrucken, 2009.

[103] G. Liu, S.-L. Zhu, S. Jiang, F. Sun, W. M. Liu, Simulating and detecting the quantum spin hall effect in the kagome optical lattice, Phys. Rev. A 82 (2010) 053605. doi:10.1103/PhysRevA.82.053605.
[104] M. Lewenstein, A. Sanpera, V. Ahufinger, Ultracold Atoms in Optical Lattices, Oxford Univ. Press, Oxford, 2012.
[105] R. Lytel, S. M. Mossman, M. G. Kuzyk, Optimization of eigenstates and spectra for quasi-linear nonlinear optical systems, J. Nonlinear Opt. Phys. Mater. 24 (02) (2015) 1550018. arXiv:http://www.worldscientific.com/doi/pdf/10.1142/S0218863515500186, doi:10.1142/S0218863515500186.
[106] M. Kac, Can one hear the shape of a drum?, The American Mathematical Monthly 73 (4) (1966) 1–23. doi:10.2307/2313748.
[107] B. Gutkin, U. Smilansky, Can one hear the shape of a graph?, J. Phys. A 34 (31) (2001) 6061–. doi:10.1088/0305-4470/34/31/301.
[108] R. Band, O. Parzanchevski, G. Ben-Shach, The isospectral fruits of representation theory: quantum graphs and drums, J. Phys. A 42 (17) (2009) 175202–. doi:10.1088/1751-8113/42/17/175202.
[109] O. Parzanchevski, R. Band, Linear representations and isospectrality with boundary conditions, J. Geom. Anal. 20 (2) (2010) 439–471–. doi:10.1007/s12220-009-9115-6.
[110] J. Boman, P. Kurasov, Symmetries of quantum graphs and the inverse scattering problem, Adv. Appl. Math. 35 (1) (2005) 58–70. doi:10.1016/j.aam.2004.10.002.
[111] P. Kurasov, M. Nowaczyk, Inverse spectral problem for quantum graphs, J. Phys. A 38 (22) (2005) 4901. doi:10.1088/0305-4470/39/4/C01.
URL http://stacks.iop.org/0305-4470/38/i=22/a=014
[112] R. Band, A. Sawicki, U. Smilansky, Scattering from isospectral quantum graphs, J. Phys. A 43 (41) (2010) 415201. doi:10.1088/1751-8113/43/41/415201.
[113] Y. Dabaghian, R. V. Jensen, R. Blümel, Exact trace formulas for a class of one-dimensional ray-splitting systems, Phys. Rev. E 63 (6) (2001) 066201–. doi:10.1103/PhysRevE.63.066201.
[114] Y. Dabaghian, R. Blümel, Explicit spectral formulas for scaling quantum graphs, Phys. Rev. E 70 (4) (2004) 046206–. doi:10.1103/PhysRevE.70.046206.
[115] Y. Dabaghian, R. Blümel, Solution of scaling quantum networks, J. Exp. Theor. Phys. Lett. 77 (9) (2003) 530–533–. doi:10.1134/1.1591985.
[116] Y. Dabaghian, R. Blümel, Explicit analytical solution for scaling quantum graphs, Phys. Rev. E 68 (5) (2003) 055201. doi:10.1103/PhysRevE.68.055201.
[117] Y. Dabaghian, R. Jensen, R. Blümel, Spectra of regular quantum graphs, J. Exp. Theor. Phys+ 94 (6) (2002) 1201–1215–. doi:10.1134/1.1493174.
[118] R. Blümel, Y. Dabaghian, R. V. Jensen, Mathematical foundations of regular quantum graphs, arXiv:quant-ph/0203126arXiv:quant-ph/0203126.
[119] V. Kostrykin, R. Schrader, Quantum wires with magnetic fluxes, Comm. Math. Phys. 237 (1-2) (2003) 161–179. doi:10.1007/s00220-003-0831-7.
[120] S. M. Badalyan, F. M. Peeters, Transport of magnetic edge states in a quantum wire exposed to a non-homogeneous magnetic field, Nanotechnology 12 (4) (2001) 570. doi:10.1088/0957-4484/12/4/340.
URL http://stacks.iop.org/0957-4484/12/i=4/a=340
[121] G. Barak, L. N. Pfeiffer, K. W. West, B. I. Halperin, A. Yacoby, Spin reconstruction in quantum wires subject to a perpendicular magnetic field, arXiv:1012.1845.
[122] P. Kurasov, A. Serio, Topological damping of aharonov-bohm effect: quantum graphs and vertex conditions, Nanosystems: physics, chemistry, mathematics 6 (2015) 309. doi:10.17586/2220-8054-2015-6-3-309-319.
[123] G. Berkolaiko, T. Weyand, Stability of eigenvalues of quantum graphs with respect to magnetic perturbation and the nodal count of the eigenfunctions, Phil. Trans. R. Soc. A 372 (2007) (2014) 20120522–. doi:10.1098/rsta.2012.0522.
[124] P. Exner, S. S. Manko, Spectra of magnetic chain graphs: coupling constant perturbations, J Phys A 48 (12) (2015) 125302–. doi:10.1088/1751-8113/48/12/125302.
[125] O. Turek, T. Cheon, Quantum graph as a quantum spectral filter, J. Math. Phys. 54 (3) (2013) 042103. doi:10.1063/1.4795404.
[126] P. Kurasov, Inverse scattering for lasso graph, J. Math. Phys. 54 (4) (2013) 042103. doi:10.1063/1.4799034.
[127] P. Kurasov, Inverse problems for aharonov-bohm rings, Math. Proc. Cambridge Philos. Soc. 148 (02) (2010) 331–362. doi:10.1017/S030500410999034X.
[128] V. Caudrelier, M. Mintchev, E. Ragoucy, Quantum wire network with magnetic flux, Phys. Lett. A 377 (31–33) (2013) 1788–1793. doi:10.1016/j.physleta.2013.05.018.
[129] S. Molchanov, B. Vainberg, Slowing down of the wave packets in quantum graphs, Waves Random Complex Media 15 (1) (2005) 101–112. doi:10.1080/17455030500053385.
URL http://dx.doi.org/10.1080/17455030500053385
[130] S. Molchanov, B. Vainberg, Wave propagation in periodic networks of thin fibers, Waves Random Complex Media 20 (2) (2010) 260–275. doi:10.1080/17455030903501857.
URL http://dx.doi.org/10.1080/17455030903501857
[131] S. Brooks, E. Lindenstrauss, Non-localization of eigenfunctions on large regular graphs, Israel J. Math. 193 (1) (2013) 1–14. doi:10.1007/s11856-012-0096-y.
[132] L. Kameni, R. Schubert, Entropy of eigenfunctions on quantum graphs, arXiv:1405.5871arXiv:1405.5871.
[133] I. Y. Popov, P. I. Smirnov, Spectral problem for branching chain quantum graph, Phys. Lett. A 377 (6) (2013) 439–442. doi:10.1016/j.physleta.2012.12.021.
[134] V. Kostrykin, R. Schrader, Kirchhoff's rule for quantum wires, J. Phys. A 32 (4) (1999) 595. doi:10.1088/0305-4470/32/4/006.
[135] E. N. Economou, Green's Functions In Quantum Physics, 3rd Edition, Springer-Verlag, Germany, 2006.
[136] G. Barton, Elements of Green's Function and Propagation, Oxford Scientific Publications, Oxford, 1995.
[137] A. G. M. Schmidt, B. K. Cheng, M. G. E. da Luz, Green function approach for general quantum graphs, J. Phys. A 36 (2003) L545.

doi:10.1088/0305-4470/36/42/L01.
[138] S. Albeverio, K. Pankrashkin, A remark on krein's resolvent formula and boundary conditions, J. Phys. A 38 (2005) 4859. doi:10.1088/0305-4470/38/22/010.
[139] V. Kostrykin, R. Schrader, Laplacians on metric graphs: Eigenvalues, resolvents and semigroups, in: G. Berkolaiko (Ed.), In Quantum Graphs and Their Applications, Vol. 415 of Contemp. Math., American Mathematical Society, Providence, RI, 2006, pp. 201–225.
[140] X. Jiang, H. Wang, S. Tang, L. Ma, Z. Zhang, Z. Zheng, A new approach to shortest paths on networks based on the quantum bosonic mechanism, New J. Phys. 13 (1) (2011) 013022. doi:10.1088/1367-2630/13/1/013022.
[141] D. U. Matrasulov, J. R. Yusupov, P. K. Khabibullaev, A. A. Saidov, Casimir effect for quantum graphs, arXiv:0707.3710arXiv:0707.3710.
[142] S. A. Fulling, Local spectral density and vacuum energy near a quantum graph vertex, in: G. Berkolaiko (Ed.), In Quantum Graphs and Their Applications, Vol. 415 of Contemp. Math., American Mathematical Society, Providence, RI, 2006, pp. 161–172.
[143] M. Coppenbarger, The green's function of the sturm-liouville operator acting on graphs, RIT Scholar Works.
URL http://scholarworks.rit.edu/article/127
[144] M. Takahashi, Thermodynamics of One-Dimensional Solvable Models, Cambridge University Press, 2005.
[145] R. Blümel, Advanced Quantum Mechanics: The Classical-Quantum Connection, Infinity Science Series, Jones & Bartlett Learning, 2011.
[146] E. Estrada, N. Hatano, M. Benzi, The physics of communicability in complex networks, Phys. Rep. 514 (3) (2012) 89–119. doi:10.1016/j.physrep.2012.01.006.
[147] P. Kuchment, Quantum graphs: I. some basic structures, Waves Random Complex Media 14 (1) (2004) S107. doi:10.1088/0959-7174/14/1/014.
[148] P. Kuchment, Quantum graphs: an introduction and a brief survey, in: P. Exner, J. P. Keating, P. Kuchment, T. Sunada, A. Teplyaev (Eds.), Analysis on Graphs and Its Applications, Vol. 77, 2008, pp. 291–314. arXiv:0802.3442.
[149] G. Berkolaiko, P. Kuchment, Introduction to Quantum Graphs, American Mathematical Society, 2012.
[150] M. G. E. da Luz, E. J. Heller, B. K. Cheng, Exact form of green functions for segmented potentials, J. Phys. A 31 (1998) 2975. doi:10.1088/0305-4470/31/13/007.
[151] M. G. E. da Luz, B. K. Cheng, M. W. Beims, Asymptotic green functions: a generalized semiclassical approach for scattering by multiple barrier potentials, J. Phys. A 34 (2001) 5041. doi:10.1088/0305-4470/34/24/303.
[152] F. M. Andrade, B. K. Cheng, M. W. Beims, M. G. E. da Luz, A generalized semiclassical expression for the eigenvalues of multiple well potentials, J. Phys. A 36 (2003) 227. doi:10.1088/0305-4470/36/1/315.
[153] V. Kostrykin, R. Schrader, The generalized star product and the factorization of scattering matrices on graphs, J. Math. Phys. 42 (4) (2001) 1563. doi:10.1063/1.1354641.
[154] S. I. El-Zanati, M. J. Plantholt, S. K. Tipnis, Extensions of some factorization results from simple graphs to multigraphs, J. Graph Theory 24 (4) (1997) 291. doi:10.1002/(SICI)1097-0118(199704)24:4<291::AID-JGT1>3.0.CO;2-J.
[155] J. Desbois, Spectral determinant of schrödinger operators on graphs, J. Phys. A 33 (2000) L63. doi:10.1088/0305-4470/33/7/103.
[156] T. Markussen, R. Stadler, K. S. Thygesen, The relation between structure and quantum interference in single molecule junctions, Nano Lett. 10 (10) (2010) 4260–4265, pMID: 20879779. arXiv:http://dx.doi.org/10.1021/nl101688a, doi:10.1021/nl101688a.
URL http://dx.doi.org/10.1021/nl101688a
[157] C. J. Lambert, Basic concepts of quantum interference and electron transport in single-molecule electronics, Chem. Soc. Rev. 44 (2015) 875–888. doi:10.1039/C4CS00203B.
URL http://dx.doi.org/10.1039/C4CS00203B
[158] R. Diestel, Graph Theory, 4th Edition, Graduate Texts in Mathematics Vol. 173, Springer, 2010.
[159] G. R. Chris Godsil, Algebraic Graph Theory, Springer-Verlag New York, 2001. doi:10.1007/978-1-4613-0163-9.
[160] A. Bondy, U. Murty, Graph Theory, Springer, 2008.
[161] J. E. Avron, P. Exner, Y. Last, Periodic schrödinger operators with large gaps and wannier-stark ladders, Phys. Rev. Lett. 72 (6) (1994) 896. doi:10.1103/PhysRevLett.72.896.
[162] R. Lytel, M. G. Kuzyk, Dressed quantum graphs with optical nonlinearities approaching the fundamental limit, J. Nonlinear Opt. Phys. Mater. 22 (04) (2013) 1350041. arXiv:http://www.worldscientific.com/doi/pdf/10.1142/S0218863513500410, doi:10.1142/S0218863513500410.
URL http://www.worldscientific.com/doi/abs/10.1142/S0218863513500410
[163] V. Pivovarchik, Characteristic functions under series and parallel connection of quantum graphs, J. Phys. A 48 (36) (2015) 365201.
URL http://stacks.iop.org/1751-8121/48/i=36/a=365201
[164] J. Yusupov, M. Dolgushev, A. Blümen, O. Muelken, Directed transport in quantum star graphs, arXiv:1503.02253arXiv:1503.02253.
[165] S. Gnutzmann, D. Waltner, Stationary waves on nonlinear quantum graphs i: General framework and canonical perturbation theory, arXiv:1510.00351arXiv:1510.00351.
[166] S. Gnutzmann, J. P. Keating, F. Piotet, Quantum ergodicity on graphs, Phys. Rev. Lett. 101 (26) (2008) 264102. doi:10.1103/physrevlett.101.264102.
URL http://dx.doi.org/10.1103/PhysRevLett.101.264102
[167] G. Teschl, Mathematical Methods in Quantum Mechanics: With Applications to Schrödinger Operators, American Mathematical Society, 2009.
[168] P. Exner, P. Seba, Quantum-mechanical splitters: How should one understand them?, Phys. Lett. A 128 (9) (1988) 493. doi:10.1016/0375-9601(88)90882-1.
[169] P. Exner, P. Seba, Free quantum motion on a branching graph, Rep. Math. Phys. 28 (1) (1989) 7. doi:10.1016/0034-4877(89)90023-2.
[170] S. Albeverio, F. Gesztesy, R. Hoegh-Krohn, H. Holden, Solvable Models in Quantum Mechanics, 2nd Edition, AMS Chelsea Publishing, Providence, RI, 2004.
[171] G. Bonneau, J. Faraut, G. Valent, Self-adjoint extensions of operators and the teaching of quantum mechanics, Am. J. Phys. 69 (3) (2001) 322. doi:10.1119/1.1328351.
[172] S. Flügge, Practical Quantum Mechanics, Springer-Verlag, Berlin, 1999.

[173] G. Baym, Lectures on quantum mechanics, Benjamin/Cummings Pub. Co, 1981.
[174] J. Kuhn, F. M. Zanetti, A. L. Azevedo, A. G. M. Schmidt, B. K. Cheng, M. G. E. d. Luz, Time-dependent point interactions and infinite walls: some results for wavepacket scattering, J. Opt. B: Quantum Semiclassical Opt. 7 (3) (2005) S77. doi:10.1088/1464-4266/7/3/011.
[175] V. Caudrelier, M. Mintchev, E. Ragoucy, The quantum nonlinear schrödinger model with point-like defect, J. Phys. A 37 (30) (2004) L367. doi:10.1088/0305-4470/37/30/L02.
[176] T. Cheon, P. Exner, P. Seba, Wave function shredding by sparse quantum barriers, Phys. Lett. A 277 (1) (2000) 1. doi:10.1016/S0375-9601(00)00690-3.
[177] L. I. Schiff, Quantum Mechanics, 2nd Edition, McGraw-Hill, New York, 1955.
[178] H. Kleinert, I. Mustapic, Summing the spectral representations of pöschl-teller and rosen-morse fixed-energy amplitudes, J. Math. Phys. 33 (2) (1992) 643–. doi:10.1063/1.529800.
[179] H. Kleinert, Path Integrals in Quantum Mechanics, Statistics, Polymer Physics, and Financial Markets, 4th Edition, World Scientific Publishing Company, Singapore, 2006.
[180] R. P. Feynman, A. R. Hibbs, Quantum Mechanics and Path Integrals: Emended Edition, Dover Publications, 2010.
[181] L. S. Schulman, Techniques and Applications of Path Integrals, Dover Publications, Mineola, New York, 2005.
[182] M. A. M. de Aguiar, Exact green's function for the step and square-barrier potentials, Phys. Rev. A 48 (4) (1993) 2567–. doi:10.1103/PhysRevA.48.2567.
[183] F. M. Andrade, Exact green's function for rectangular potentials and its application to quasi-bound states, Phys. Lett. A 378 (2014) 1461. arXiv:1403.5964, doi:10.1016/j.physleta.2014.03.042.
[184] Y. Golovaty, 1d schrödinger operators with short range interactions: Two-scale regularization of distributional potentials, Integr. Equ. Oper. Theory 75 (3) (2013) 341–362. doi:10.1007/s00020-012-2027-z.
URL http://dx.doi.org/10.1007/s00020-012-2027-z
[185] H.-J. Stöckmann, J. Stein, "quantum" chaos in billiards studied by microwave absorption, Phys. Rev. Lett. 64 (19) (1990) 2215. doi:10.1103/PhysRevLett.64.2215.
[186] H. Schanze, E. R. P. Alves, C. H. Lewenkopf, H.-J. Stöckmann, Transmission fluctuations in chaotic microwave billiards with and without time-reversal symmetry, Phys. Rev. E 64 (6) (2001) 065201. doi:10.1103/PhysRevE.64.065201.
[187] F. M. Zanetti, J. Khun, G. J. Delben, B. K. Cheng, M. G. E. da Luz, Classifying the general family of 1D point interactions: a scattering approach, J. Phys. A 39 (2006) 2493. doi:10.1088/0305-4470/39/10/016.
[188] M. G. E. da Luz, B. K. Cheng, Exact propagators for moving hard-wall potentials, J. Phys. A 25 (17) (1992) L1043–L1047. doi:10.1088/0305-4470/25/17/005.
URL http://dx.doi.org/10.1088/0305-4470/25/17/005
[189] M. da Luz, B. K. Cheng, On the propagators for hard-wall potentials oscillating periodically with constant velocity, Physica D 72 (3) (1994) 244–258. doi:10.1016/0167-2789(94)90213-5.
URL http://dx.doi.org/10.1016/0167-2789(94)90213-5
[190] M. G. E. da Luz, B. K. Cheng, Quantum-mechanical results for a free particle inside a box with general boundary conditions, Phys. Rev. A 51 (1995) 1811–1819. doi:10.1103/PhysRevA.51.1811.
URL http://link.aps.org/doi/10.1103/PhysRevA.51.1811
[191] M. Van Vessen, M. C. Santos, B. K. Cheng, M. G. E. da Luz, Origin of quantum chaos for two particles interacting by short-range potentials, Phys. Rev. E 64 (2001) 026201. doi:10.1103/PhysRevE.64.026201.
URL http://link.aps.org/doi/10.1103/PhysRevE.64.026201
[192] A. G. M. Schmidt, B. K. Cheng, M. G. E. da Luz, Green functions for generalized point interactions in one dimension: A scattering approach, Phys. Rev. A 66 (2002) 062712. doi:10.1103/PhysRevA.66.062712.
[193] A. G. M. Schmidt, M. G. E. da Luz, Wave-packet dynamics for general contact interactions on a circular setup:revivals, bouncing, and trapping, Phys. Rev. A 69 (5) (2004) 052708. doi:10.1103/PhysRevA.69.052708.
[194] K. Chadan, P. C. Sabatier, Inverse Problems in Quantum Scattering Theory, 2nd Edition, Springer, New York, 1989.
[195] F. A. B. Coutinho, Y. Nogami, J. F. Perez, Generalized point interactions in one-dimensional quantum mechanics, J. Phys. A 30 (11) (1997) 3937. doi:10.1088/0305-4470/30/11/021.
[196] S. M. Blinder, Green's function and propagator for the one-dimensional δ-function potential, Phys. Rev. A 37 (1988) 973. doi:10.1103/PhysRevA.37.973.
[197] S. Gnutzmann, H. Schanz, U. Smilansky, Topological resonances in scattering on networks (graphs), Phys. Rev. Lett. 110 (9) (2013) 094101. doi:10.1103/PhysRevLett.110.094101.
[198] I. Carneiro, M. Loo, X. Xu, M. Girerd, V. Kendon, P. L. Knight, Entanglement in coined quantum walks on regular graphs, New J. Phys. 7 (1) (2005) 156–. doi:10.1088/1367-2630/7/1/156.
[199] B. Tregenna, W. Flanagan, R. Maile, V. Kendon, Controlling discrete quantum walks: coins and initial states, New J. Phys. 5 (2003) 83. doi:10.1088/1367-2630/5/1/383.
[200] V. PotoCek, A. Gabris, T. Kiss, I. Jex, Optimized quantum random-walk search algorithms on the hypercube, Phys. Rev. A 79 (1) (2009) 012325. doi:10.1103/PhysRevA.79.012325.
[201] S. E. Venegas-Andraca, Quantum walks for computer scientists, Synthesis Lectures on Quantum Computing 1 (1) (2008) 1. doi:10.2200/S00144ED1V01Y200808QMC001.
[202] H. Krovi, T. A. Brun, Hitting time for quantum walks on the hypercube, Phys. Rev. A 73 (3) (2006) 032341. doi:10.1103/PhysRevA.73.032341.
[203] C. Moore, A. Russell, Quantum walks on the hypercube, in: RANDOM, 2002, p. 164. arXiv:quant-ph/0104137, doi:10.1007/3-540-45726-7.
[204] J. Košik, V. Bužek, Scattering model for quantum random walks on a hypercube, Phys. Rev. A 71 (2005) 012306. doi:10.1103/PhysRevA.71.012306.
[205] E. Farhi, J. Goldstone, S. Gutmann, A quantum algorithm for the hamiltonian nand tree, Theory of Computing 4 (1) (2008) 169–190.

doi:10.4086/tOC.2008.v004a008.
[206] A. M. Childs, R. Cleve, S. P. Jordan, D. Yonge-Mallo, Discrete-query quantum algorithm for nand trees, Theory of Computing 5 (1) (2009) 119–123. doi:10.4086/tOC.2009.v005a005.
[207] E. Farhi, S. Gutmann, Quantum computation and decision trees, Phys. Rev. A 58 (2) (1998) 915. doi:10.1103/PhysRevA.58.915.
[208] A. M. Childs, E. Farhi, S. Gutmann, An example of the difference between quantum and classical random walks, Quantum Inf. Process. 1 (2002) 35. arXiv:quant-ph/0103020, doi:10.1023/A:1019609420309.
[209] A. M. Childs, R. Cleve, E. Deotto, E. Farhi, S. Gutmann, D. A. Spielman, Exponential algorithmic speedup by a quantum walk, in: STOC '03: Proceedings of the thirty-fifth annual ACM symposium on Theory of computing, ACM, New York, NY, USA, 2003, p. 59. doi:http://doi.acm.org/10.1145/780542.780552.
[210] S. Perseguers, G. J. L. Jr, D. Cavalcanti, M. Lewenstein, A. Acín, Distribution of entanglement in large-scale quantum networks, Rep. Prog. Phys. 76 (9) (2013) 096001. doi:10.1088/0034-4885/76/9/096001.
URL http://stacks.iop.org/0034-4885/76/i=9/a=096001
[211] V. Caudrelier, E. Ragoucy, Direct computation of scattering matrices for general quantum graphs, Nucl. Phys. B 828 (3) (2010) 515–535. doi:10.1016/j.nuclphysb.2009.10.012.
[212] J. Shang, Y. Wang, M. Chen, J. Dai, X. Zhou, J. Kuttner, G. Hilt, X. Shao, J. M. Gottfried, K. Wu, Assembling molecular sierpiński triangle fractals, Nat Chem 7 (5) (2015) 389–393, article. doi:10.1038/nchem.2211.
URL http://dx.doi.org/10.1038/nchem.2211
[213] I. Stewart, Four encounters with sierpińriski's gasket, The Mathematical Intelligencer 17 (1) (1995) 52. doi:10.1007/BF03024718.
[214] P. Alonso-Ruiz, U. R. Freiberg, Hanoi attractors and the sierpiński gasket, International Journal of Mathematical Modelling and Numerical Optimisation 3 (4) (2012) 251–265, pMID: 49601. arXiv:http://www.inderscienceonline.com/doi/pdf/10.1504/IJMMNO.2012.049601, doi:10.1504/IJMMNO.2012.049601.
URL http://www.inderscienceonline.com/doi/abs/10.1504/IJMMNO.2012.049601
[215] A. Bondarenko, V. Dedok, Surgery of quantum graphs, in: Science and Technology, 2004. KORUS 2004. Proceedings. The 8th Russian-Korean International Symposium on, 2004, p. 108. doi:10.1109/KORUS.2004.1555559.
[216] A. Bondarenko, V. Dedok, Anderson localization in 1-D quantum random walk, in: Science and Technology, 2005. KORUS 2005. Proceedings. The 9th Russian-Korean International Symposium on, 2005, p. 27. doi:10.1109/KORUS.2005.1507636.
[217] L. Barriere, F. Comellas, C. Dalfo, Fractality and the small-world effect in sierpinski graphs, J. Phys. A 39 (38) (2006) 11739. doi:10.1088/0305-4470/39/38/003.
[218] C. A. Moyer, A unified theory of quasibound states, AIP Adv. 4 (2) (2014) 027109. doi:10.1063/1.4865998.
URL http://scitation.aip.org/content/aip/journal/adva/4/2/10.1063/1.4865998
[219] L. D. Landau, E. M. Lifschitz, Quantum Mechanics, Pergamon, Oxford, 1981.
[220] G. N. Gibson, G. Dunne, K. J. Bergquist, Tunneling ionization rates from arbitrary potential wells, Phys. Rev. Lett. 81 (13) (1998) 2663. doi:10.1103/PhysRevLett.81.2663.
[221] E. Torrontegui, J. Muñoz, Y. Ban, J. G. Muga, Explanation and observability of diffraction in time, Phys. Rev. A 83 (4) (2011) 043608. doi:10.1103/PhysRevA.83.043608.
[222] A. del Campo, J. G. Muga, Dynamics of a tonks-girardeau gas released from a hard-wall trap, Europhys. Lett. 74 (6) (2006) 965. doi:10.1209/epl/i2006-10061-5.
[223] M. Sato, H. Aikawa, K. Kobayashi, S. Katsumoto, Y. Iye, Observation of the fano-kondo antiresonance in a quantum wire with a side-coupled quantum dot, Phys. Rev. Lett. 95 (6) (2005) 066801. doi:10.1103/PhysRevLett.95.066801.
[224] J. J. Sakurai, J. Napolitano, Modern Quantum Mechanics, 2nd Edition, Addison-Wesley, 2011.
[225] E. Merzbacher, Quantum Mechanics, 3rd Edition, Wiley, New York, 1998.
[226] F. M. Andrade, Funções de green semiclássicas generalizadas e aplicações a sistemas ligados, Master's thesis, Universidade Federal do Paraná, Curitiba (2001).
[227] P. Dita, Parametrisation of unitary matrices, J. Phys. A 15 (11) (1982) 3465. doi:10.1088/0305-4470/15/11/023.
[228] R. Newton, Scattering Theory of Waves and Particles, 2nd Edition, Dover Books on Physics Series, Dover Publications, 1982.
[229] L. Hostler, Coulomb green's functions and the furry aproximation, J. Math. Phys. 5 (1964) 591. doi:10.1063/1.1704153.
[230] S. M. Blinder, Nonrelativistic coulomb green's function in parabolic coordinates, J. Math. Phys. 22 (1981) 306. doi:10.1063/1.524879.